

SYNTHESIS OF 2,7-DIHYDROXYCADALENE, A COTTON
PHYTOALEXIN; PHOTO-ACTIVATED ANTIBACTERIAL
ACTIVITY OF PHYTOALEXINS FROM COTTON;
EFFECT OF REACTIVE OXYGEN SCAVENGERS
AND QUENCHERS ON BIOLOGICAL ACTIVITY
AND ON TWO DISTINCT DEGRADATION
REACTIONS OF DHC

By

JOY RANDALL STEIDL

Bachelor of Science
University of Illinois
Urbana, Illinois
1977

Master of Science
State University of New York
Albany, New York
1981

Submitted to the Faculty of the Graduate College
of the Oklahoma State University
in partial fulfillment of the requirements
for the Degree of
DOCTOR OF PHILOSOPHY
December, 1988

SYNTHESIS OF 2,7-DIHYDROXYCADALENE, A COTTON
PHYTOALEXIN; PHOTO-ACTIVATED ANTIBACTERIAL
ACTIVITY OF PHYTOALEXINS FROM COTTON;
EFFECT OF REACTIVE OXYGEN SCAVENGERS
AND QUENCHERS ON BIOLOGICAL ACTIVITY
AND ON TWO DISTINCT DEGRADATION
REACTIONS OF DHC

Thesis Approved:

Margaret K. Essenberg

Thesis Adviser

Robert K. Johnson

Richard C. Essenberg

Roger E. Hoff

E. L. Lintz

Norman N. Durham

Dean of the Graduate College

PREFACE

This research was undertaken with the intent to discover how a particular phytoalexin inhibits one bacterial pathovar. It sounded straightforward, but, like many questions in science, turned out to be quite complex. I scaled back my expectations, and was able to answer parts of my original question, plus some interesting questions I had not foreseen. That, too, is common in science.

I thank my advisor, Margaret Essenberg, for restoring my belief in fine principles in research and in the joys of intellectual behavior. I thank Drs. E. J. Eisenbraun and Robert Stipanovic, who gave generously and patiently of their time and knowledge, during the organic synthesis of DHC. Without my dear friends, this would have been a much less happy time. I thank Randy Turner, Marlee Pierce, Gordon Davis and Judy Hall for their help and support.

Finally, I thank my parents for teaching me the joy of learning new things. Without this, and their belief in me, I would never have undertaken this work.

TABLE OF CONTENTS

| Chapter | Page |
|---|------|
| I. INTRODUCTION | 1 |
| II. REVIEW OF SELECTED LITERATURE | 3 |
| Resistant Response of Cotton to Xcm | 5 |
| Reported Mechanisms of Toxicity of Some Phytoalexins | 6 |
| Photo-activation and Photo-oxidation | 7 |
| Reactive Oxygen Species | 9 |
| Strategy of Scavenging and Quenching Reactive Oxygen | 10 |
| III. SYNTHESIS OF 2,7-DIHYDROXYCADALENE; OXIDATIVE REARRANGEMENT OF SUBSTITUTED ARYLAKYL KETONES WITH THALLIUM (III) NITRATE | 12 |
| Introduction | 13 |
| Results and Discussion | 13 |
| Experimental | 22 |
| Synthesis of 2,7-dihydroxycadalene | 22 |
| Thallium (III) Nitrate Oxidative Rearrangements | 29 |
| References | 30 |
| IV. PHOTOACTIVATED ANTIBACTERIAL ACTIVITY OF PHYTOALEXINS FROM COTTON AND EFFECT OF REACTIVE OXYGEN SCAVENGERS AND QUENCHERS ON PHOTODYNAMIC ACTION OF DHC | 32 |
| Abstract | 33 |
| Introduction | 33 |
| Materials and Methods | 34 |
| Preparation of Phytoalexins | 34 |
| Bioassay Methods | 35 |
| Results | 36 |
| Comparison of Plant-derived and Synthetic DHC | 36 |
| Effect of Xcm Concentration on the Toxicity of DHC | 38 |
| Effect of Light on the Biological Activity of Several Cotton Sesquiterpenoids | 38 |
| Biological Activity of Some Products of DHC | 48 |
| Effects of Scavengers or Quenchers of Activated Oxygen on DHC Toxicity | 52 |
| Discussion | 75 |

| Chapter | Page |
|---|------|
| References | 81 |
| | |
| V. TWO REACTIONS OF DHC UNDER BIOASSAY CONDITIONS: A PHOTOACTIVATED GENERATION OF A FREE RADICAL, AND AN Fe^{+3} -DEPENDENT OXIDATION TO FORM LACINILENE C | 84 |
| Abstract | 85 |
| Introduction | 85 |
| Results | 86 |
| Effect of Fe and Light on DHC Degradation | 86 |
| Effect of Fe on LC Degradation | 101 |
| Effects of Selected Enzymes on DHC Degradation..... | 101 |
| Inhibition of the Degradation of DHC Under Anaerobic Conditions | 103 |
| Effect of Selected Scavengers or Quenchers of Activated Oxygen | 111 |
| Photo-degradation of HMC | 113 |
| Spin Trapping of a Free Radical Produced by DHC in the Light | 119 |
| Separation of Degradation Products of DHC | 119 |
| Discussion | 119 |
| Fe-Dependent DHC Degradation in Dark Conditions | 127 |
| Photo-Degradation of DHC | 133 |
| Experimental | 140 |
| Preparation and Purification of Phytoalexins | 140 |
| Time-Course Degradations | 140 |
| Ferrous and Ferric Ion/DHC Degradations | 141 |
| Protein/DHC Degradation Experiments | 141 |
| Crocine/DHC Experiments | 142 |
| Spin-Trapping of Free Radical | 142 |
| References | 142 |
| | |
| BIBLIOGRAPHY | 144 |
| | |
| APPENDICES | 147 |
| APPENDIX A – EFFECT OF TWO ALCOHOLS ON GROWTH OF XCM | 148 |
| APPENDIX B – EFFECT OF AET ON GROWTH OF XCM | 149 |
| APPENDIX C – EFFECT OF CROCIN ON GROWTH OF XCM | 150 |

LIST OF FIGURES

| Figure | | Page |
|-------------|---|------|
| Chapter II | | |
| 1. | Types I & II Photosensitization Reactions | 8 |
| Chapter III | | |
| 1. | Synthesis of 2,7-Dihydroxycadalene by the Method of Teresa <i>et al.</i> (3)..... | 14 |
| 2. | Synthesis of 2,7-Dihydroxycadalene by the Method of Stipanovic and Steidl (4)..... | 15 |
| 3. | ¹ H NMR Spectrum, Detail of Aromatic Region, of Nitrated Ester..... | 17 |
| 4. | Thallium (III) Nitrate Oxidative Rearrangements of Alkyl Phenones..... | 18 |
| 5. | Proposed Mechanism of Thallium (III) Oxidative Rearrangement of Alkyl Phenones..... | 19 |
| 6. | ¹ H NMR Spectrum of Methyl 2-(3'-methoxy-4'-methylphenyl) propionate..... | 20 |
| 7. | Substituted Acetophenones Used for Thallium (III) Nitrate Oxidative Rearrangement | 21 |
| Chapter IV | | |
| 1. | Comparison of Toxicity of Plant-derived and Synthetic DHC | 37 |
| 2a. | Comparison of Toxicity of Plant-derived and Synthetic DHC; Light Conditions, Time-Course | 39 |
| 2b. | Comparison of Toxicity of Plant-derived and Synthetic DHC; Dark Conditions, Time-Course | 40 |
| 3. | Effect of Concentration of Xcm on DHC Toxicity | 41 |
| 4. | Photo-stimulation of Antibacterial Activity of DHC | 44 |

| Figure | Page |
|---|------|
| 5. Photo-stimulation of Antibacterial Activity of LC | 45 |
| 6. Effect of HMC on Xcm; Light and Dark Conditions | 46 |
| 7. Effect of Light on Toxicity of LCME Toward Xcm | 47 |
| 8. Bioassay of an Unidentified Red Compound, Produced by Degradation of DHC in the Dark; Dark Conditions | 49 |
| 9. Toxicity of Photo-Degradation Products of DHC Toward Xcm | 50 |
| 9a. Toxicity of Photo-Degradation Products of DHC Toward Xcm | 51 |
| 10a. Test of Toxicity of DABCO Toward Xcm | 54 |
| 10b. Bioassay of DABCO with Xcm in Light | 54 |
| 11a. Effect of DABCO on Toxicity of Xcm in Light | 55 |
| 11b. Effect of DABCO on Toxicity of Xcm in Dark | 56 |
| 12a. Effect of Bixin on Xcm ; Light and Dark Conditions | 57 |
| 12b. Effect of Bixin on Xcm; Light and Dark Conditions | 57 |
| 13a. Effect of Bixin on Toxicity of DHC; Light Conditions | 58 |
| 13b. Effect of Bixin on Toxicity of DHC; Dark Conditions | 59 |
| 14a. Effect of Sodium Benzoate on Toxicity of DHC; Light Conditions | 60 |
| 14b. Effect of Sodium Benzoate on Toxicity of DHC; Dark Conditions | 61 |
| 15a. Effect of SOD and Catalase on Toxicity of DHC; Light Conditions | 63 |
| 15b. Effect of SOD and Catalase on Toxicity of DHC; Dark Conditions | 64 |
| 16a. Toxicity of Vitamins E and C Toward Xcm; Light Conditions | 66 |
| 16b. Toxicity of Vitamins E and C Toward Xcm; Dark Conditions | 67 |
| 17a. Effect of Vitamin E on Toxicity of DHC; Light Conditions | 68 |
| 17b. Effect of Vitamin E on Toxicity of DHC; Dark Conditions | 69 |
| 18. Toxicity of Sequestrene 138 Toward Xcm; Light Conditions | 70 |
| 19a. Effect of Sequestrene 138 on Toxicity of DHC; Light Conditions | 71 |
| 19b. Effect of Sequestrene 138 on Toxicity of DHC; Dark Conditions | 72 |
| 20a. Effect of DTPA on Toxicity of DHC; Light Conditions | 73 |

| Figure | Page |
|--|------|
| 20b. Effect of DTPA on Toxicity DHC; Dark Conditions | 74 |

Chapter V

| | |
|---|-----|
| 1. UV-visible Absorption Spectrum of DHC, 10.3 μM in MOPS Medium; Scanned with MOPS Medium Blank | 87 |
| 2. UV-visible Absorption Spectrum in MOPS Medium of an Equal Sample from DHC Solution Shown in Fig. 1, After Exposure to Light for 7 h | 88 |
| 3. UV-visible Absorption Spectrum in MOPS Medium of Degradation Products of 10.9 μM DHC, 12 h in Dark, in MOPS Medium | 90 |
| 4. UV-visible Absorption Spectrum of LC, 85.4 μM LC, in MOPS Medium | 91 |
| 5a. Effect of Fe and Light on Degradation of DHC | 92 |
| 5b. Rate of DHC Degradation with/without Fe or Light; Semilog Plot | 93 |
| 5c. Effects of Fe on Rate of Appearance of DHC Degradation Products; Dark Conditions | 94 |
| 6. Effect of Fe on Degradation of DHC; DTPA Used to Remove Fe | 95 |
| 7. Effect of DTPA and Fe on Degradation of DHC; Dark Conditions | 97 |
| 8. Effects of DTPA and Fe on Appearance of DHC Degradation Products; Dark Conditions | 98 |
| 9. Effects of Excess Fe^{+2} and Fe^{+3} on DHC Degradation; Dark Conditions | 99 |
| 10. Effects of Fe^{+2} and Fe^{+3} on Disappearance of DHC in the Dark | 100 |
| 11. Effects of Fe and Light on Degradation of LC | 102 |
| 12. Effects of Some Proteins on Light Degradation of DHC | 104 |
| 13. Effect of SOD on DHC Degradation in the Dark | 105 |
| 14. Effect of KCN on the Degradation of DHC by SOD in the Dark | 106 |
| 15. Effect of SOD, Catalase and Cytochrome c on Degradation of DHC; Dark Conditions | 107 |
| 16. Effect of Peroxidase on the Degradation of DHC; Dark Conditions | 108 |
| 17. Effect of Anaerobic Conditions on Degradation of DHC; Light Conditions | 109 |

| Figure | Page |
|---|------|
| 18. Effect of Anaerobic Conditions on Appearance of DHC Degradation Products; Dark Conditions | 110 |
| 19. Effect of Crocin, Na-benzoate and DABCO on Light Degradation of DHC | 112 |
| 20. Effect of Mannitol and AET on Light Degradation of DHC | 114 |
| 20a. Effect of Mannitol and AET on Rate of Light Degradation of DHC; Semilog Plot | 115 |
| 20b. Effect of AET Concentration on Degradation of DHC; Light Conditions | 116 |
| 21. Effect of AET on Degradation of DHC; Dark Conditions | 117 |
| 22. Light Degradation of DHC and HMC in Methanol | 118 |
| 23. Spin Trapping by PBN of a Free Radical Produced by DHC in the Light | 120 |
| 24. UV-visible Absorption Spectrum of a Degradation Product of DHC; Dark Conditions | 121 |
| 25a. UV-visible Spectra of Light Degradation Products of DHC | 122 |
| 25b. | 123 |
| 25c. | 124 |
| 25d. | 125 |
| 25e. | 126 |
| 26. Proposed Mechanism for Fe-Dependent DHC Degradation in the Dark | 129 |
| 27. Transguanylation Rearrangement of AET | 132 |
| 28. Resonance Stabilization of Amino-thiol Free Radical | 132 |
| 29. Proposed Toxic Reaction Pathways of Light-Activated DHC | 140 |

LIST OF ABBREVIATIONS

| | |
|------------------------------|---|
| AET | S-2-aminoethyl isothiuronium bromide hydrobromide |
| 9-BBN | 9-borabicyclo[3.3.1]nonane |
| BSA | bovine serum albumin |
| DABCO | diazabicyclo(2,2,2)octane |
| DHC | 2,7-dihydroxycadalene |
| DMPO | 5,5-dimethylpyrroline N-oxide |
| DTPA | diethylene triaminepentaacetic acid |
| EPR | electron paramagnetic resonance |
| GED | bis(2-guanidinoethyl)disulfide |
| HMC | 2-hydroxy, 7-methoxycadalene |
| HR | hypersensitive response |
| LC | lacinilene C |
| LCME | lacinilene C 7-methyl ether |
| MEG | 2-mercaptoethylguanidine hydrobromide |
| MOPS | 3-(N-morpholino)propanesulfonic acid |
| O ₂ ¹ | singlet oxygen |
| O ₂ ^{·-} | superoxide anion |
| OH [·] | hydroxyl radical |
| PA | phytoalexin |
| PBN | phenyl <i>t</i> -butylnitron |
| SOD | superoxide dismutase |
| TLC | thin layer chromatography |

LIST OF ABBREVIATIONS (Continued)

| | |
|------|--|
| TMOF | trimethylorthoformate |
| TTN | thallium (III) nitrate |
| Xcm | <i>Xanthomonas campestris</i> pv. <i>malvearum</i> |

CHAPTER I

INTRODUCTION

Bacterial leaf blight of cotton in susceptible cotton plants causes water-soaked lesions, which spread from the site(s) of infection, and under favorable infection conditions, lead to withering and loss of the leaf. Lines of cotton highly resistant to bacterial leaf blight have been developed. Inoculation of a resistant cotton plant with *Xanthomonas campestris* pv. *malvacearum* (Xcm), the causative agent of bacterial leaf blight, leads to dry pin-point lesions, which do not spread, and thus no further visible symptoms develop.

The pin point lesions are the site of a rapid local response, called the hypersensitive response (HR), to the invading pathogen. At the site of the HR, the plant cells actually die much more rapidly than do cells of a susceptible plant inoculated with Xcm. However, the growth of Xcm is inhibited, and lesions do not spread.

The HR is a complex series of events which has been and still is being intensively studied. It is clear that many factors contribute to a successful resistant disease interaction. The particular part of this complex interaction which constitutes the focus of this study is the ability of a group of sesquiterpenoid phytoalexins, synthesized during the resistant response, to inhibit the growth of Xcm. The phytoalexins (DHC, LC, and LCME) are inhibitory to Xcm in liquid culture, and DHC is the most potent of these in its inhibitory effect. The mechanism of the antibacterial activity of DHC is the subject of the following investigation.

Although a thorough understanding of the role of these compounds in disease resistance will encompass their activity *in planta*, the search for their mechanism of toxicity

was, of necessity, undertaken in a simpler system: bacterial liquid culture in a defined medium.

The first approach to understanding the toxicity of DHC which was taken in this study was use of a variety of reagents and conditions in an attempt to block or partially interfere with the toxicity of DHC in liquid culture, and so gain insight into the reactions involved.

This approach met with only limited success, and an even simpler system was employed to study the chemical reactions which DHC undergoes in bioassay conditions: Xcm was omitted, and spectral studies were carried out in the bioassay medium.

CHAPTER II

REVIEW OF SELECTED LITERATURE

Plants have developed a variety of techniques for defense against invasion by the pathogens in their environment. Morphological adaptations which greatly reduce the ability of the pathogen to gain access to the plant tissue have been observed in many plant/pathogen systems, including the resistance of alfalfa to *Corynebacterium insidiosum*. Resistant varieties of alfalfa have shorter vessels and fewer vascular bundles, severely restricting the movement of the bacteria (1).

In some plants, constitutive compounds which are capable of inhibiting bacterial, fungal or viral growth are present and active in uninfected tissue. Saponins, widely distributed glycosides capable of disrupting membranes, and phenolics, which are present in most plant tissues, and can inhibit bacteria and fungi, are two examples. Only a few systems have been described in which a preformed (prior to infection) compound has been convincingly shown to be responsible for disease resistance. One such plant system is onions, which contain certain phenolic compounds in the onion scales. The phenolics are present only in plants resistant to *Colletotrichum circinans*, which causes smudge disease (2).

Many disease resistance interactions consist of a series of events in the plant which are initiated by invasion by the pathogen. There is evidence that the immediate signal for the response within the plant (called an elicitor) is, in some cases, fragments of pathogen or host cell wall (3). One of the most notable of these resistance events is a rapid collapse and death of plant cells in the immediate area of the infection, called a hypersensitive response (HR) (4). The collapse of tissue caused by HR, or the death of single plant cells

seen with very low pathogen inoculum (5), appears to be necessary for the containment of pathogen which is a characteristic of plants responding with HR. However, the mechanism of this containment is not yet established. The immediate agent of cell death is likewise not defined. A sudden rise in extracellular pH is observed during development of HR in tobacco (6). Ammonia accumulates in bacterially inoculated cotton leaves, and rises to higher levels during a resistant than a susceptible interaction (7). In tobacco suspension cultures, stimulated by an elicitor (8), and in potato leaves responding hypersensitively to infection with *Phytophthora infestans* (9), the rise in extracellular pH is accompanied by an increase in H_2O_2 or O_2^- . Reactive oxygen such as H_2O_2 or O_2^- is capable of causing membrane damage, which would lead to the loss of membrane integrity observed in the HR by Novacky et al.(10). No such cause-and-effect relationship has been established, however.

In the cotton/Xcm resistant interaction, the local cell death does not appear to be a sufficient condition to cause bacterial inhibition. Inoculated resistant cotton lines held continuously in the dark showed the cell collapse and death of the HR, but allowed Xcm to grow to the high populations seen in the susceptible lines (11). Phytoalexin synthesis was suppressed under these conditions.

Many successful resistance responses include more than line of action by the plant which produce conditions or compounds potentially lethal or inhibitory toward the pathogen. Some resistant plants synthesize low molecular-weight antimicrobial compounds, called phytoalexins (PAs) following infection. Envelopment of pathogens by fibrillar material synthesized by the host cells is also observed in resistant (incompatible) responses (12,13), but in most studies was absent or less frequent in susceptible (compatible) interactions (13,14).

Resistant Response of Cotton to Xcm

Resistant lines of Upland cotton (*Gossypium hirsutum*), when inoculated with incompatible strains of Xcm, initiated an HR at the sites of infection. During the incompatible response, three sesquiterpenoid phytoalexins [2,7-dihydroxycadalene (DHC), lacinilene C (LC), and lacinilene C 7-methyl ether (LCME)] accumulated in cells near the infection (15).

Small lesions of collapsed tissue developed, but did not spread, and the Xcm, after dividing rapidly for 3-4 days in the intercellular spaces, was inhibited from further growth (16). The mesophyll cells immediately adjoining bacterial colonies died rapidly, and a small bacteriostatic zone around each colony was produced (15). Fluorescence microscopy of resistant cotton leaves which had been inoculated with incompatible Xcm has shown the presence of mesophyll cells with a bright yellow fluorescence (17). This fluorescence is similar to the fluorescent emission of lacinilene C, and the fluorescent cells correspond with irregularly shaped brown cells which are the sites of extracellular bacterial colonies (18).

Mesophyll cells from inoculated resistant cotyledons were isolated and the fluorescent cells were separated using a fluorescence-activated cell sorter. DHC, LC and LCME were found to be highly enriched in the fluorescent cell fraction, indicating these cells as the site of phytoalexin accumulation (19). The local concentration of PAs in the fluorescent cells was calculated and found to be adequate to account for inhibition of Xcm (20). The fluorescent cells have damaged membranes as detected by Evans blue staining of these cells (M. Pierce & M. Essenberg, unpublished work), and the PAs should be free to diffuse into the extracellular space where the bacteria are located. The observed onset of bacteriostatic conditions following inoculation of highly resistant cotton with Xcm, at 3-4 days following inoculation, coincided with the initial rise in concentration of the PAs (20).

This early concentration, although well below the maximum levels accumulated, was sufficient for inhibition (21).

Reported Mechanisms of Toxicity of Some Phytoalexins

Phytoalexin accumulation in disease resistance has been reported for many resistance interactions. In a few of these interactions, the mechanism of toxicity of the phytoalexin has been studied and characterized.

Glycinol, a pterocarpan phytoalexin is synthesized by soybeans in response to inoculation with *Erwinia carotovora*. Incubation of *E. carotovora* with glycinol at bacteriostatic concentrations inhibited the ability of *E. carotovora* to incorporate $^3\text{[H]}$ leucine, $^3\text{[H]}$ thymidine and $^3\text{[H]}$ uridine into biopolymers (22). Exposure of *E. coli* membrane vesicles to the same levels of glycinol resulted in the leakage of accumulated $^{14}\text{[C]}$ methyl-glucoside-6-phosphate. Glycinol also inhibited membrane transport of labelled lactose or glycine. All the membrane-associated processes examined were impaired by glycinol, suggesting that glycinol acts as a nonspecific membrane antibiotic, similar to polymixin B, altering the structural integrity of the membrane, and interfering with membrane-dependent processes.

In the same study, glyceollin and coumestrol, two other soybean PAs, were shown to have similar effects on membrane-dependent activities.

Glyceollin also was shown to inhibit mitochondrial electron transport of soybean and corn mitochondria in a manner similar to rotenone, acting at site I (between NADH dehydrogenase and coenzyme Q) (23).

Phaseollin, an isoflavonoid PA produced by beans (*Phaseolus vulgaris*) caused loss of membrane integrity in the tonoplast of beet root protoplasts and cultured bean cells. Electrolytes were lost from beet root tissue following exposure to phaseollin (24). Phaseollin also inhibited O_2 uptake by bean suspension culture cells (25).

Capsidiol is a sesquiterpenoid phytoalexin produced by pepper (*Capsicum annuum*) in response to fungal infection. When isolated membranes of *Phytophthora capsici*, a parasitic fungus of *C. annuum*, were incubated with capsidiol, they underwent marked compositional changes, losing up to half of the membrane proteins and undergoing changes in phospholipid composition (26).

These reported mechanisms of toxicity all relate to effects on membrane proteins or membrane integrity. Electrolyte leakage or loss of activity of membrane proteins (including mitochondrial membrane proteins) are proposed to account for the toxic effects of these phytoalexins.

Gossypol is a terpenoid compound isolated from pigment glands of cotton, with the same cadinane carbon skeleton as DHC. Gossypol caused an increase in order in the membrane lipid matrix of liposomes, and increased permeability in this system. Gossypol also inhibited the insulin-sensitive transport of glucose into rat adipocytes (27).

Other phenolics have been reported to affect membrane order, function and integrity, including phenol itself (28) and the food preservatives butylated hydroxytoluene (29), and butylated hydroxyanisole (30).

Photo-activation and Photo-oxidation

Bakker *et al.* reported the photoactivation of several isoflavonoid phytoalexins, including phaseollin, glyceollin, tuberosin and pisatin. In these experiments, the enzyme glucose-6-phosphate dehydrogenase was inactivated by the PAs upon UV-irradiation. Phaseollin and pisatin gave rise to EPR signals when irradiated by UV light. (31).

Gossypol is also reported to be photo-activated, causing damage to animal cells when irradiated by light (32).

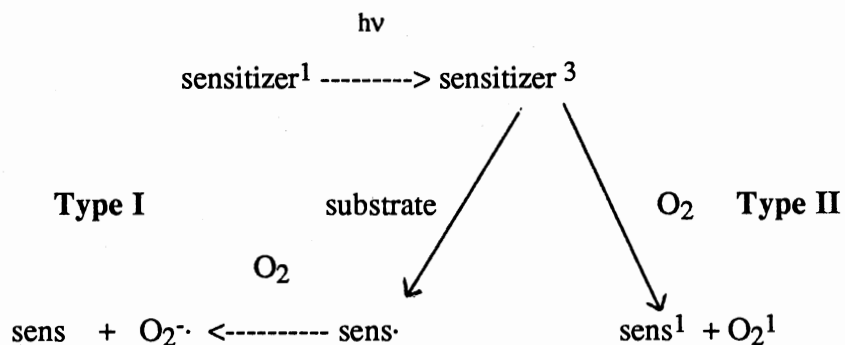
The only other report of photo-activation of a phytoalexin is the study by T. J. Sun, on DHC. Sun noted that the antibacterial action of DHC was stimulated by light, and that DHC inactivated malate dehydrogenase and nicked DNA upon irradiation (33).

Cercosporin, a nonspecific fungal toxin, produced by members of *Cercospora*, has been demonstrated to sensitize cells to visible light (34). In the presence of light, cercosporin generated both singlet oxygen and superoxide anion, leading to killing of suspension culture tobacco cells. The toxicity was reduced by DABCO and bixin, which react with singlet oxygen (35).

Photoactivation of compounds with extended systems of conjugated double bonds is a common phenomenon, and all three cotton phytoalexins, and HMC (the 7-methyl ether of DHC), would appear to be candidates for photochemical activation.

Photodynamic action resulting in stimulated toxicity is frequently mediated by interaction of the photo-excited compound (often called a sensitizer) with O_2 in an energy transfer to generate the highly reactive singlet oxygen state [type II reaction].

Fig. 1 Types I & II Photosensitization Reactions



Alternatively, the excited-state sensitizer (probably a triplet state) may interact with some substrate capable of donating an electron or hydrogen, to generate a free radical. This free radical may react further with O_2 , generating $O_2^{\cdot-}$. Good substrates for this reaction are electron-rich or have easily abstractable hydrogens, e.g., aromatic amines,

phenols and sulfhydryl compounds. Note that DHC may possibly act both as photosensitizer and as (a second molecule) substrate in this pathway.

A competition exists between Type I & II reactions, with the balance dependent on the concentration of substrate and oxygen, and presence of a reasonable substrate for singlet oxygen, as well as the relative efficiencies of the two photochemical reactions.

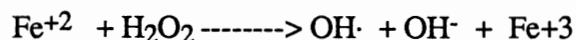
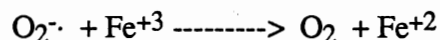
Reactive Oxygen Species

Singlet oxygen is metastable, with a lifetime varying from 4 μ sec, in water, to 25 to 100 μ sec in nonpolar organic media (36) which are reasonable models for lipid membrane environments. The O_2^1 molecule is highly reactive, adding to electron-rich organic molecules to give peroxides or other oxidized products (37). If singlet oxygen fails to react with an appropriate substrate, it returns to ground (triplet) state. It is quite selective. The major sites of cellular damage by singlet oxygen are membranes (lipid peroxidation) and nucleic acids (destruction of guanine).

Superoxide anion, which may be generated by a photosensitizer in a type-I reaction, readily undergoes electron-transfer with many compounds, either as a reductant, or as an oxidant. In organic solvents (or in the lipid milieu of the membrane), $O_2^{\cdot-}$ is a powerful base and nucleophile (38). In aqueous solution, it is far less reactive, acting as a reductant and undergoing the dismutation:



The Fenton reaction shows a mechanism for generation of OH^{\cdot} when $O_2^{\cdot-}$ is present with traces of Fe^{+3} (or other reducible metal ion):



The hydroxyl radical is the most damaging of the reactive oxygen species in aqueous solutions. It is highly reactive, relatively nonselective, and relatively stable (compared to singlet oxygen or superoxide). Hydroxyl radical may abstract a hydrogen atom, leading to

secondary radicals of ethanol (39) and DNA (40). Addition to double bonds by OH· radical occurs readily, and several amino acids react very rapidly with OH·, including histidine, methionine and tryptophan (41).

Confirmation or identification of reactive oxygen species is complicated by their extreme reactivity and short lifetimes. The presence of one form of reactive oxygen in a complex aqueous system is almost certain to lead to production of other reactive oxygen species.

Strategy of Scavenging and Quenching Reactive Oxygen

One strategy for inferring the presence of reactive oxygen species in complex systems is use of a list of compounds capable of quenching or scavenging these species. If the quenchers successfully block the effect suspected to be due to reactive oxygen, then more explicit evidence (such as an epr signal) will help to confirm the presence of the reactive oxygen.

Compounds which quench a species are not consumed in the interaction. Scavengers react very readily with the reactive oxygen, competing with the site of biological damage. The scavengers may themselves then form a stable free radical, not highly reactive with other compounds.

Compounds reported to quench or scavenge singlet oxygen are: β -carotene (42), DABCO (43), histidine, and vitamin A compounds (44).

SOD, with catalase, can be used to scavenge O_2^- .

Hydroxyl radical is scavenged by ethanol, Na-benzoate (45), mannitol (*ibid*), and urea.

Removal of iron salts from the medium should be done with a chelator which inhibits redox reactions of the bound Fe. Desferrioxamine, DTPA and bathophenanthroline sulfonate are effective inhibitors (46).

Some scavengers react with a variety of free radicals, including, but not confined to $\text{OH}\cdot$. AET and α -tocopherol are among the most effective of these, although α -tocopherol has very limited water solubility.

CHAPTER III

SYNTHESIS OF 2,7-DIHYDROXYCADALENE; OXIDATIVE REARRANGEMENT OF SUBSTITUTED ARYLALKYL KETONES WITH THALLIUM (III) NITRATE

Joy Steidl¹, E. J. Eisenbraun¹ and Robert D. Stipanovic²

¹Depts of Biochemistry and Chemistry, Oklahoma State University, Stillwater, OK
74078

²Cotton and Grain Crops Research Laboratory, U.S. Department of Agriculture,
Agricultural Research Service, P.O. Drawer JF, College Station, TX 77841

INTRODUCTION

2',7' dihydroxycadalene (DHC) is one of a group of sesquiterpenoids synthesized by resistant cotton lines in response to infection by *Xanthomonas campestris* pv. *malvacearum*, the causative agent of bacterial blight of cotton (1). DHC has the most potent antibacterial activity of the sesquiterpenoids found in the responding resistant tissue, and has recently been shown to undergo photostimulation in its biological activity (2). The mechanism of toxicity is unknown, as is its cellular site of action. In order to inquire into these properties, a synthesis of DHC for biological testing was undertaken.

Teresa *et al.* (3) reported a pathway for synthesis of 2-hydroxy 7-methoxy cadalene (HMC), (Fig. 1) starting either from limonene **2** or carvone **10**. HMC can be demethylated to produce DHC. This route, however, included a hydroboration reaction, using 9-borabicyclo[3.3.1]nonane (9-BBN). Since gram quantities of the final product were desired, and the hydroboration is the initial step, large-scale reactions with 9-BBN would be needed. A large-scale hydroboration, with its concomitant risk of fire, seemed unnecessarily hazardous, and an alternate route was proposed by R. D. Stipanovic (Fig. 2) (4).

RESULTS AND DISCUSSION

The initial reaction, nitration of 4'-methyl propiophenone, proceeded readily in good yield and with high specificity. This was dependent on carefully maintaining the reaction mixture at -20° or below throughout the addition of H₂SO₄/HNO₃.

Reduction of the nitro group was attempted using first Raney nickel, then Pd/C as catalyst in a Parr shaker. Yields were poor, and recovery of product was difficult. The three-step conversion of an aromatic nitro group to a phenol described by R. B. Woodward (5) was carried out on the 3'-nitro,4'-methyl propiophenone **14**. This group of reactions had the advantages of being carried out rapidly in sequence and, for the diazotization and hydrolysis reactions, of proceeding well on unpurified products. The

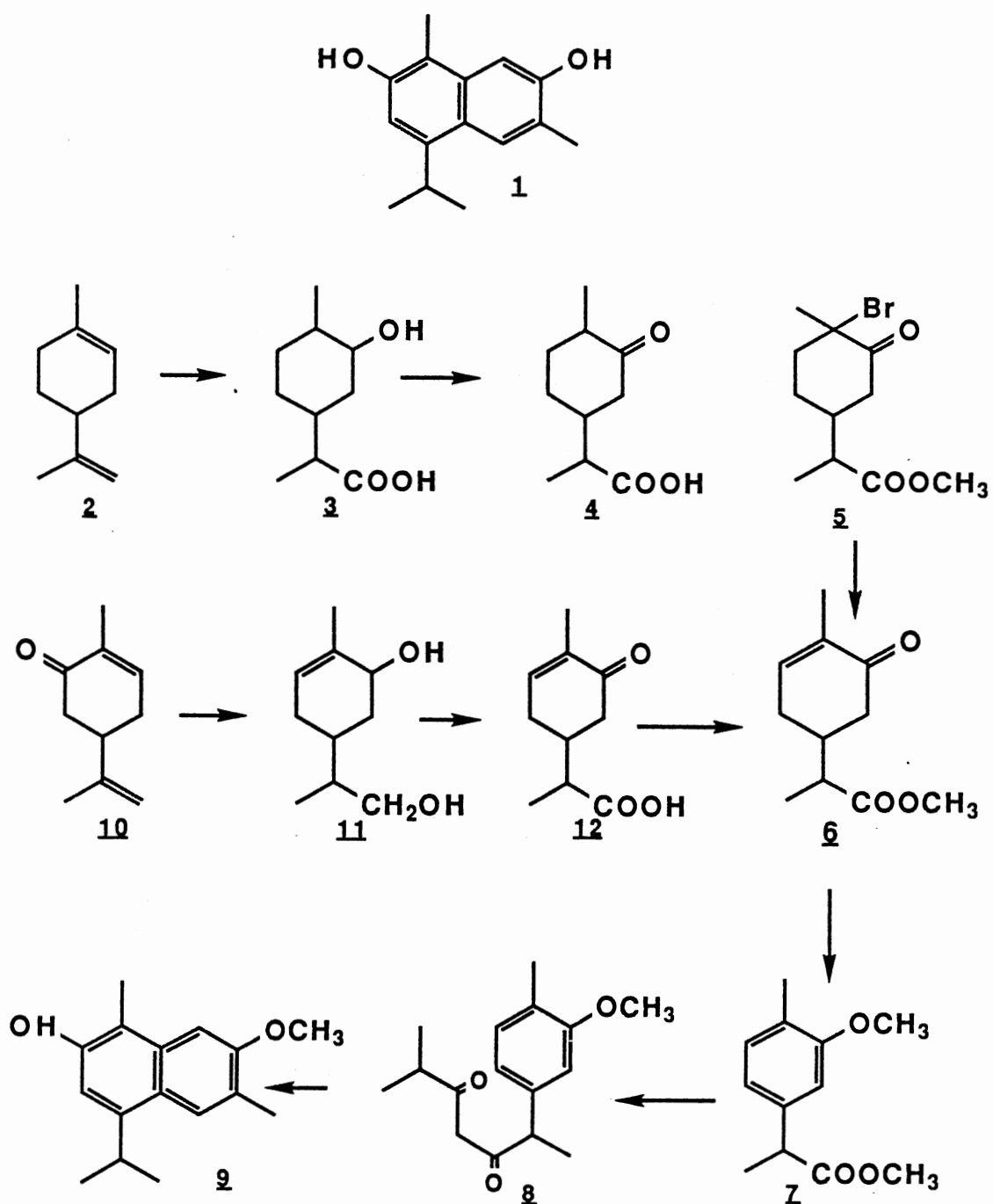


Fig. 1 Synthesis of 2,7-Dihydroxycadalene by the Method of Teresa *et al.* (3).

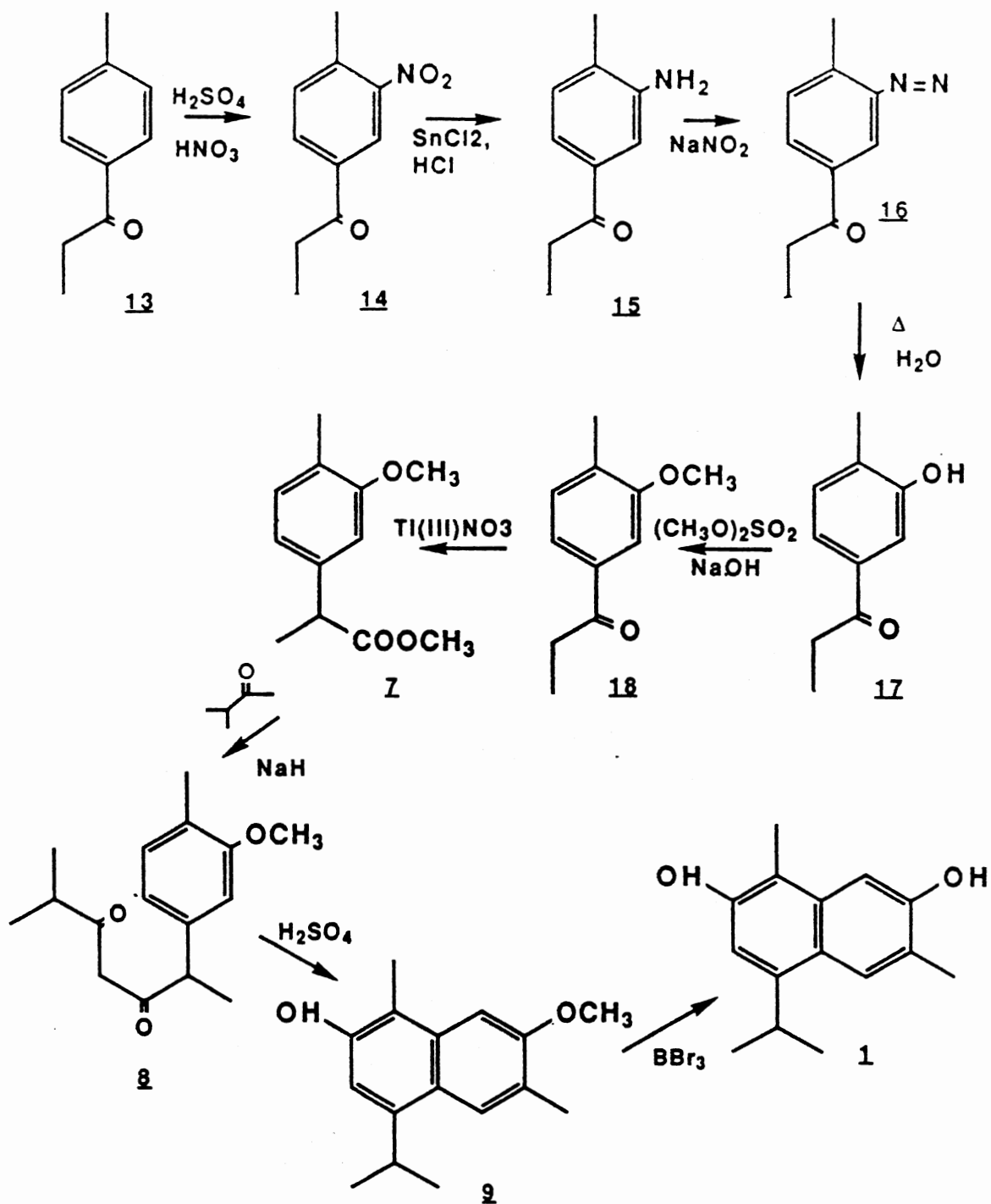


Fig. 2 Synthesis of 2,7-Dihydroxycadalene by the Method of Stipanovic and Steidl (4).

presence of a phenol in the final product was confirmed by a bathochromic shift in the absorption spectrum at the 310 nm peak, when the spectrum was taken in alkaline ethanol. The presence of the phenol, **17** in subsequent batches was confirmed by strip TLC.

Without purification the phenol was methylated using the method of Icke *et al.* (6) to give 3'-methoxy, 4'-methyl propiophenone **18**. A complete extraction of the product **18** was most consistently achieved by checking the pH of the reaction mixture, and adjusting to pH 11, if necessary. The methoxy propiophenone **18** was purified in good yield by vacuum distillation.

The thallium (III) nitrate (TTN) rearrangement of alkyl aryl phenones to form α -substituted phenylacetates described by Taylor *et al.* (6) facilitated by an acidic montmorillonite clay catalyst (K-10 clay) was used to convert **18** to the α -methyl ester **7**, but without success. Throughout repeated attempts with some variation of conditions, the reaction either failed to proceed at all, and starting material was recovered, or almost 100% of the rearranged ester recovered was nitrated on the aromatic ring. The predominance of nitrated products was detected by ^1H NMR and confirmed by mass spectroscopy. The ^1H NMR of the aromatic protons of the nitrated ester, shown in Fig. 3, indicates a major product with nitration at either the 5' or 6' position, and a minor product nitrated at the 2' carbon. This mixture gave prominent mass spectral peaks at $m/e = 252, 238, 222, 207$ and 194, indicating the presence of a single nitro group on the aromatic ring of the α -methyl ester.

The reaction was also attempted, without the K-10 catalyst, with trimethylorthoformate (TMOF) in methanol (see method C, in experimental section), essentially according to Taylor *et al.* (7). Under these conditions, the desired rearrangement proceeded more consistently, but a nitro group appeared on all of the recovered ester. The report of Taylor *et al.* (6) described successful rearrangements of a variety of alkyl phenones, (Fig. 4), with unsubstituted or *p*-substituted rings. *Ortho*-substituted

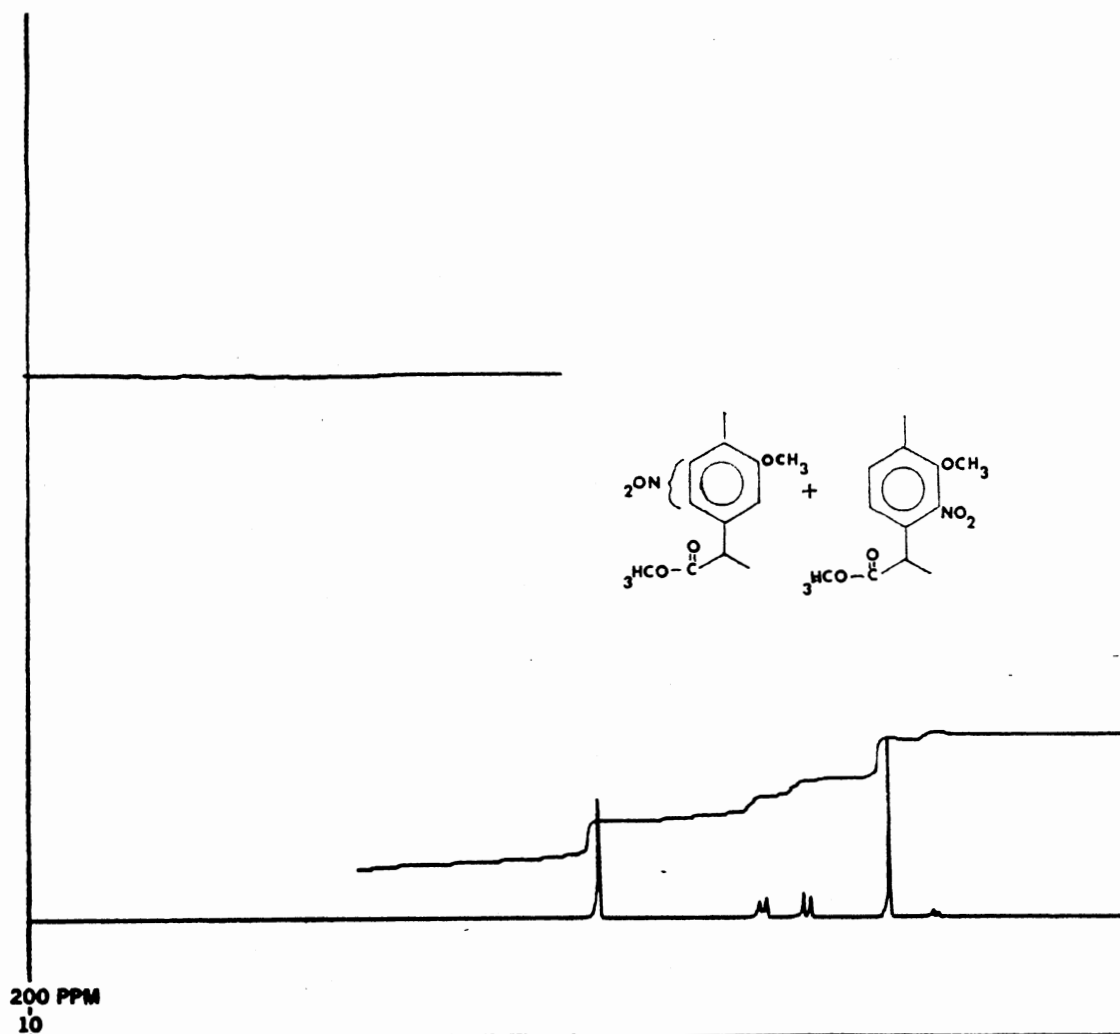
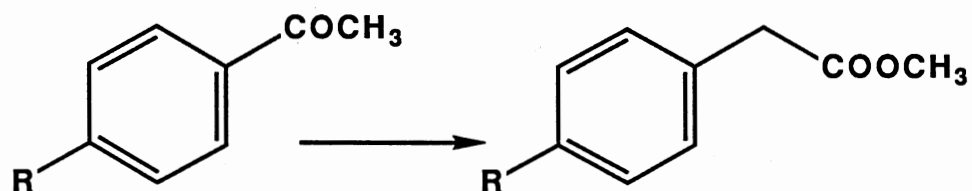


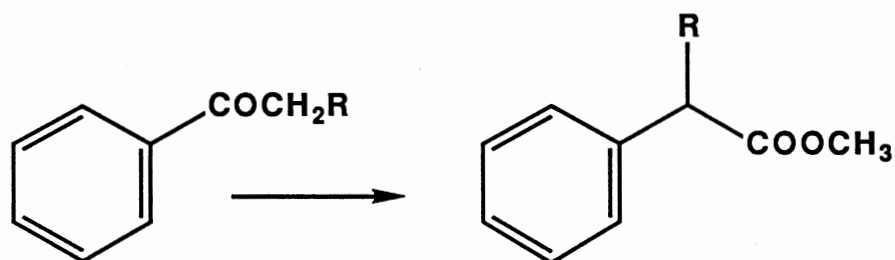
Fig. 3 ¹H NMR Spectrum, Detail of Aromatic Region, of Nitrated Ester. Methyl 2-(3'-methoxy-4'-methylphenyl)propionate with mixed nitration on aromatic ring, product of TTN oxidative rearrangement, experimental method C. Spectrum taken in CDCl₃.

propiophenone rearrangements have been reported (8), and one successful rearrangement of a *meta*-substituted acetophenone has been described (9).

Figure 4. Thallium (III) Nitrate Oxidative Rearrangements of Alkyl Phenones



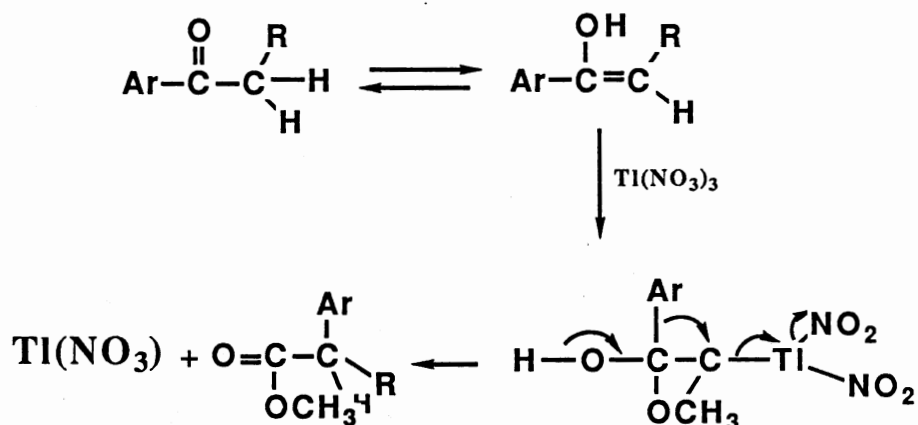
$R = H, CH_3, CH_3, F, Br$



$R = CH_3, C_2H_5$

Two reports (7,10) mention the importance of formation of an enol intermediate from the ketone in the reaction mechanism. McKillop *et al.* (8) proposed the mechanism shown in Fig. 5 for the oxidative rearrangement by TTN.

Figure. 5 Proposed Mechanism of Thallium (III) Oxidative Rearrangement of Alkyl Phenones



The electron-withdrawing *m*-methoxy group of **18** may inhibit formation of the enol intermediate, while slightly activating the aromatic ring toward nitration. A third method reported for oxidative thallium rearrangements uses HClO_4 (**8**), presumably as an acid catalyst, to assist enol formation. McKillop *et al.* described a mixture of products from the oxidative rearrangement of propiophenone under these conditions, with the major products being α -methyl phenylacetate (45%) and α -methoxypropiophenone (32%).

We attempted the 4'-methyl-3'-methoxy propiophenone rearrangement under these conditions (described in the experimental section) and found that the reaction proceeded smoothly, although more slowly, with high yields and no detectable nitration. ^1H NMR of the product, (Fig. 6) showed the expected proton pattern in the aromatic region for the three aromatic protons.

Since nitration is a potentially useful starting point for addition of functional groups to an aromatic ring, three methoxyacetophenones and a bromoacetophenone were tested with TTN, using method C (Fig 7) to determine if nitration is a general side reaction under these circumstances. 3',4'-dimethoxyacetophenone rearranged slowly, with a very low yield and was not nitrated under these conditions. The other three acetophenones

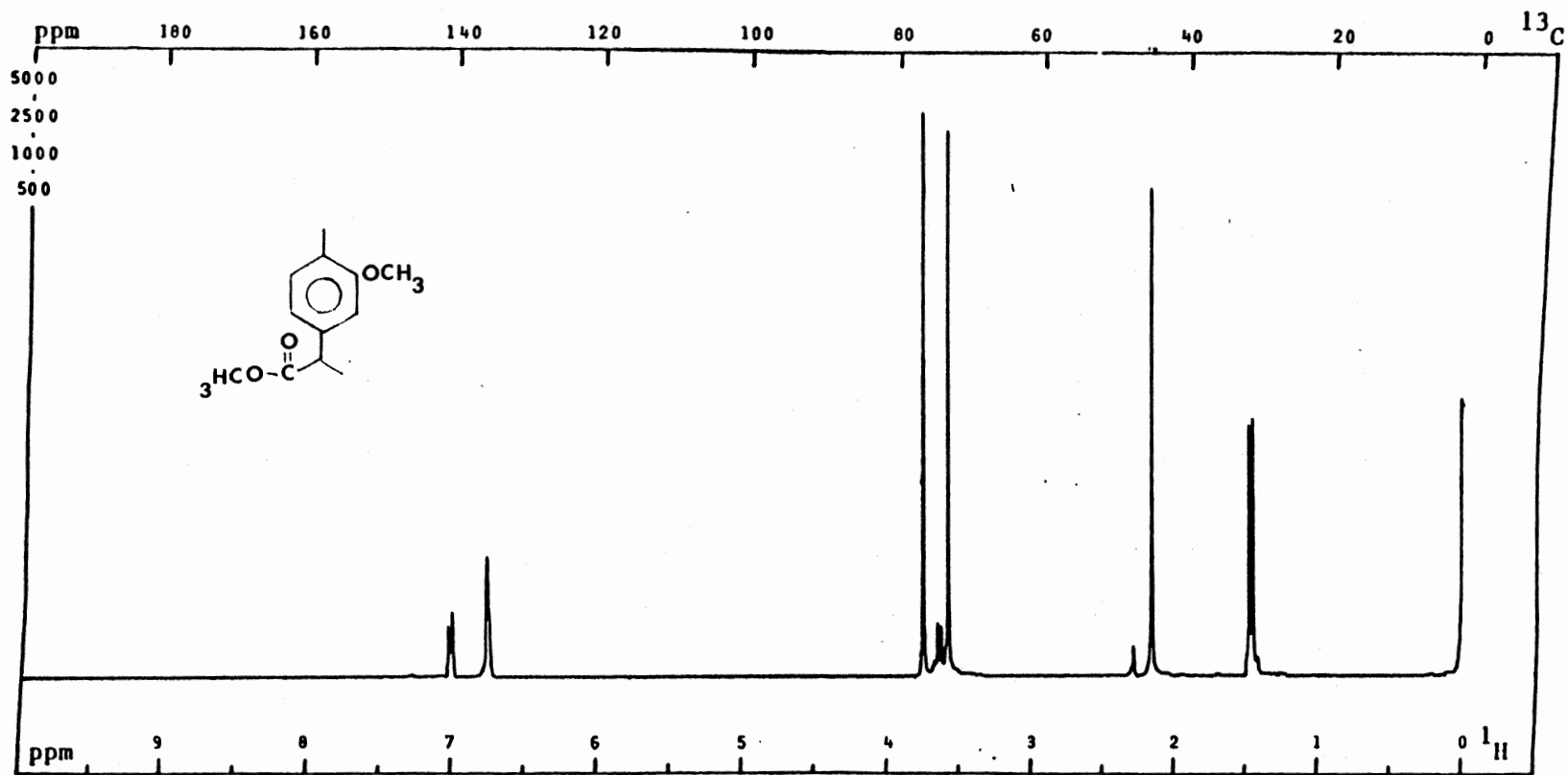
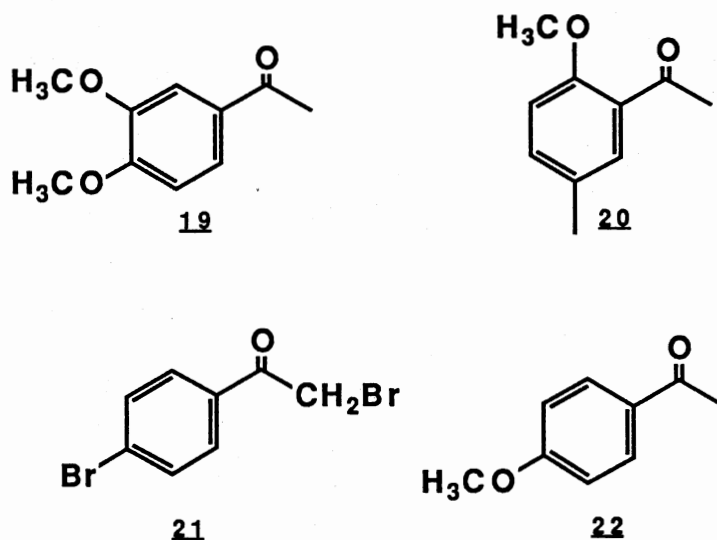


Fig. 6 ^1H NMR Spectrum of Methyl 2-(3'-methoxy-4'-methylphenyl) propionate. Ester product of TTN oxidative rearrangement by TMOF/ HClO_4 method. Spectrum in CDCl_3 .

rearranged readily, and only 2'-methoxy-5'-methylacetophenone underwent any nitration of the aromatic ring. The nitrated methyl phenylacetate was a minor product, as seen on the ^1H NMR spectrum (not purified).

Figure 7 Substituted Acetophenones Used for Thallium (III) Nitrate Oxidative Rearrangements



Thus nitration is not a general side reaction with TTN oxidative rearrangement, but should be considered as a possibility when electron-withdrawing groups are present on the aromatic ring of an alky phenone.

The ester produced by the rearrangement was used to alkylate methyl isopropyl ketone in a condensation reaction carried out according to Miles *et al.* (11). Specificity of enolate alkylation in this reaction is maintained by 1) adding excess ester relative to the ketone, and 2) adding the pre-mixed reactants slowly to the hot base solution. The first point helps inhibit ketone self-condensation, and the second helps ensure a kinetic, rather than thermodynamic, distribution of enolate anion, to give alkylation chiefly at the α -

methyl carbon rather than the tertiary carbon of the isopropyl group. The excess ester was recovered during the work-up in the acid form, esterified with diazomethane, and used later.

Since this condensation reaction is the last step at which additional carbons were introduced into the cadalene synthesis, it was considered as a possible point of introduction of a ^{14}C label into DHC. Several attempts to synthesize a methyl isopropyl ketone using starting materials which are commercially available with ^{14}C labels were made, including a Grignard reaction and a lithium/alkyl chloride substitution. Yield and recovery were prohibitively poor in all methods attempted.

The route to DHC synthesis described here proceeds with excellent or satisfactory yields at all steps, with the exception of the final demethylation. At this step, the tendency of DHC to decompose in air poses extreme problems with the purification and work-up, leading to low yields. Improvement of the purification methods at this step would greatly enhance the yield of this pathway, which, in terms of speed, simplicity, and yield at all other steps, is the best available.

EXPERIMENTAL

Synthesis of 2,7-dihydroxycadalene

Nitration of 4' methylpropiophenone

In a typical batch reaction, 164 mL of concentrated H_2SO_4 was pre-cooled in an alcohol bath to $-30\text{ }^\circ\text{C}$, and 80 mL 4' methylpropiophenone was added to the H_2SO_4 from a syringe, with mechanical stirring. A mixture of 43.7 mL concentrated HNO_3 and 65.5 mL concentrated H_2SO_4 was cooled on ice, placed in a dripping funnel, and added to the cooled H_2SO_4 and phenone in a very slow drip, with constant mechanical stirring. The rate of addition was regulated to keep the reaction mixture at $-25\text{ }^\circ\text{C}$ ($\pm 5\text{ }^\circ\text{C}$). The solution became highly viscous during the reaction. Addition was completed in

approximately 4 hours, and stirring was continued for an additional 15 minutes. The mixture was removed from the cooling bath, allowed to warm briefly, then poured into 2.5 L of a slurry of ice and water, with rapid stirring. The aqueous mixture was filtered on Whatman 52 filter paper, and the yellow-white crystals were washed with 3 L of distilled water.

The crystals were dissolved in 300 mL of methanol, with gentle heat, and the hot solution was rapidly filtered. The solution was cooled in the refrigerator, and the resulting crystals were collected by vacuum filtration on a chilled funnel, with two rapid washes using methanol pre-chilled to 0°C. Melting point of the crystals was 47-49° C. A second and third crop of crystals were collected in the same manner. The yield of first-crop crystals was 40 - 41% (in three different batches). The yield of combined crystals was 61 - 69%. ¹H NMR [as reported (4)], in CDCl₃, δ = 1.27 (3H, t, CH₃); 2.69 (3H, s, Ar-CH₃); 3.04 (2H, q, CH₂); 7.47 (1H, d, ArH); 8.10 (d of d, J=7.9 Hz and J=1.7 Hz, 1H, ArH); 8.54 (1H, d, J=1.7 Hz, ArH).

3'-Hydroxy 4'-methylpropiophenone

A solution of 176.6 g of powdered SnCl₂·H₂O in 235.5 mL concentrated HCl was prepared and cooled to 5°C on ice, with mechanical stirring. 3'-nitro-4'-methylpropiophenone, 50 g, was added in one portion. The ice bath was removed, and the reaction mixture was heated briefly to initiate reaction. The temperature rose rapidly to 100°C, and the solution was allowed to cool slowly on an asbestos pad, with very slow mechanical stirring. When the solution cooled to room temperature, the vessel was placed in an ice bath and maintained at 5 °C, with slow stirring for an additional 2 hours. The mixture was then filtered on sintered glass, and the damp precipitate was added to 235.5 mL concentrated HCl and cooled on ice to 0-5 °C. A dripping funnel was arranged with its tip extended below the surface of the solution, and a solution of 18 g NaNO₂ in 58.9 mL of H₂O was dripped in slowly, maintaining the reaction temperature at 4-5 °C. Stirring

was continued on ice for 1 hour following addition of the NaNO_2 , then the solution was filtered on sintered glass.

The damp precipitate was added cautiously, in small portions to 667 mL boiling water in a 2 L Erlenmeyer flask. Vigorous frothing followed each addition. Boiling was continued 5 minutes after addition was complete.

Filtration was used to collect the product in the initial batches, but was extremely slow. Later batches were extracted into ether, and a brown oil collected when the ether was removed by evaporation. In neither case were further attempts made to purify the phenol. Absorption spectra of a dilute solution of the product in neutral ethanol showed absorption peaks, $\lambda_{\text{max}} = 310 \text{ nm}$, 258 nm . In ethanol with one drop N NaOH , the peaks were shifted: $\lambda_{\text{max}} = 358 \text{ nm}$, 244.5 nm . Ethanol with one drop N HCl gave a spectrum with peaks at $\lambda_{\text{max}} = 310 \text{ nm}$ and $\lambda_{\text{max}} = 259.5 \text{ nm}$. Estimated (crude) yields of the three-step reaction: 50 - 74%.

3'-Methoxy-4'-methylpropiophenone

3'-hydroxy-4'-methylpropiophenone (35.13 g, crude, prepared as described above) was added to 180 mL 2N NaOH warmed in a three-neck flask with N_2 bubbled through. The solution was stirred in a water bath at $40 \text{ }^\circ\text{C}$, until it became homogeneous. Dimethyl sulfate (30 mL) was added slowly from a dripping funnel. Following the addition, the solution was stirred an additional 5 minutes, then 90 mL 2N NaOH was added in one portion with stirring, followed by a second slow addition of 15 mL of dimethyl sulfate. The solution was stirred at $50 \text{ }^\circ\text{C}$ for 30 minutes after all additions, then allowed to cool, and extracted three times with diethyl ether.

The ether solution was washed three times with dilute HCl , water, and saturated NaCl , respectively, then dried (Na_2SO_4), filtered and evaporated. TLC was used to check both aqueous and organic fractions, and unreacted phenol was recovered from the aqueous layer in some batches by acidifying and extracting with ether. The oil extracted

into the ether phase was vacuum distilled, collected at 130°C and 20 mm. Yields were 90 - 92%. ¹H NMR, in CDCl₃ [as reported (4)], δ = 1.24 (3H, t, CH₃); 2.28 (3H, s, Ar-CH₃); 3.00 (2H, q, CH₂); 3.91 (3H, s, OCH₃); 7.20 (1H, d, ArH); 7.45 (1H, s, ArH); 7.46 (1H, d, ArH).

Methyl 2-(3'-methoxy-4'-methylphenyl)-propionate

3'-methoxy-4'-methylpropiophenone (16.32 g) was dissolved in 229 mL methanol and 229 mL trimethyl orthoformate; 70% HClO₄ (22.9 mL) was added, and the solution was stirred at room temperature for 1 hour. Thallium (III) nitrate [Tl(NO₃)₃·3H₂O] was added in one portion of 48.87 g, and the solution was stirred for 24 hours at room temperature. The white precipitate (probably Tl(I)NO₃) was allowed to settle, and the orange solution was carefully decanted. The precipitated Tl(I)NO₃ was washed with CH₂Cl₂ until all color was rinsed away. (NOTE: Thallium is highly toxic, and was disposed of as a toxic waste).

An approximately equal volume of H₂O was added to the methanol solution, and the H₂O/MeOH phase was extracted with CH₂Cl₂ four times, or until no color remained in the aqueous phase. The CH₂Cl₂ phases were combined, and washed three times, once each with NHCl, H₂O, and saturated NaCl, in order, and evaporated under reduced pressure to give a light brown oil. This oil was purified by vacuum distillation to give the ester - (b.p. 93°C, 0.4 mm Hg), yields 88-96%. ¹H NMR, in CDCl₃, δ = 1.46 (3H, d, CH₃); 2.16 (3H, s, ArCH₃); 3.69 (3H, s, OCH₃); 3.65 (1H, q, CH); 3.77 (3H, s, OCH₃); 6.76 (1H, d, ArH); 6.80 (1H, s, ArH); 7.03 (1H, d, ArH).

2,6-dimethyl- 6 (3'-methoxy, 4'-methylphenyl)-3,5-heptadione

Rigorously anhydrous conditions were maintained throughout this alkylation. Glassware was dried at 150 °C overnight, assembled while hot, and flushed immediately with a N₂ stream which was fitted with a drying tube of molecular sieves. Methyl

isopropyl ketone was stored over molecular sieves, as was the solvent, glyme, which had been distilled over CaH_2 . A 3-neck flask was equipped with a condenser, mechanical stirrer and a side-arm dripping funnel. N_2 flow was established, exiting through the condenser. Following assembly, the apparatus was warmed with a heat gun to drive off any remaining moisture. In the side arm dripping funnel, 20.2 g of methyl 2-(3'methoxy-4'methyl) propionate and 8.3 mL of methyl isopropyl ketone were mixed, but not initially allowed to drip into the flask.

Glyme (150 mL) and 9.34 g of dry NaH were placed in the flask, and the slurry was warmed with a heating mantle while stirring to reflux. When reflux was established a slow drip of the ester-ketone mixture in the funnel was begun. Complete addition took 1 hour, and the reaction was stirred while refluxing under N_2 for 6 more hours. The heating mantle was then removed, and an ice bath installed. After allowing the mixture to cool, 150 mL cold water (from an ice/water slurry) was dripped in from the funnel, pausing between drops at first to allow H_2 evolution to subside.

The reaction mixture was extracted three times with ether, and the pooled ether extracts were washed twice with H_2O and once with 1% NaOH. The ether layers were dried (MgSO_4), filtered and evaporated under reduced pressure, to give a light yellow oil; crude yield, 68% (based on ketone).

The aqueous extracts were combined, neutralized with HCl, and extracted with ether to recover unreacted 2(3'methoxy-4'methyl) propionic acid. The acid was later esterified with diazomethane for use in later alkylation batches.

The diketone was purified on a Silica-R-CC-7 gel column, 3 cm x 50 cm. The column was packed dry with constant tapping. The crude dione (16.9 g) was adsorbed on 20 g of Silica-R in a minimal volume of benzene. The slurry was evaporated slowly on a solvent stripper. Rotation was very rapid, and the flask was not warmed in the water bath until evaporation was nearly complete. Drying was complete in 2 hours, and the free-flowing light yellow powder was loaded on the top of the clean Silica-R column, and

tapped extensively to ensure smooth packing. A cap of approximately 2 cm of clean sea sand was carefully packed on the top.

Pure hexane was loaded on top of the dry column and flow was established, with 7 mL fractions being collected by a fraction collector (Isco Retriever II). After approximately one column volume of hexane was collected (350 mL), the head was drawn off, and the reservoir was filled with hexane : ether 90:10. This mixture was allowed to flow through the column until approximately two column volumes were collected. The position of peaks of the dione and contaminating compounds in the fractions was monitored by a hand-held uv lamp, and spot-checked by strip TLC. Like fractions were pooled, concentrated, and identified by nmr. ^1H NMR, in CDCl_3 , δ = 1.08 (6H, d, CH_3); 1.47 (3H, d, CH_3); 2.18 (3H, s, ArCH_3); 2.38 (1H, heptet, CH); 3.61 (1H, q, CH); 3.80 (3H, s, OCH_3); 7.50 (2H, s, CH_2); 6.77 (1H, d, ArH); 6.76 (1H, s, ArH); 7.06 (1H, d, ArH).

2-Hydroxy-7-methoxycadalene

The dione **8** (2.002 g) was weighed into a round-bottom flask containing a stirring bar. Concentrated H_2SO_4 (3.75 mL) was pipetted in, and the resulting deep reddish brown mess was stirred for 15 minutes at room temperature. An excess of an ice/water slurry was added, stirred, and extracted with CH_2Cl_2 . Saturated NaCl was added to the aqueous layer, which was extracted a second time with CH_2Cl_2 , then once with hexane. The combined organic layers were washed with brine, dried (MgSO_4), filtered, and the concentrated by evaporation. The reddish crystals were redissolved in a small quantity of ether, and recrystallized with a hexane/ether system. The first crop of white crystals had a melting point of 168-169°C, yields 38-48%. ^1H NMR, in CDCl_3 , δ = 1.35 (6H, d, CH_3); 2.40 (3H, s, OCH_3); 2.44 (3H, s, ArCH_3); 3.66 (1H, heptet, CH); 3.98 (3H, s, OCH_3); 4.77 (1H, s, ArOH); 6.86 (1H, s, ArH); 7.13 (1H, s, ArH); 7.81 (1H, s, ArH).

Low purity crops of crystals were combined and purified on a small column of acidic alumina packed in hexane.

2,7-Dihydroxycadalene

The glassware, stirring bar, and syringe used in this reaction were pre-dried in an oven overnight (150°C) and cooled to room temperature in a dessicator. One gram of 2-hydroxy-7-methoxy cadalene (HMC) was weighed, placed in a two-neck 100 mL round bottom flask with a stirring bar, and 60 mL of CH₂Cl₂ (stored over molecular sieves) was added. Gentle warming in a water bath was needed to dissolve the HMC. In some batches, a small volume of CHCl₃ was added to assist solvation. N₂ flow was established, entering through a needle in a septum and exiting via an adapter, and an isopropanol/dry ice bath was placed around the flask.

After 10 minutes of cooling, 3.78 mL BBr₃ was added to the flask via syringe through the septum. All subsequent steps in the reaction, work-up and purification were carried out under very low light or under special blue-deficient lights. The solution was allowed to stir for a few minutes, then the dry ice bath was removed, and the solution was stirred at room temperature for 1.5 hours. The reaction was then terminated by cautiously adding ice-water, pausing to allow brief, violent frothing to subside. When no frothing occurred upon further addition of water, the white solution was stirred for an additional 30 minutes.

The following work-up was done as quickly as possible due to the tendency of DHC to oxidize in the air. Glassware and solutions were arranged in advance. The reaction mixture was added to 50 mL H₂O in a separatory funnel, shaken, and the CH₂Cl₂ layer was removed. The aqueous layer was extracted three times with ether, and the combined organic layers were dried over anhydrous MgSO₄ and filtered. The solvent was then evaporated at reduced pressure with only sufficient warming of the flask to prevent ice

formation. The crude product was stored under argon in the freezer. Estimated (crude) yield: 47%.

DHC was purified on a Silica-R column, 1.5 x 50 cm. The crude DHC was washed on with 100% hexane. Successive washes of the column with hexane : ether solvent systems with increasing proportions of ether [hexane:ether, 90:10, to 50:50 (v/v)] were used to elute the DHC, which was monitored by its fluorescence under a hand-held uv lamp. A bright-red contaminant closely followed the DHC in elution and was a useful visible marker. DHC was recovered from the solvent fraction by evaporation under reduced pressure and identified by nmr. ^1H NMR, in CDCl_3 , δ = 1.35 (6H, d, CH_3); 2.40 (3H, s, ArCH_3); 2.43 (3H, s, ArCH_3); 3.65 (1H, heptet, CH); 4.87 (1H, s, ArOH); 5.16 (1H, s, ArOH); 6.86 (1H, s, ArH); 7.81 (1H, s, ArH). Yield of pure DHC: 2 - 7%.

Thallium (III) Nitrate Oxidative Rearrangements

A) The oxidative rearrangement conditions optimized to exclude nitration were carried out as described above under methyl 2-(3'-methoxy-4'-methylphenyl)-propionate.

B) Thallium (III) Rearrangements on K-10 catalyst

The TTN [Thallium (III) Nitrate] was adsorbed onto K-10 clay in the following manner: 46.12 g of clay was dried overnight in a 100°C oven, then added to a flask containing a mixture of 20.5 g TTN, 53 mL TMOF (trimethyl orthoformate) and 42 mL methanol. Precautions were taken to keep all reagents dry, including storage of TTN in a vacuum dessicator, and storage of methanol and TMOF over dried molecular sieves. After being stirred for 5 minutes, the clay slurry was placed on a rotary evaporator, and dried for 2 hours under reduced pressure, using a 70°C water bath to warm the flask. Recovery was 71.44 g, with an estimated 0.64 mmoles TTN per gram reagent clay.

The TTN/K-10 reagent was added to an approximately equimolar amount (based on estimated TTN quantity) of the alkyl aryl ketone to be rearranged, in either heptane or methylene chloride. The suspension was stirred until the reaction was complete, as

monitored by either 1) a negative starch iodide paper test [for thallium (III)] or 2) a negative DNPH reaction with the major spot on a small test TLC strip. The suspension was then filtered, and the clay was washed several times with heptane (or CH_2Cl_2). The organic phase was washed with saturated NaHCO_3 , then water, dried over anhydrous MgSO_4 , and evaporated. The resulting product was purified by recrystallization or chromatography on a small basic alumina column. The spent thallium/K-10 reagent was dried and disposed of as toxic waste.

C) Thallium-Induced Rearrangement in Methanol

A mixture of TTN (6 mmoles, 2.7 g), TMOF (25 mmoles, 2.74 mL) and 13 mL methanol was gently warmed in a round-bottom flask fitted with a condenser. After a few minutes, the alkyl aryl ketone (5 mmoles) was added, and the solution was stirred at $55\text{ }^\circ\text{C}$ for 1 hour. The white precipitate was allowed to settle, and the solution to cool to room temperature. The clear solution was decanted, and the precipitate was washed twice with CH_2Cl_2 . The organic layers were combined and extracted with water. The water extract was shaken with an equal volume of CH_2Cl_2 , which was drawn off and added to the other organic phases. The combined organic extracts were washed with dilute HCl, and twice with saturated NaCl, then dried over anhydrous MgSO_4 and evaporated on a solvent stripper. The collected product was purified as described in B. The precipitate collected by decanting the reaction mixture was dried and disposed of as toxic waste. The aqueous extracts were allowed to evaporate to check for dissolved thallium.

REFERENCES

1. M. Essenberg, M. Doherty, B. Hamilton, V. Henning, E. Cover, S. McFaul and W Johnson, *Phytopathology*, 72, 1349 (1982)
2. T.J. Sun, M. Essenberg and U. Melcher, manuscript submitted
3. J. deP. Teresa, A. Mateos and R. Gonzales, *Tetrahedron Lett.*, 23, 3405 (1982)
4. R. D. Stipanovic and J. Steidl, *Syn. Comm.*, 16, 1809 (1986)

5. R. B. Woodward, *Org.Syn ., Coll.Vol. 3*, John Wiley and Sons, New York, 453 (1955)
6. R. N. Icke, C. E. Redemann;, B. B. Wisegarver, and G. A. Alles, *ibid*, 564
7. E. C. Taylor, C-S. Chiang, A. McKillop and J. F. White, *J. Am. Chem. Soc.*, 98, 6750 (1976)
8. E. C. Taylor, R. L. Robey, K-T. Liu, B. Favre, H. T. Bozimo R. A. Conley, C-S. Chiang, A. McKillop and M. E. Ford, *J. Am. Chem. Soc.* 98, 3037 (1976)
9. P. Belanger, C. S. Rooney, F. Robinson and L. Sarrett, *J. Org. Chem.* 43, 906 (1978)
10. J. A. Walker and M. Pillai, *Tetrahedron Lett.* 42, 3707 (1977)
11. M. L. Miles, T. M. Harris and C. R. Hauser, *Org.Syn .,Coll. Vol. V*, John Wiley and Sons, New York, 718 (1973)

CHAPTER IV

PHOTOACTIVATED ANTIBACTERIAL ACTIVITY OF PHYTOALEXINS FROM COTTON AND EFFECT OF REACTIVE OXYGEN SCAVENGERS AND QUENCHERS ON PHOTODYNAMIC ACTION OF DHC

Joy Steidl¹, and Robert D. Stipanovic², and Margaret Essenberg¹

¹Department of Biochemistry, Oklahoma State University, Stillwater, Oklahoma, 74078, U.S.A.

²Cotton and Grain Crops Research Laboratory, U.S. Department of Agriculture, Agricultural Research Service, P.O. Drawer JF, College Station, Texas, 77841, U.S.A.

Abbreviations used: DHC, 2,7-dihydroxy cadalene; LC, lacinilene C; LCME, lacinilene C 7-methyl ether; HMC, 2-hydroxy, 7-methoxy cadalene; Xcm, *Xanthomonas campestris* pv. *malvacearum*; SOD, superoxide dismutase; DABCO, diazobicyclo (2,2,2) octane, DTPA, diethylenetriamine pentaacetic acid; MOPS, 3-(N-morpholino) propanesulfonic acid.

ABSTRACT

The antibacterial activity of two phytoalexins (DHC and LC), produced by cotton in response to infection by *Xanthomonas campestris* pv *malvacearum* (Xcm) was markedly stimulated by light. A closely related cotton phytoalexin was not photo-activated. The products of the photodegradation of DHC inhibited Xcm, as did an *ortho*-quinone product of DHC. The photoactivation of DHC was partially prevented by DABCO, a singlet oxygen scavenger.

INTRODUCTION

Part of the resistant response of certain lines of Upland cotton (*Gossypium hirsutum*) to inoculation with incompatible strains of *Xanthomonas campestris* pv. *malvacearum* (Xcm), the causative agent of bacterial blight of cotton, is *de novo* synthesis of a group of sesquiterpenoid phytoalexins (1). Three of these phytoalexins, DHC, LC, and LCME, and a fourth closely related compound, HMC, have been assayed for biological activity toward Xcm. Of the four compounds, DHC is the most toxic toward Xcm. The inhibition of Xcm by DHC is markedly stimulated by light, (300-700 nm) (2), as is that of LC.

Since these compounds are inhibitory in the absence of light, they cannot function solely as photosensitizers, although photosensitized oxidation may be the mechanism of part of their toxic effect. Photosensitizers from plants and plant pathogens have been reported in other systems, and usually generate singlet oxygen and/or superoxide anion (3, 4). The mechanism of toxicity of DHC, which is investigated here, may also involve these or other activated oxygen species, including hydroxyl radical, or other free radical species. Accordingly, this study includes a series of bioassays with various compounds reported to quench or scavenge activated oxygen species: DABCO, bixin, Na-benzoate, SOD, catalase, and vitamin E. Two compounds capable of chelating iron salts were also

tested to probe the possible involvement of Fe^{+2} or Fe^{+3} in generation of activated oxygen.

DHC, LC, and LCME are all sensitive to exposure to light and air. DHC degrades rapidly in light to a group of compounds which have been isolated but not yet identified. In the dark, DHC is also degraded, but forms different products than those seen in the light reaction. Identification of the light products is underway, and the effect of the light degradation products of DHC is reported here.

MATERIALS AND METHODS

Preparation of Phytoalexins

DHC and LCME isolated from cotton were prepared essentially as described (5), except that the solvent used during loading on the Sep-Pak was methanol/water (30:70, v/v). Synthetic DHC used in the first comparison with plant-derived DHC was synthesized by R.D. Stipanovic, by the method of Teresa *et al.* (6). The DHC used in all remaining experiments, and HMC, were synthesized by J. Steidl, as described in Chapter III, this work.

LC was prepared by dissolving 12.96 mg DHC in 3 ml methanol, with addition of 30 ml MOPS medium and 15 ml 10 mM $\text{FeNH}_4(\text{SO}_4)_2$. This solution was covered with foil, and stirred 24 hours at room temperature, with periodic spectral and strip TLC monitoring of the reaction progress. The final mixture was extracted 4 times with approximately 20 ml CHCl_3 and the extract was purified by HPLC essentially as previously described (5).

DHC, HMC, and LCME were also purified by essentially the same reverse-phase HPLC method.

Except where specifically described, the phytoalexins were handled only under blue-deficient light from General Electric F06T12/GO gold fluorescent lamps, or a

Westinghouse 100 Watt bug-a-way bulb. Where possible, the phytoalexin solutions were handled under N₂.

Bioassay Methods

The Xcm used in all bioassays was a streptomycin-resistant mutant of the previously described Race 3 (1).

All bioassays and bacterial culture were carried out in a defined medium, referred to here as MOPS medium, based on that developed by Niedhardt *et al.* (7), and modified by K. McNally *et al.* (8). The amino acids added to the medium, and their concentrations, were: L-alanine, 0.47 mM, L-arginine-HCl, 0.60 mM, L-asparagine, 0.32 mM, L-histidine-HCl, 0.10 mM, L-isoleucine, 0.30 mM, L-threonine, 0.30 mM, and L-phenylalanine, 0.30 mM. Sucrose, at 2.5%, was used as the carbon source.

Inhibitory effects of phytoalexins upon Xcm were bioassayed by determining effects of the phytoalexins upon bacterial cfu/ml in liquid culture. The dark condition in the bioassays was achieved by double-wrapping each bioassay tube to be so treated in aluminum foil. The light condition was provided by a cool-white fluorescent lamp, which emits 300-700 nm radiation (9). Both the dark- and light-condition tubes were mounted, 9-10 cm directly below the lamp, with the bioassay tubes held at an approximately 30° angle below the horizontal. The mounted tubes were agitated on an orbital shaker at 30° C during the period of the bioassay. At the stated times, samples were removed from the shaker, diluted appropriately (to approximately 5×10^3 cfu/ml, if possible) in saturated sterile calcium carbonate, and plated (1) on Difco nutrient agar containing 0.02% streptomycin, using a Spiral Systems Spiral Plater.

Two slightly different methods for preparing the bioassay mixtures were used, and are designated in the figure legends as method I and method II.

Method I: The phytoalexin being assayed was transferred in individual aliquots of methanol solution to 1.5 ml conical polypropylene centrifuge tubes, with a separate tube

used for each replication and each time point. The methanol was evaporated under a N₂ stream fitted with a sterile cotton plug. Equal volumes of Xcm in MOPS medium were added to all tubes, vortexed for 40 seconds and mounted under the light as described above. If the effect of a second compound on the phytoalexin/Xcm interaction was being assayed, two suspensions of Xcm in MOPS were prepared: one with the added compound, and one without it as a control. All steps up to the vortexing were carried out in a laminar flow hood.

Method II : The phytoalexin being assayed was transferred to a single conical tube, in a quantity sufficient to prepare a MOPS medium stock solution for all the bioassay tubes to be used at that concentration. If a second phytoalexin concentration was being assayed, it was prepared in a separate tube. The methanol was evaporated as described in Method I, and sufficient MOPS medium was added to the tube to make a solution twice the desired final concentration. The tube was then vortexed thoroughly (up to five minutes), with careful inspection to assure complete solvation. The phytoalexin solution was pipetted into sterile conical tubes, and an equal volume of Xcm in MOPS medium (also prepared at twice the desired final cfu/ml) was added. As in method I, if the effect of a second compound was being assayed, it was added to the Xcm-MOPS suspension.

The DABCO used was purchased from Aldrich. DTPA, horseradish SOD, d- α -tocopherol acetate, and bovine liver catalase were obtained from Sigma. Sequestrene 138 was obtained in a crude preparation from CIBA-GEIGY.

RESULTS

Comparison of Plant-derived and Synthetic DHC

The toxicity of DHC isolated from infected cotton leaves and that of a synthetic sample of DHC, prepared by Dr. R. D. Stipanovic, were compared in a bioassay with Xcm, performed in the absence of light (Fig. 1) The results were calculated as total

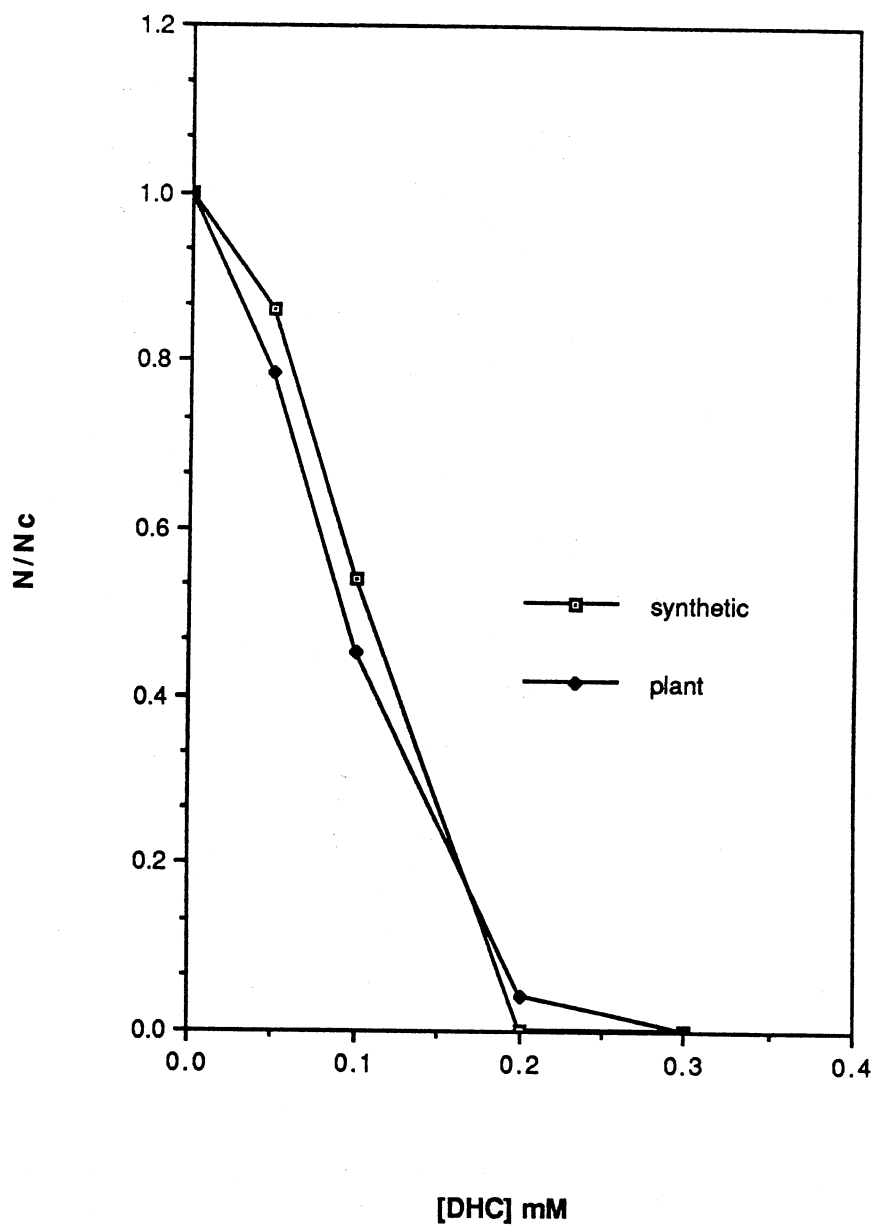


Fig. 1 Comparison of Toxicity of Plant-derived and Synthetic DHC. Plant-derived and synthetic DHC were bioassayed with *Xcm* at DHC concentrations of 0.05, 0.10, 0.20, and 0.30 mM. The bacterial population, in cfu/ml, at the end of 43 hours was expressed as a population doubling during the bioassay (N) divided by total doublings in a control (N_c). Initial [*Xcm*] was 6.65×10^3 ; assay volume = 25 μ l. All conditions were assayed in the absence of light; method I.

bacterial doublings during the bioassay period (43 hours) divided by the doublings in the untreated control (N/N_c). The toxicity of the two DHC preparations was essentially the same, with 50% inhibition occurring at approximately 0.1 mM DHC for both.

Following the DHC synthesis described in this work, a second comparative bioassay again indicated very similar toxicities in the two DHC preparations (Figs. 2a & 2b). This bioassay, with bacterial population sampled at various times, was performed concurrently in light and dark conditions. As reported by Sun *et al.* (2), the toxicity of DHC was markedly activated by irradiation. The light- and dark-condition bioassays displayed a similar pattern of toxicity for plant-derived and synthetic preparations of DHC.

Effect of Xcm Concentration on the Toxicity of DHC

The toxic effects of 0.1 mM and 0.2 mM DHC solutions on Xcm, both in the presence and absence of light, were assayed using Xcm cultures with starting concentrations of 1.06×10^5 , 1.01×10^6 , and 1.27×10^7 cfu/ml (Figs 3a, 3b & 3c). In each case, 0.2 mM DHC in light and dark conditions was at least bacteriostatic, and sometimes bactericidal. In the presence of light, 0.1 mM DHC was bacteriostatic toward the two lower population conditions. The photodynamic effect of 0.1 mM DHC was less pronounced at the higher bacterial concentrations.

Effect of Light on the Biological Activity of Several Cotton

Sesquiterpenoids

The two major phytoalexins (DHC and LC) found in resistant cotton lines, and their 7-methyl ethers (HMC and LCME, respectively) were tested in bioassays for photodynamic toxic effects against Xcm. The DHC, LC and HMC tested in the following experiments were synthetically prepared. The LCME was isolated from Xcm-inoculated plant material.

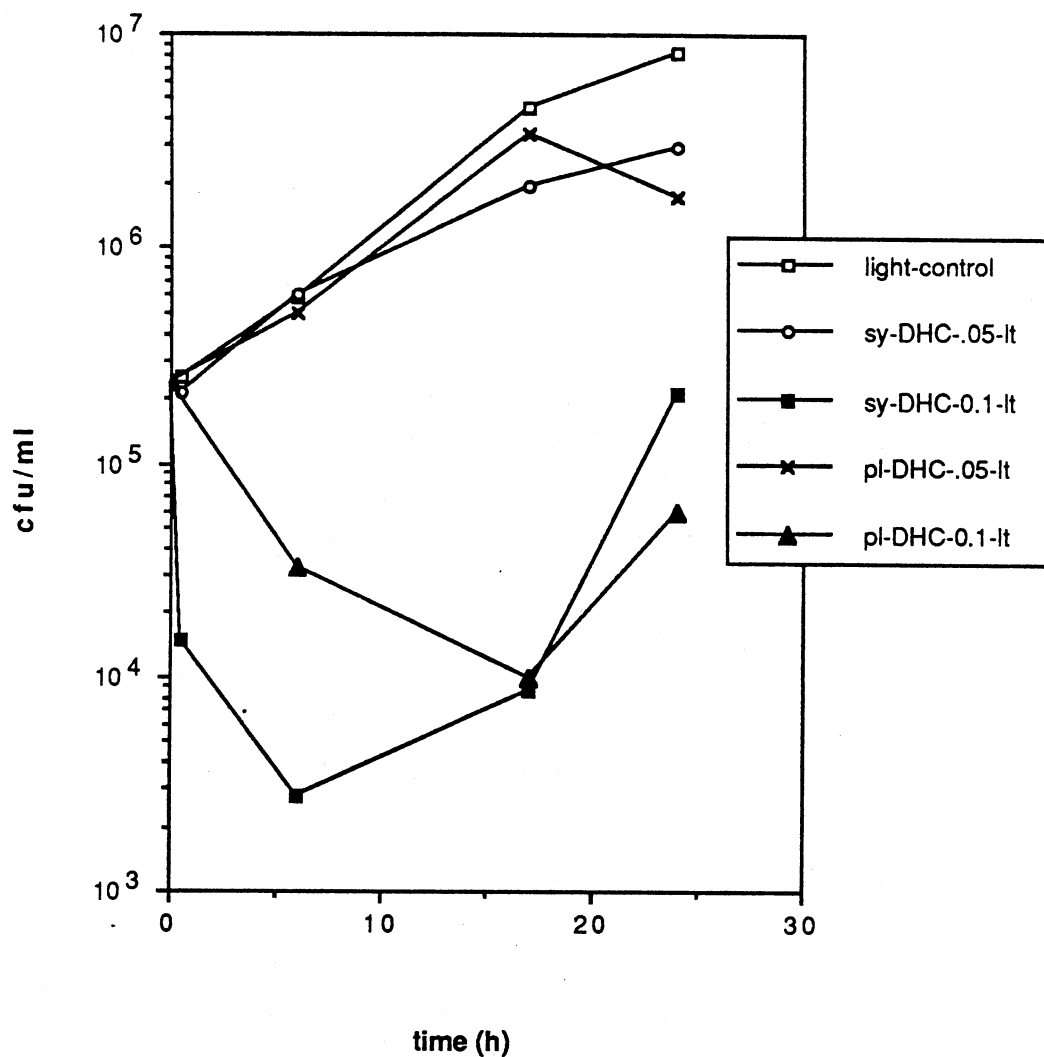


Fig. 2a Comparison of Toxicity of Plant-derived and Synthetic DHC; Light Conditions, Time-course. *Xcm* was bioassayed with 0.05 and 0.10 mM DHC concentrations of plant and synthetic DHC. Assay tubes were exposed to radiation from cool-white fluorescent tubes during bioassay; volume = 200 μ l; bioassay method I.

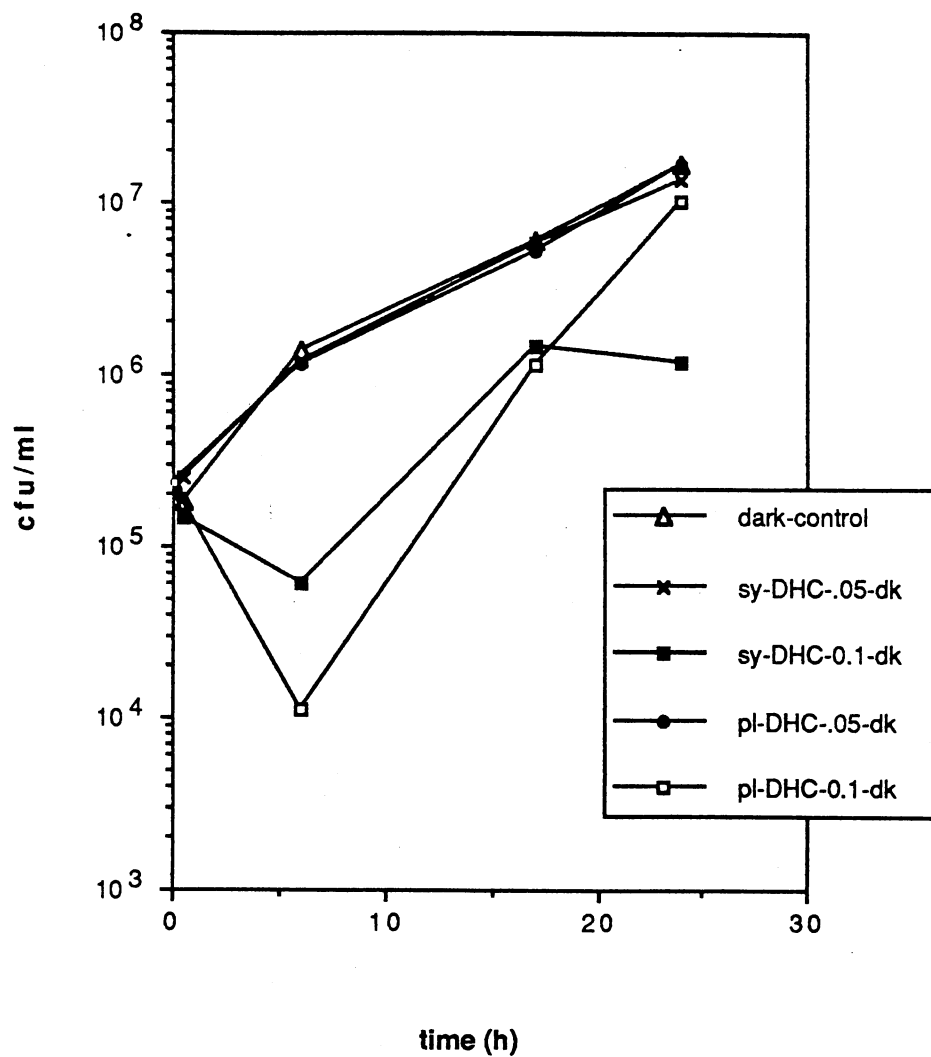


Fig. 2b Comparison of Toxicity of Plant-derived and Synthetic DHC; Dark Conditions, Time-Course. Performed concurrently with and under same conditions as Fig. 2a, except all tubes were protected from exposure to light with double-wrapped aluminum foil.

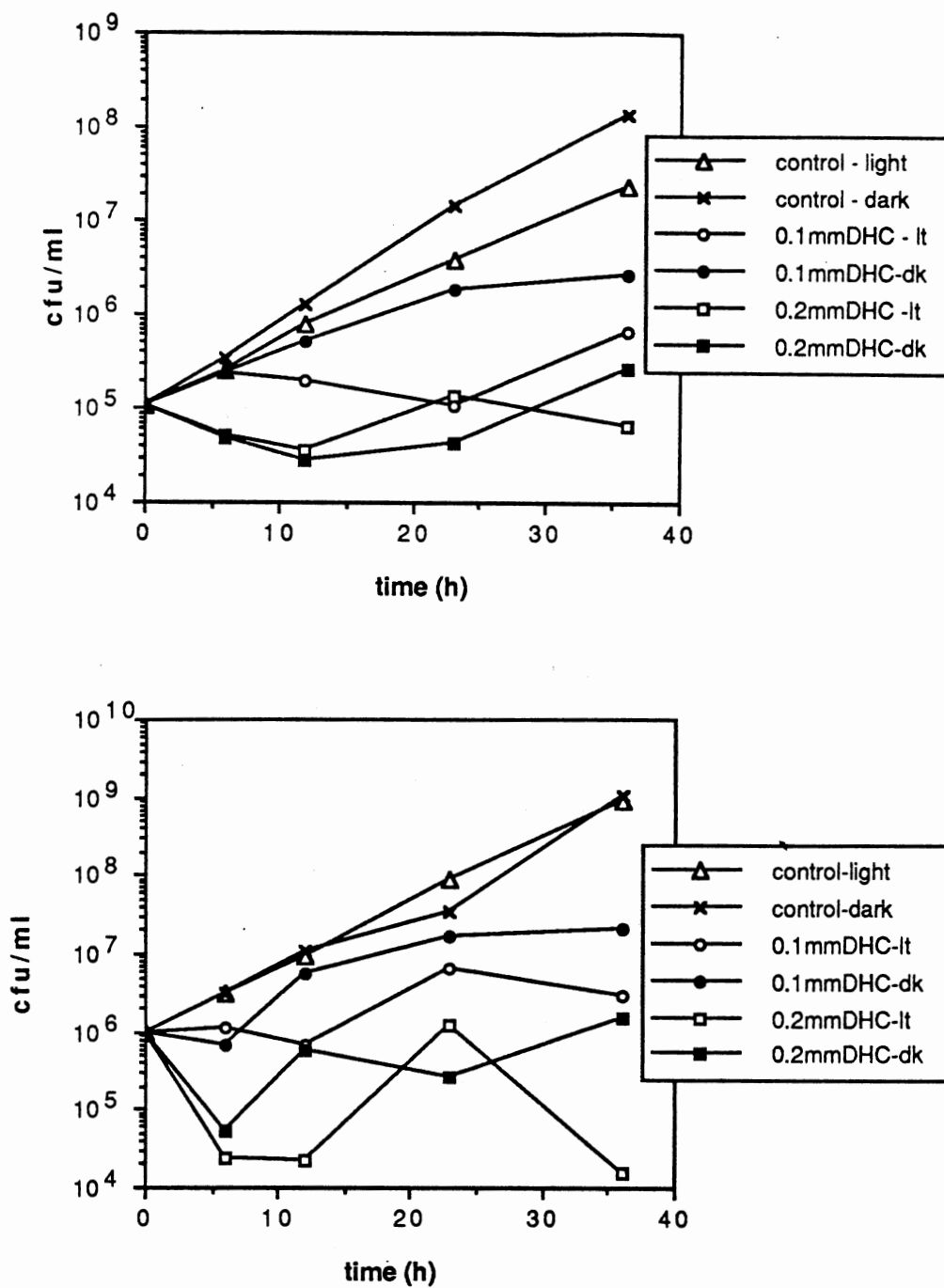


Fig. 3a - c Effect of Concentration of Xcm on DHC toxicity. Xcm in three different starting concentrations was assayed in light and dark conditions. DHC concentrations of 0, 0.1 and 0.2 mM were used. Initial Xcm concentrations : 3a 1.06×10^5 cfu/ml; 3b 1.01×10^6 cfu/ml; and 3c 1.27×10^7 cfu/ml. Bioassay method I.

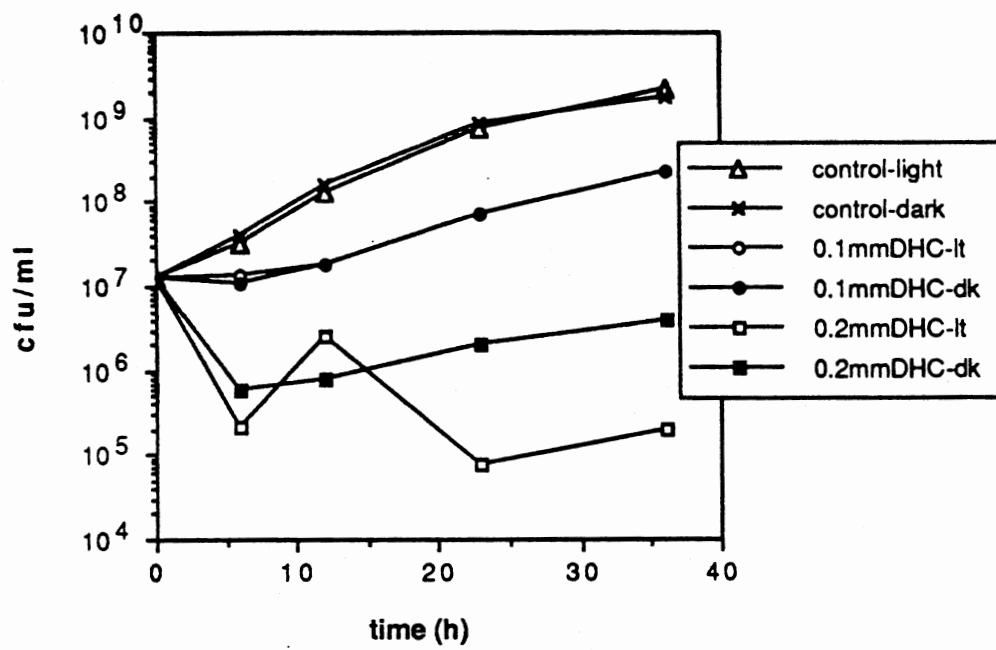


Fig. 3c

The previous report (2) of the photo-activation of the antibacterial action of DHC was supported in the experiment shown in Fig. 4. Even under conditions in which the radiation used was not inhibitory toward Xcm growth, as displayed by the light and dark growth controls, the stimulation of toxicity by light was quite marked.

LC was similarly photo-activated (Fig. 5). LC at 0.75 mM was used in this bioassay, a concentration which was not inhibitory under these conditions toward Xcm in the absence of light. When this concentration of LC was irradiated in the presence of Xcm, it was bacteriostatic. The final time point of the LC/light condition represents a maximum possible value for cfu/ml. Due to very low plate counts, the exact concentration could not be calculated with high confidence and may be lower than the value indicated. This condition with LC may well be bactericidal, therefore.

HMC has the lowest solubility in water (< 0.08 mM, Cover & Essenberg, unpublished results) of the four related sesquiterpenes assayed in this study. Previous attempts to test the activity of HMC toward Xcm in the dark had indicated no inhibition by HMC in saturated solutions. In order to investigate the possibility that HMC might be photo-activated, a bioassay was performed using methanol in a final concentration of 2% to achieve a 0.5 mM solution of HMC (Fig. 6). A previous study (see Appendix) indicated that this concentration of methanol does not inhibit Xcm growth, and the growth of the control samples in this study supported this observation. HMC was shown under these conditions not to inhibit Xcm growth, even in the presence of light.

LCME was assayed with Xcm at a concentration of 0.8 mM (Fig. 7) and displayed a slight loss of antibacterial activity when the assay was performed in the light, relative to the same conditions assayed in the absence of light.

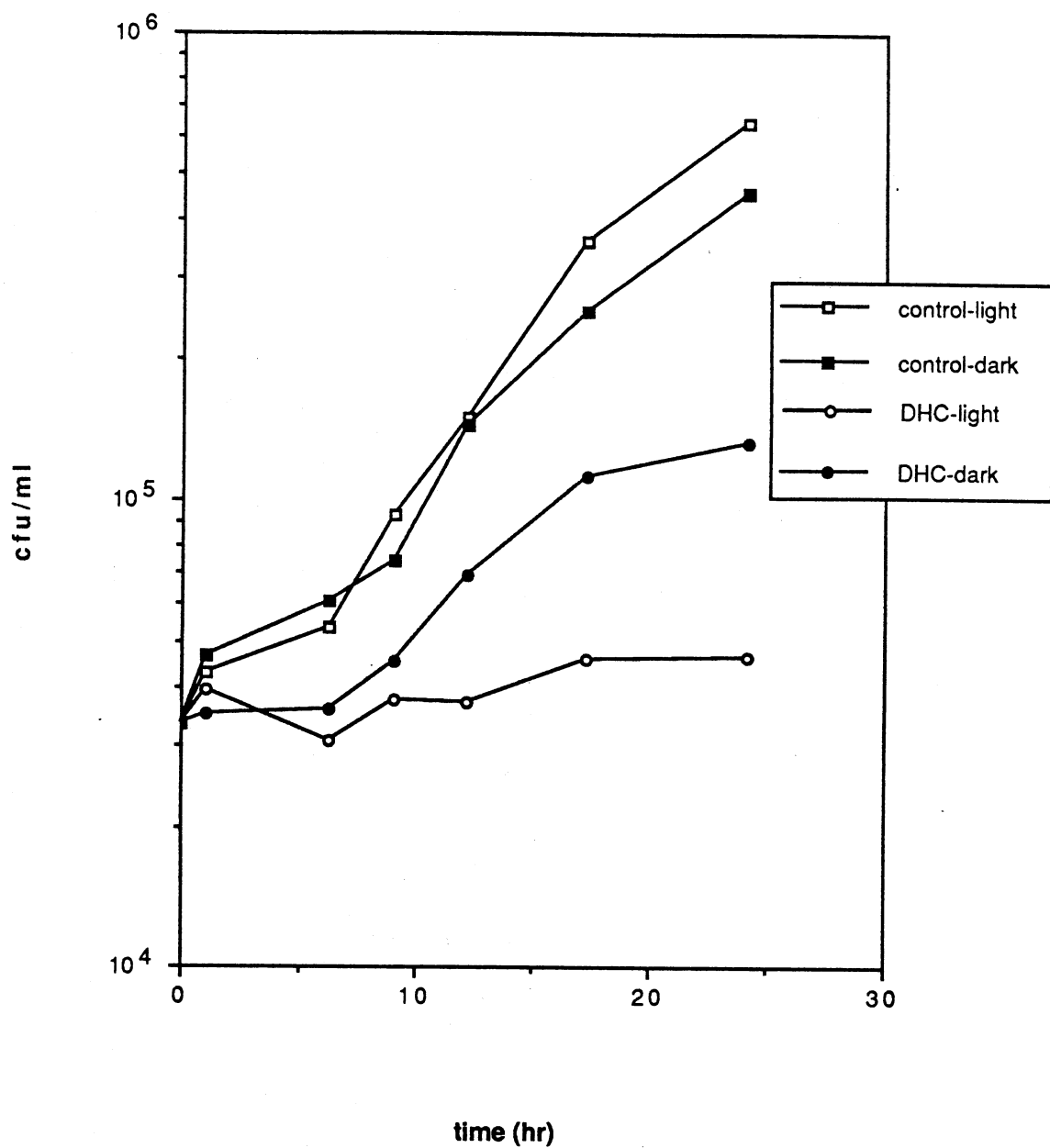


Fig. 4 Photo-stimulation of Antibacterial Activity of DHC. Xcm at an initial concentration of 3.33×10^4 cfu/ml was bioassayed with 0.1 mM DHC in the presence and absence of light. Assay volume was 100 μ l; bioassay method II.

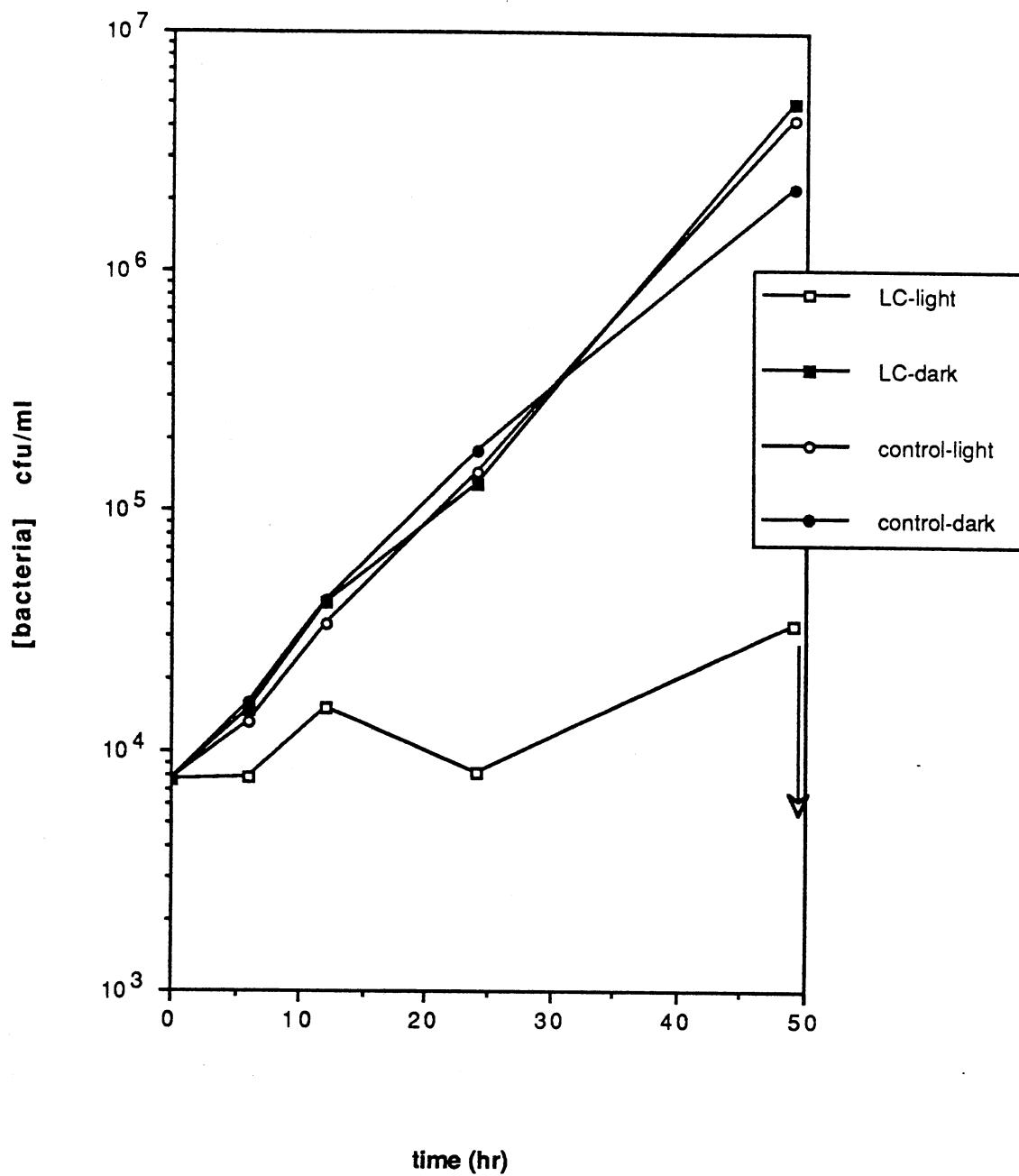


Fig. 5 Photo-stimulation of Antibacterial Activity of LC. LC (0.75 mM) was bioassayed with Xcm at an initial concentration of 7.67×10^3 cfu/ml. Light and dark conditions. Assay volume was 100 μ l; method II.

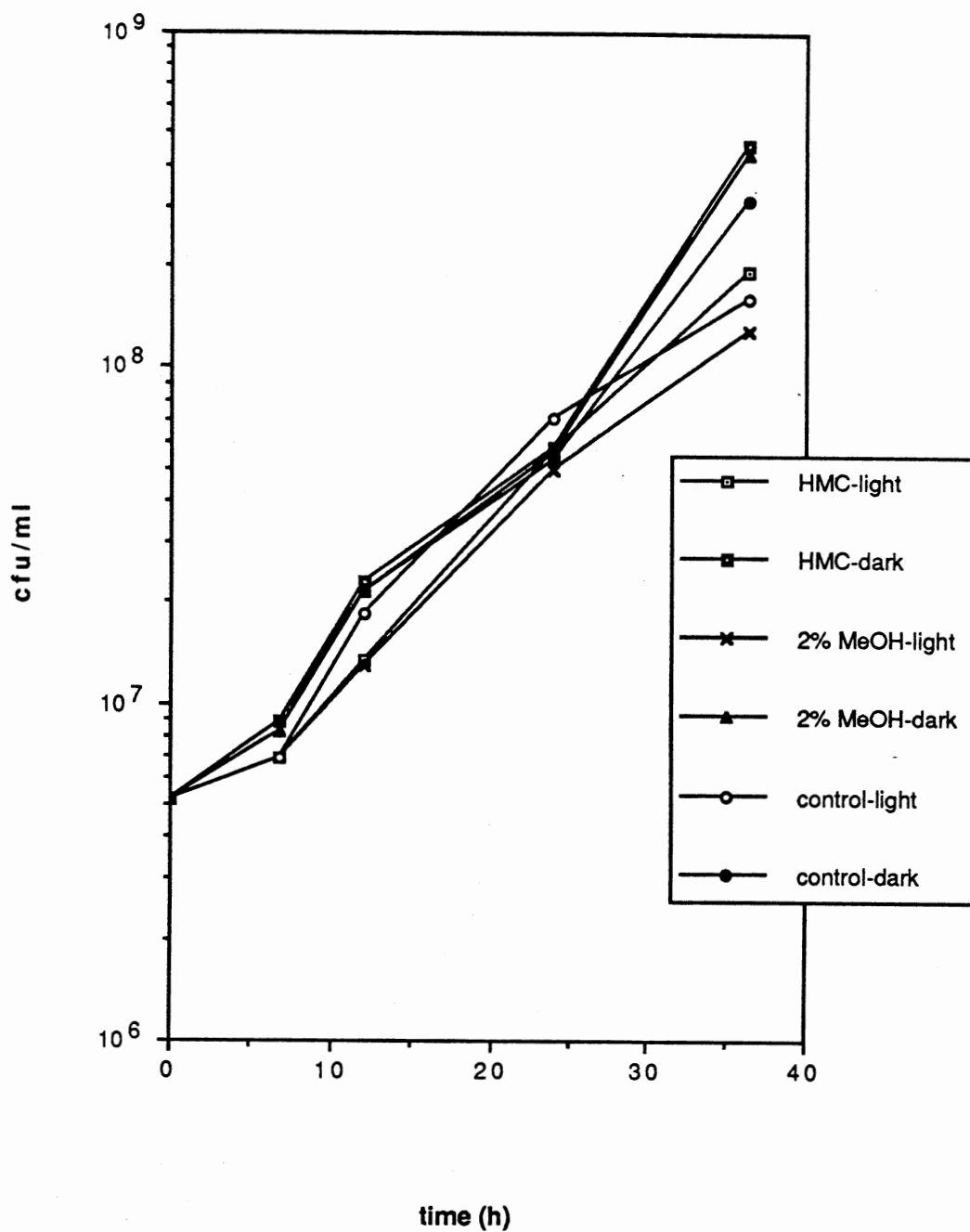


Fig. 6 Effect of HMC on Xcm; Light and Dark Conditions. HMC at 0.5 mM, dissolved in 2% methanol in MOPS was assayed with Xcm at an initial concentration of 5.21×10^6 cfu/ml. Controls with 2% methanol in light and dark included. Assay volume 100 μ l; Method II.

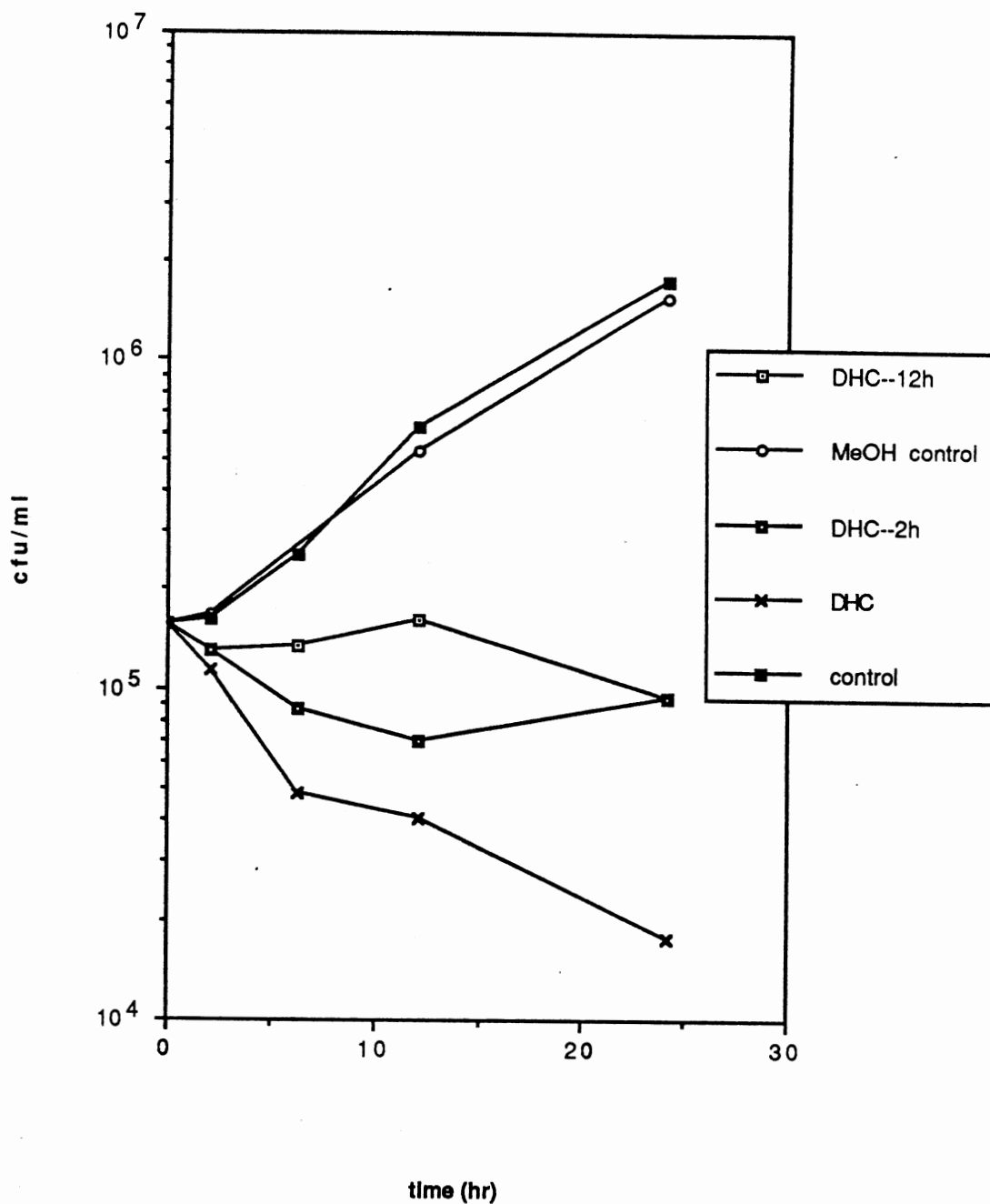
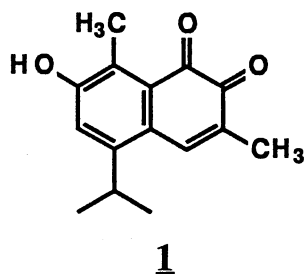


Fig. 7 Effect of Light on Toxicity of LCME Toward Xcm. LCME derived from Xcm-inoculated cotton cultivar OK 1.2, assumed to be chiefly *R*- isomer; 0.8 mM assayed in light and dark with Xcm at an initial concentration of 1.135×10^4 cfu/ml; Method II.

Biological Activity of Some Products of DHC



When DHC is repeatedly evaporated and transferred from the methanol solutions in which it is typically handled, an intensely red contaminant is frequently observed. The reaction which produces this red compound occurs in the dark, (or under blue-deficient lights). Dr. Robert Stipanovic has isolated this red compound, and has proposed structure **1**, based on nmr spectral findings. The proposed *ortho*-quinone was bioassayed with Xcm, in the dark, and the results are shown in Figure 8. At a concentration of 0.15 mM, the *ortho*-quinone was slightly inhibitory toward Xcm, and was bactericidal at 0.75 mM. Preparation of higher concentrations was attempted, but the water solubility of this compound appears to be approximately 1.0 mM or slightly less.

When exposed to light, DHC undergoes a reaction, or series of reactions, producing a group of compounds which have been isolated by HPLC, but not yet identified (see Chapter V, this work). Spectral studies of solutions of DHC exposed to light under bioassay conditions indicate that the degradation of DHC is essentially complete in 1.5 hours. Most of the spectral studies were performed at higher DHC concentrations than were used in bioassays: 0.37 or 0.40 mM DHC in the spectral studies, as opposed to 0.1 or 0.2 mM DHC in most bioassays. The toxicity of these products of the interaction of DHC with light was assayed, and the results are shown in Figs. 9 and 9a. Solutions of 0.2 mM DHC were pre-treated with light, in the bioassay medium, for 0, 2, or 12 hours (Fig. 9). The light-degraded samples were bacteriostatic toward the Xcm, while the fresh DHC was bactericidal. The DHC sample exposed to light for 2 hours prior to the start of

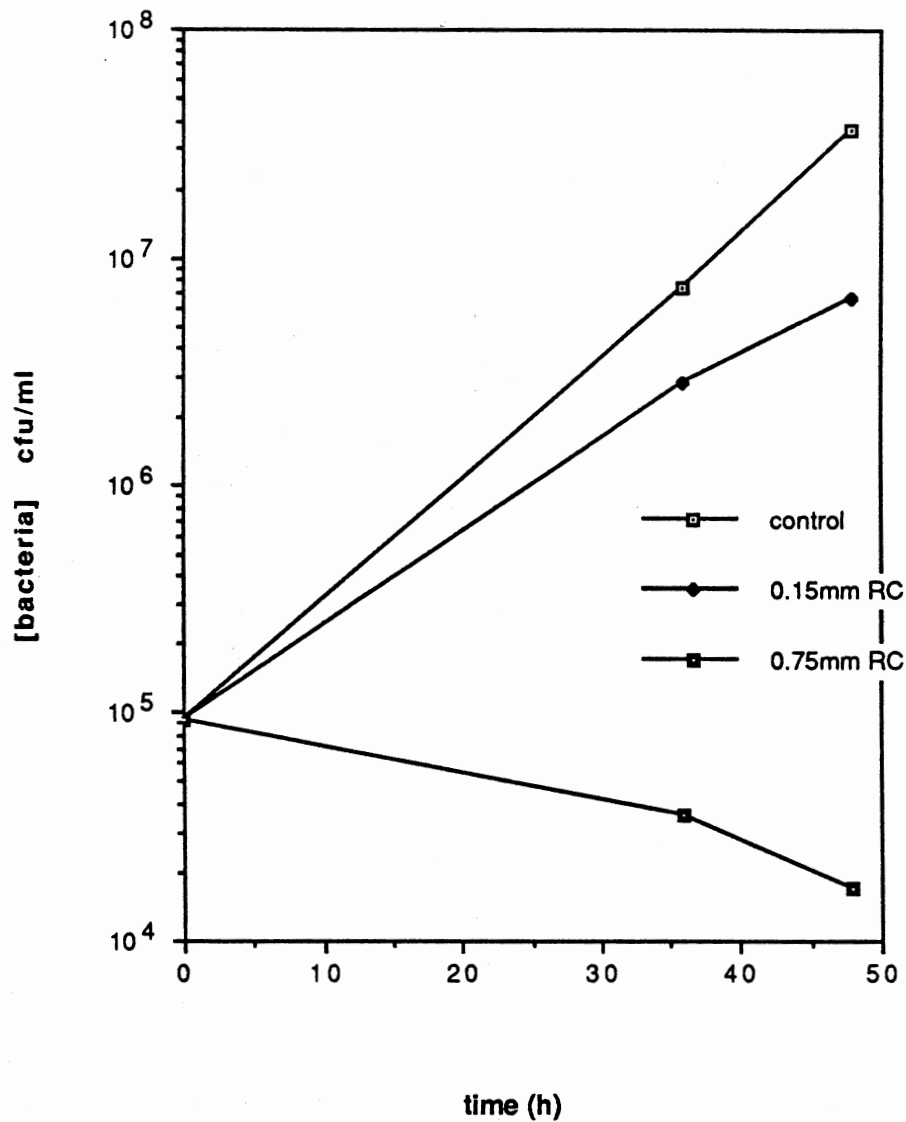


Fig. 8 Bioassay of an Unidentified Red Compound, Produced by Degradation of DHC in the Dark; Dark Conditions. Using the molecular weight of the proposed *ortho*-quinone structure (1) the red compound (RC) was assayed at 0.15 mM and 0.75 mM concentrations, with Xcm at an initial concentration of 9.40×10^4 cfu/ml. Assay carried out in the dark; Method II.

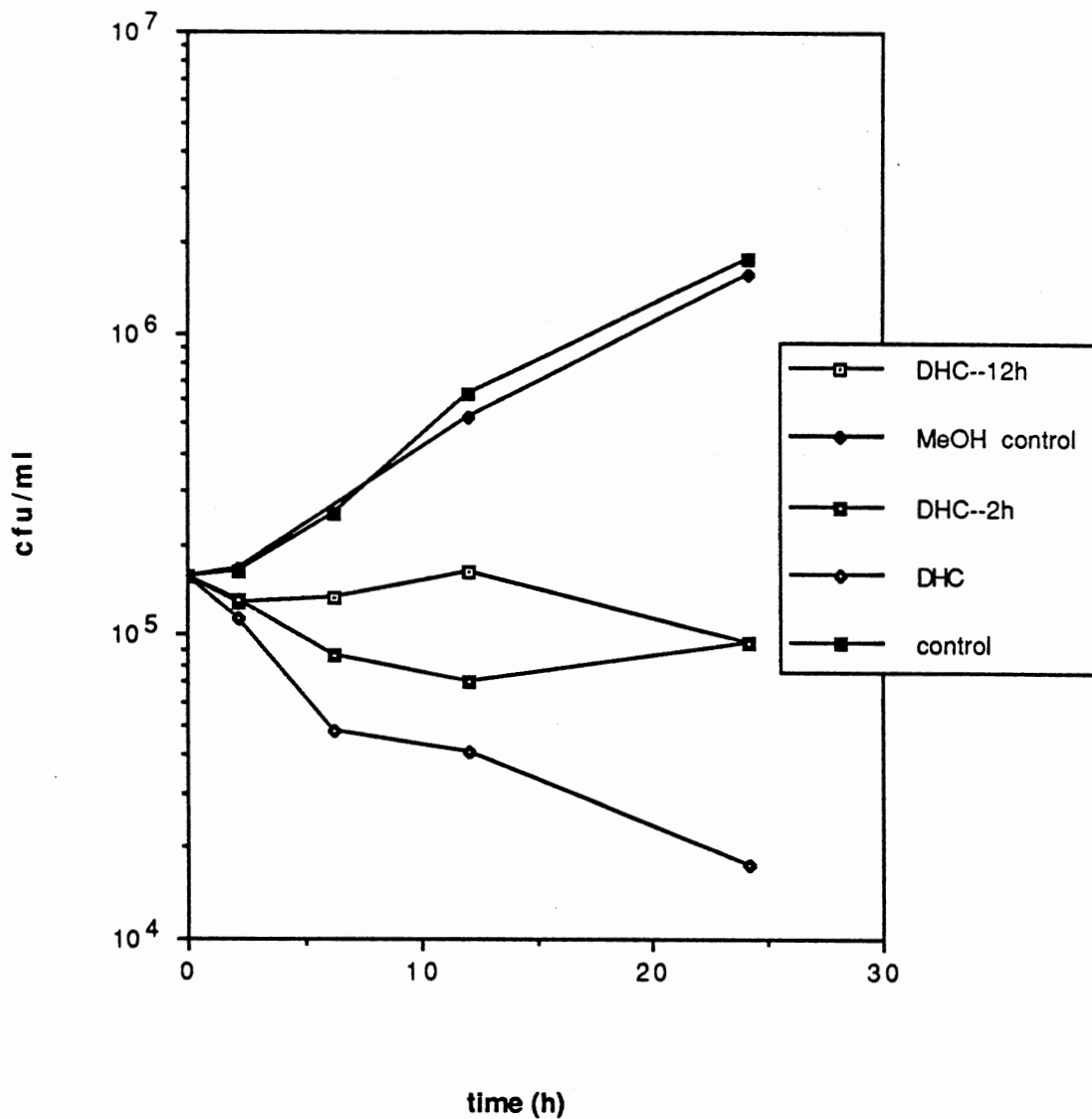


Fig. 9 Toxicity of Photo-Degradation Products of DHC Toward Xcm. DHC (0.2 mM) was exposed to light for 0, 2, or 12 hours in MOPS medium before being added to an Xcm suspension in MOPS. As a control, a sample of the growth medium was exposed to light for 12 hours. Initial [Xcm] = 3.13×10^5 cfu/ml. Experiment carried out in the light; Method II.

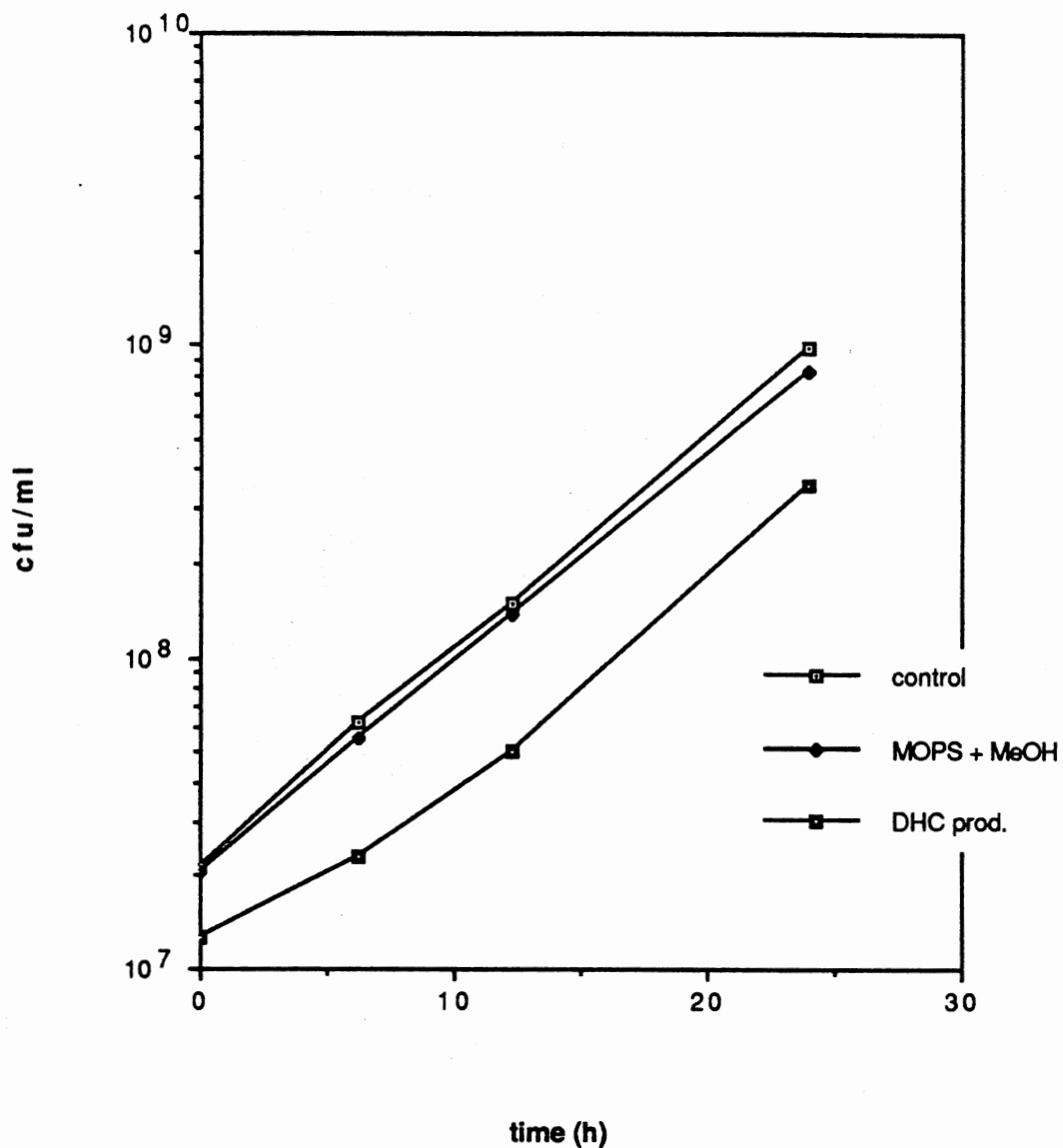


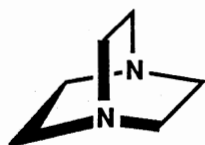
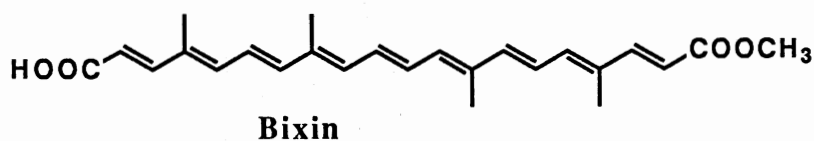
Fig. 9a Toxicity of Photo-Degradation Products of DHC Toward Xcm. DHC (0.1 mM) was exposed to light in MOPS medium for 2 hours before being added to an Xcm suspension. MOPS medium was exposed to light for 2 hours as a control. Initial Xcm concentration = 1.157×10^7 cfu/ml; method II.

the bioassay was slightly more inhibitory than that exposed to light for 12 hours. In a similar study performed at higher bacterial concentration, the products of DHC exposed to light for two hours were only very slightly inhibitory to Xcm (Fig. 9a).

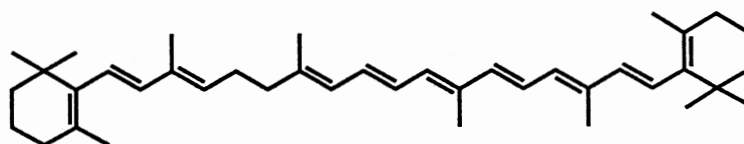
*Effects of Scavengers or Quenchers of Activated Oxygen
on DHC Toxicity*

Several compounds reported to quench or scavenge various activated oxygen species were combined with DHC in bioassays to investigate the possible involvement of some form of activated oxygen in the toxic interaction of DHC with Xcm. In the event that DHC generated, or caused generation of, one of these reactive species in the culture medium, the appropriate scavenger or quencher would be expected to markedly decrease the inhibitory effect of DHC toward the bacteria.

Several of these compounds are themselves potential bacterial inhibitors. Thus, preliminary tests of the quenchers and scavengers with Xcm were necessary.



DABCO



β -Carotene

DABCO (structure above). DABCO, an efficient quencher of singlet oxygen (O_2^1) (10) was tested for inhibitory activity toward Xcm in liquid culture under low light conditions

at an Xcm concentration starting near 1×10^8 (Fig. 10a); and under bioassay conditions (Fig. 10b) with starting Xcm concentrations of approximately 1×10^4 cfu/ml. Using the results of this test, concentrations of 1 mM and 10 mM DABCO were chosen for the bioassay with DHC and Xcm (Figs. 11a and 11b). When DABCO was present in the DHC bioassay performed in the light (Fig. 11a), a decrease in toxicity was observed. A large excess of DABCO relative to DHC was apparently necessary for this effect, as only the 10 mM DABCO solution was capable of appreciably decreasing the toxicity of 0.1 mM DHC.

DABCO exerted no apparent protective effect in the DABCO/DHC assay performed in the absence of light and even appeared to potentiate the effect of 0.2 mM DHC (Fig. 11b).

Bixin (structure above). The specificity of bixin toward activated oxygen has not been reported, but is generally assumed to be similar to that of β -carotene, which is a good singlet oxygen quencher (11, 12). The water solubility of bixin is limited, and the stock solution (134 mM) used in this study contained 46.5% methanol, 53.5% aqueous 0.2N NaOH. The effect of this preparation on Xcm growth was tested (Figs. 12a & 12b), and a 2 mM bixin concentration was chosen for the combined bixin/DHC bioassay (Figs. 13a & 13b). In the presence of light, bixin was somewhat inhibitory, and provided no protection from DHC toxicity. DHC was assayed at 0.2 mM with and without bixin, but in the presence of light this concentration of DHC was completely toxic, and is not shown in Figure 13a. Figure 13b shows the bixin/DHC bioassay performed in the absence of irradiation. Under these conditions, bixin provided partial protection against the inhibition by DHC at 0.1 mM and 0.2 mM DHC. As indicated by the bixin control, this compound was not inhibitory toward Xcm in the dark.

Na-Benzoyate. Sodium benzoate interacts with hydroxyl radical (OH^\cdot) fairly specifically. (13) In a bioassay with sodium benzoate and DHC (Figs. 14a & 14b), concentrations of

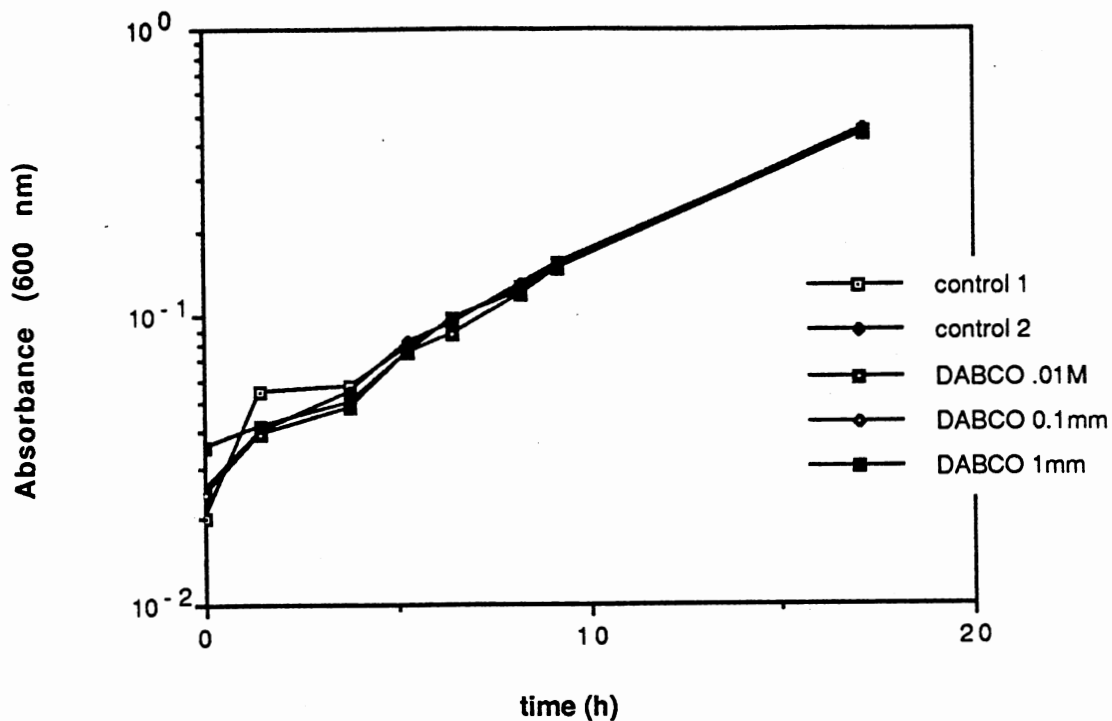


Fig. 10a Test of Toxicity of DABCO Toward Xcm. DABCO in three concentrations (10, 1, and 0.1 mM) was added to logarithmically growing Xcm cultures; assay volume = 10 ml; initial Xcm concentration $\sim 1 \times 10^8$ cfu/ml. Assay was carried out under low light, and bacterial concentration was monitored using a Coleman, Jr. spectrometer.

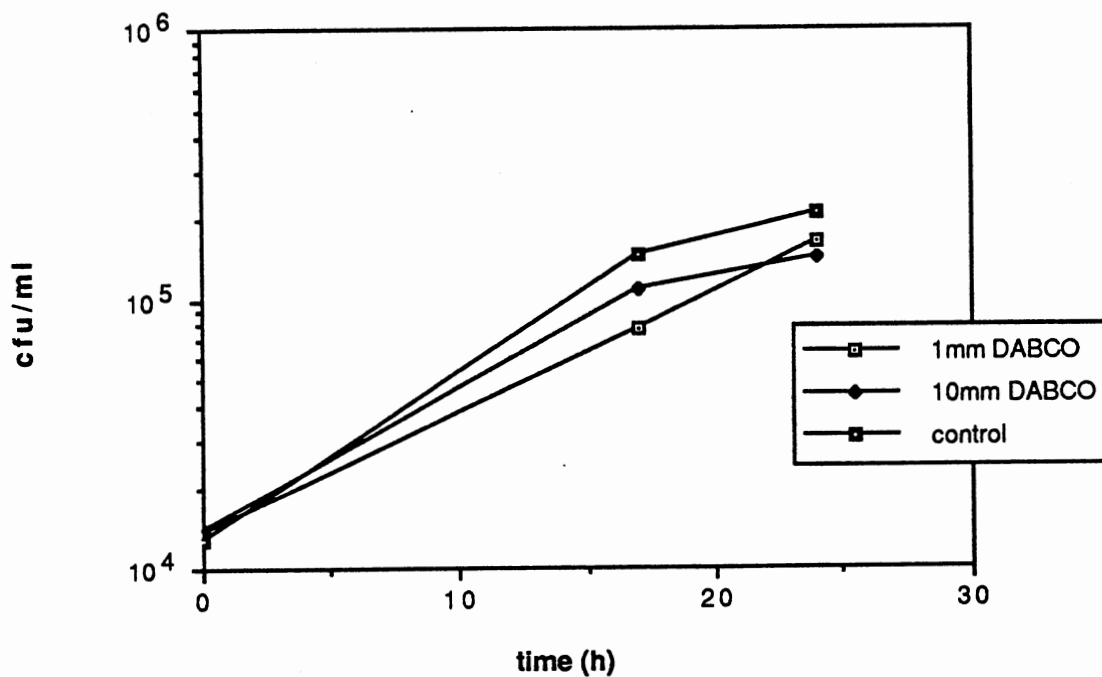


Fig. 10b Bioassay of DABCO with Xcm in Light. DABCO, at 1 and 10 mM concentrations, was added to Xcm in MOPS medium in μ guge tubes; bioassay Method I.

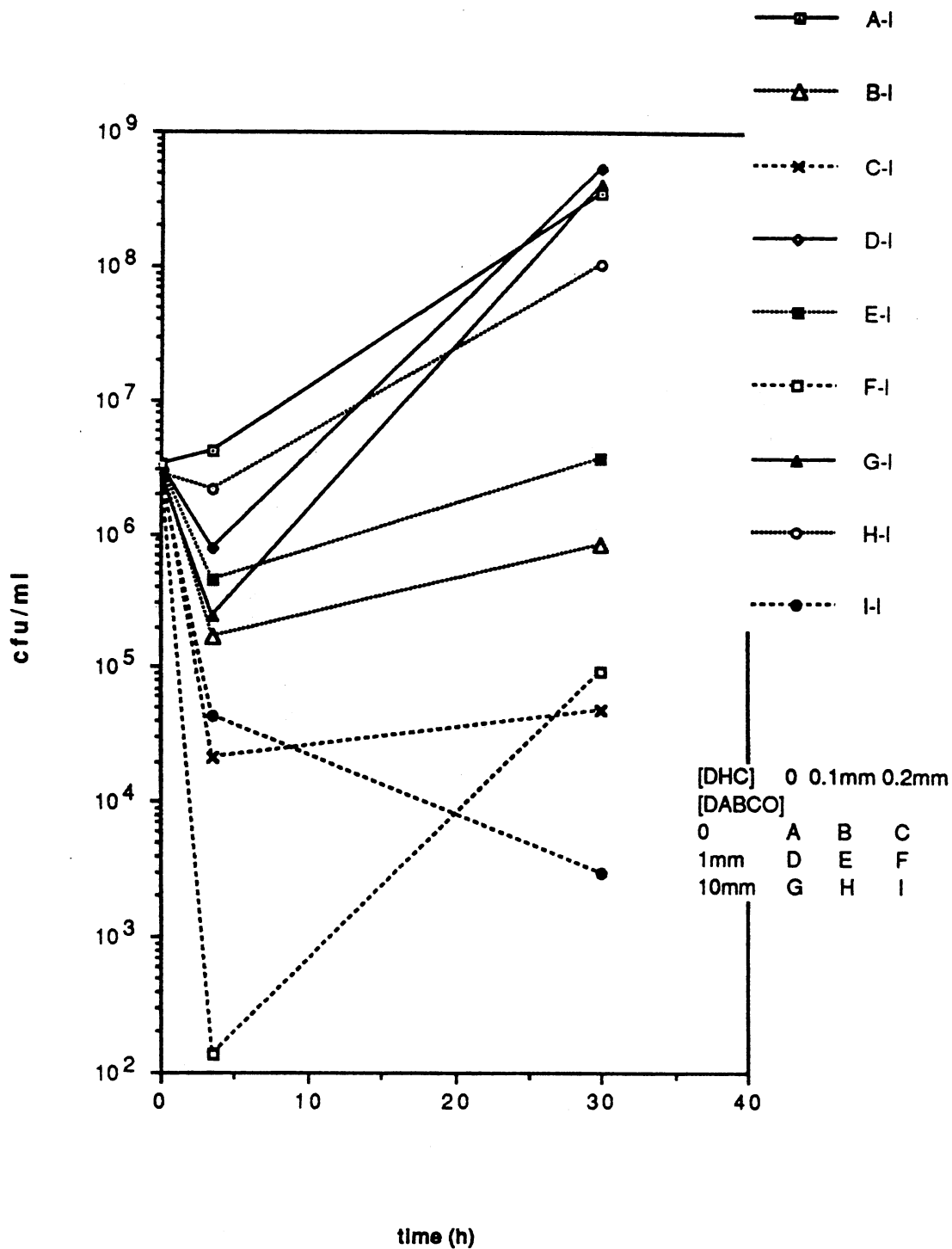


Fig. 11a Effect of DABCO on Toxicity of Xcm in Light. DHC, at 0, 0.1, and 0.2 mM, was dissolved in suspensions of Xcm with DABCO (at 0, 1, and 10 mM concentrations). Combinations shown in table at lower right. Assay volume = 50 μ l, bioassay Method I.

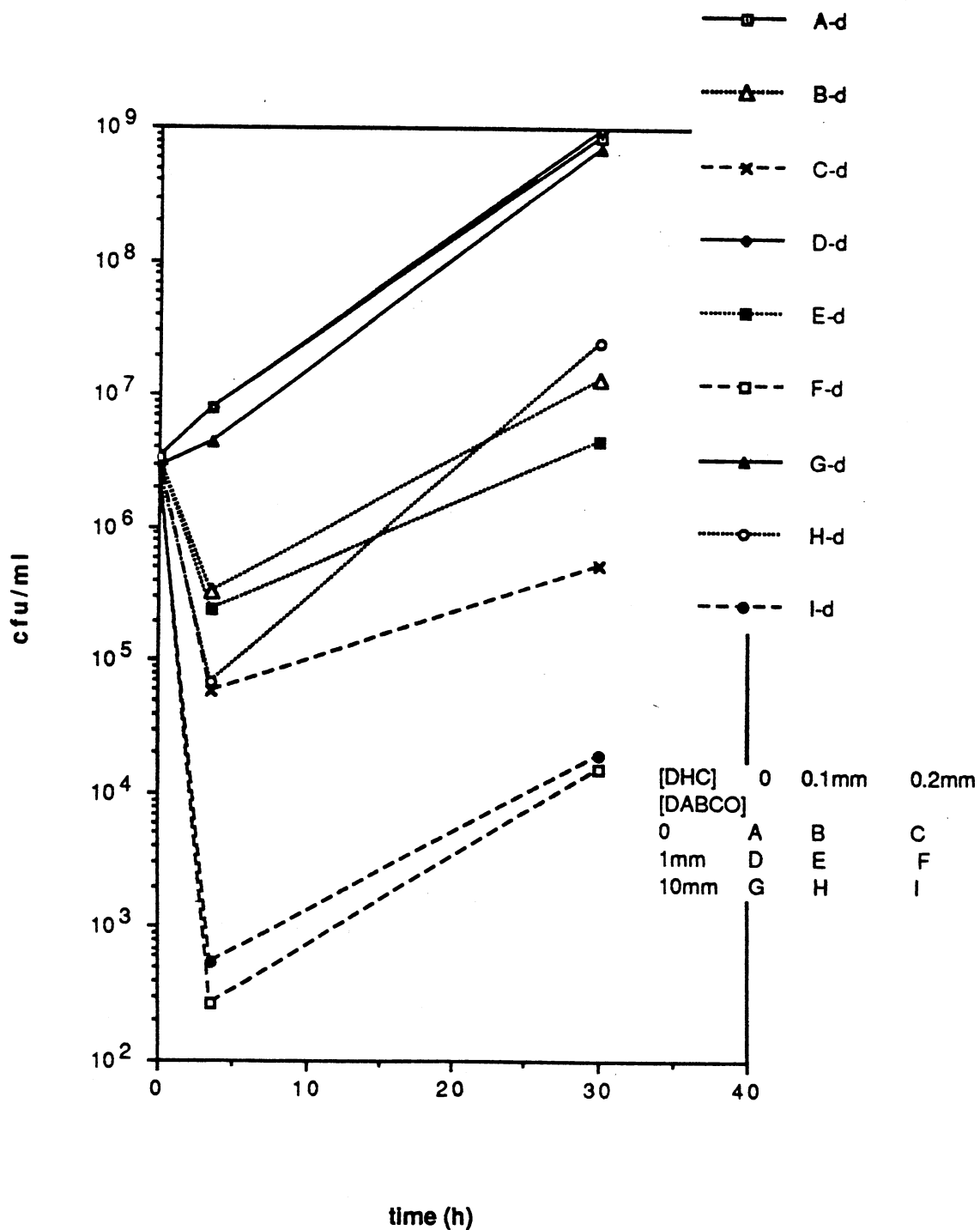


Fig. 11b Effect of DABCO on Toxicity of Xcm in Dark. DHC and DABCO were bioassayed concurrently and under the conditions described in Fig.11a, except bioassay tubes were protected from light with foil.

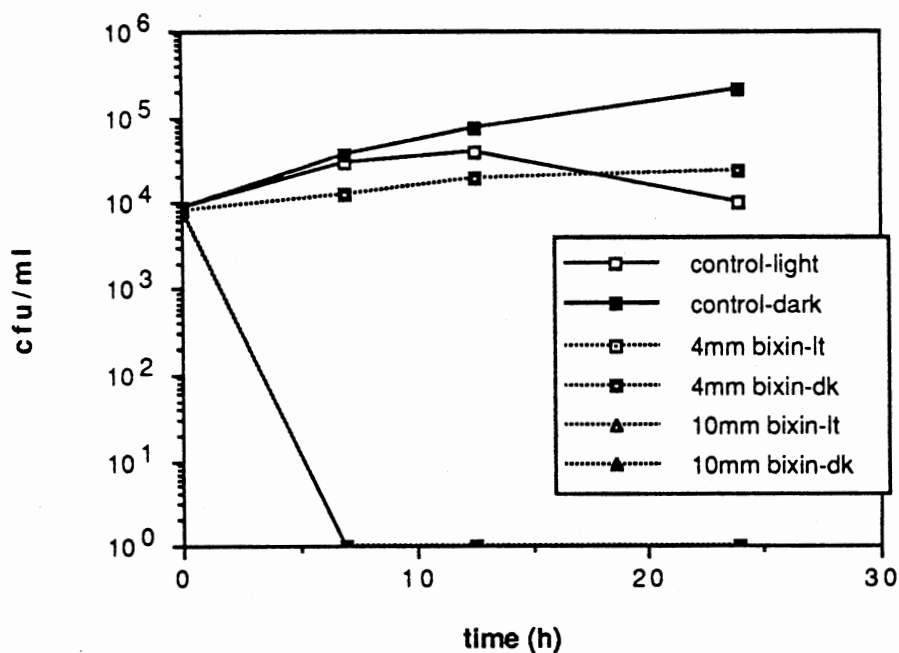


Fig. 12a Effect of Bixin on Xcm ; Light and Dark Conditions. Bixin, at 4 and 10 mM was added to Xcm in MOPS medium. Bioassay Method I, light and dark conditions.

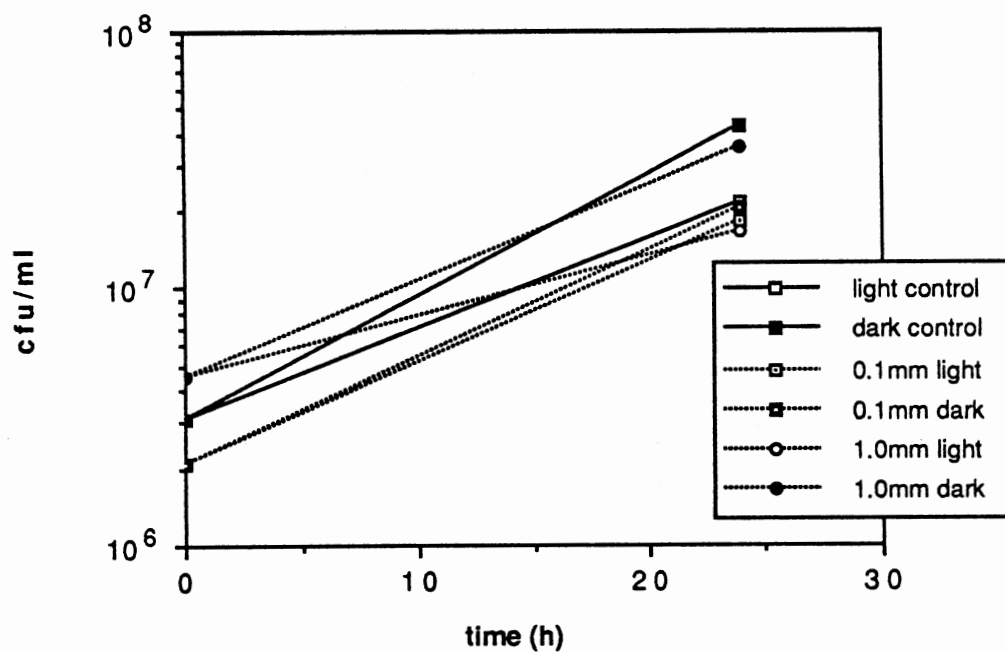


Fig. 12b Effect of Bixin on Xcm; Light and Dark Conditions. Bixin, at 0.1 and 1 mM, was added to suspensions of Xcm in MOPS. Light and dark conditions, Bioassay Method I.

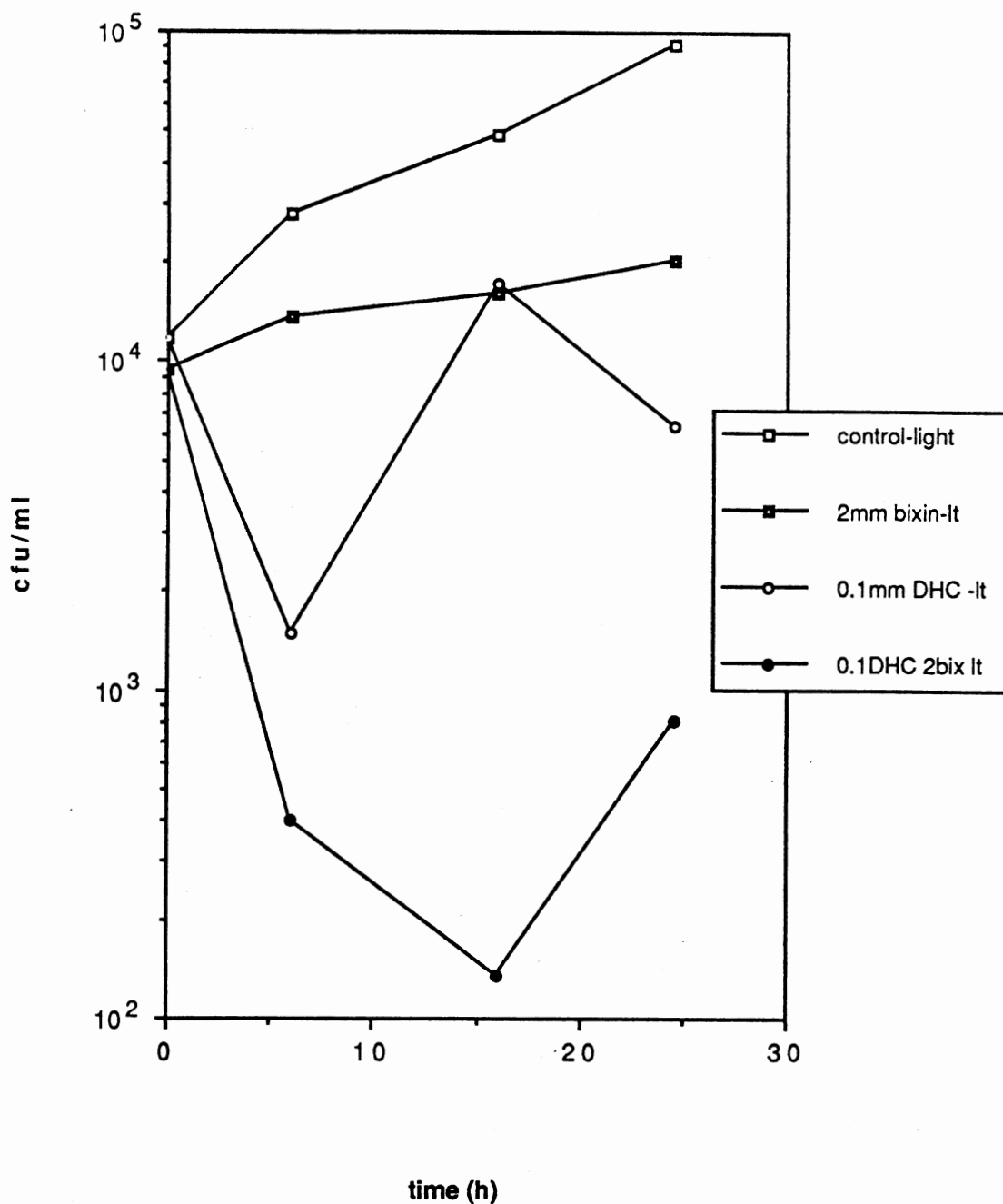


Fig. 13a Effect of Bixin on Toxicity of DHC; Light Conditions. DHC, at 0, 0.1 and 0.2 mM was added to Xcm suspensions in MOPS with 0 or 2 mM bixin. The 0.2 mM DHC treatment was completely toxic to both Xcm suspensions, and the data does not appear on the graph. All tubes exposed to light, bioassay method I, assay volume = 50 μ l.

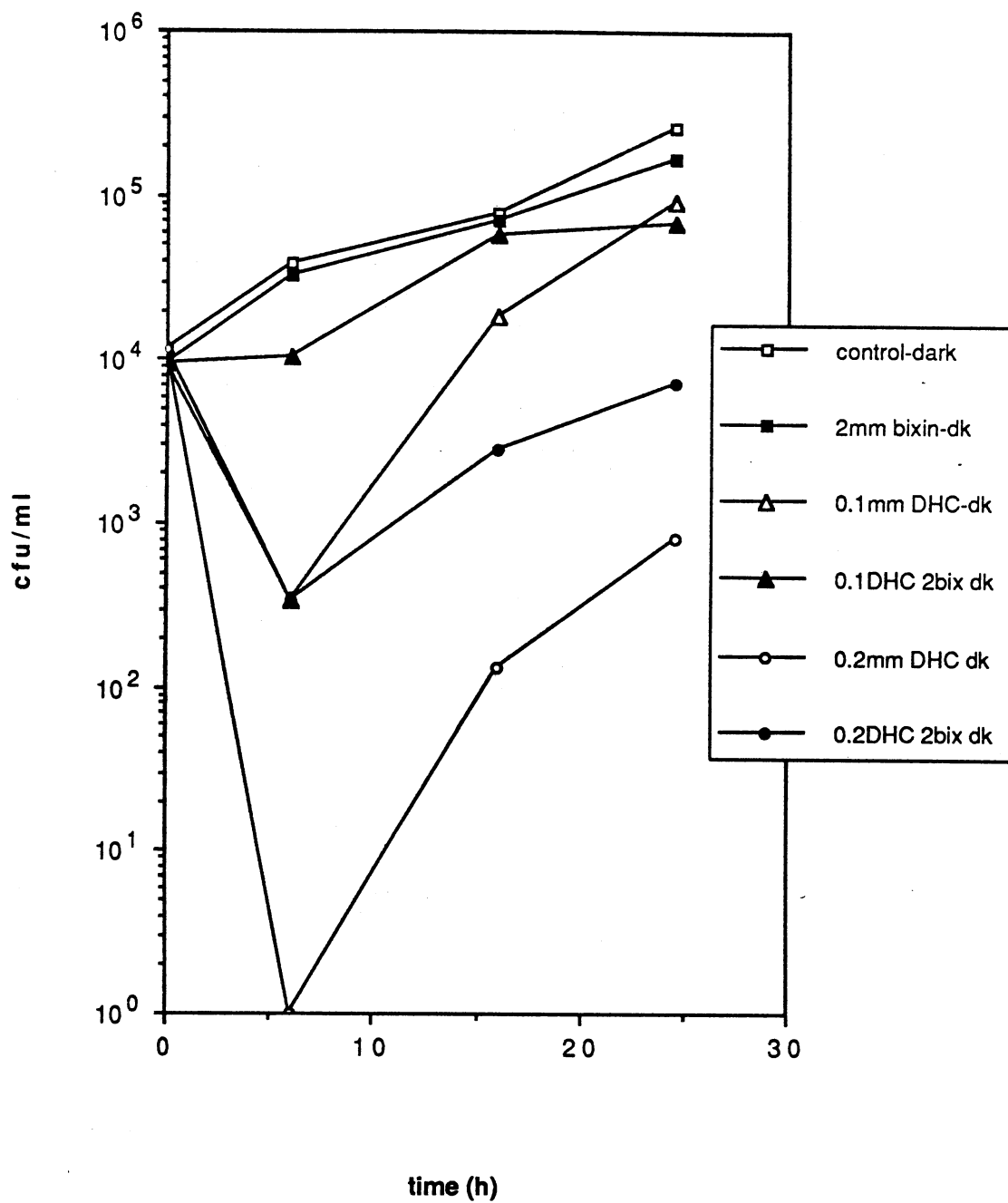


Fig. 13b Effect of Bixin on Toxicity of DHC; Dark Conditions. DHC and bixin were bioassayed with Xcm concurrently with and using the conditions in Fig. 13a, except all tubes were protected from light with foil.

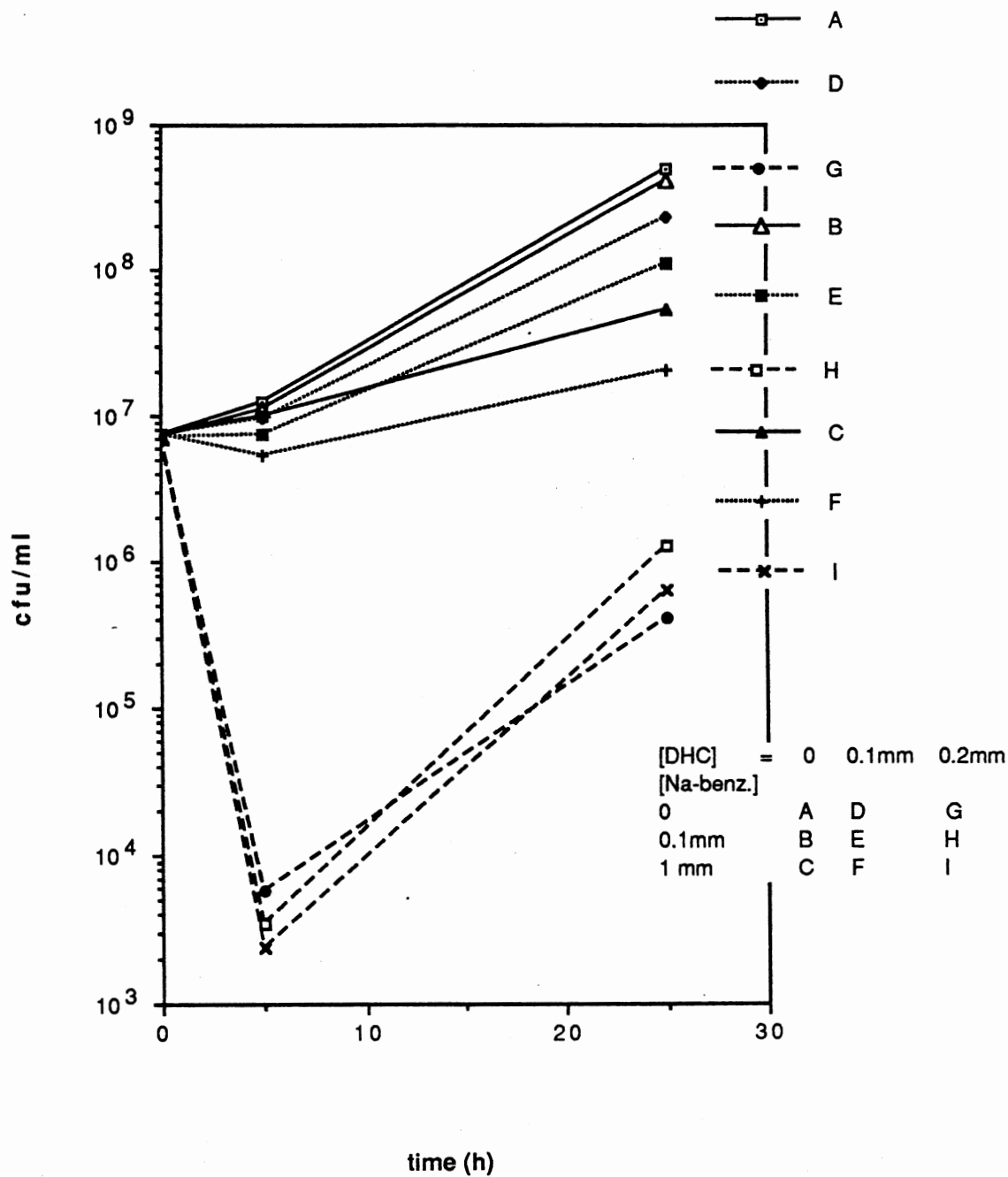


Fig. 14a Effect of Sodium Benzoate on Toxicity of DHC; Light Conditions. DHC, at 0, 0.1, and 0.2 mM was dissolved in an Xcm suspension containing 0, 0.1 or 1.0 mM Na-benzoate. (Combinations shown in table, lower right). Light conditions; volume = 50 μ l; bioassay method I.

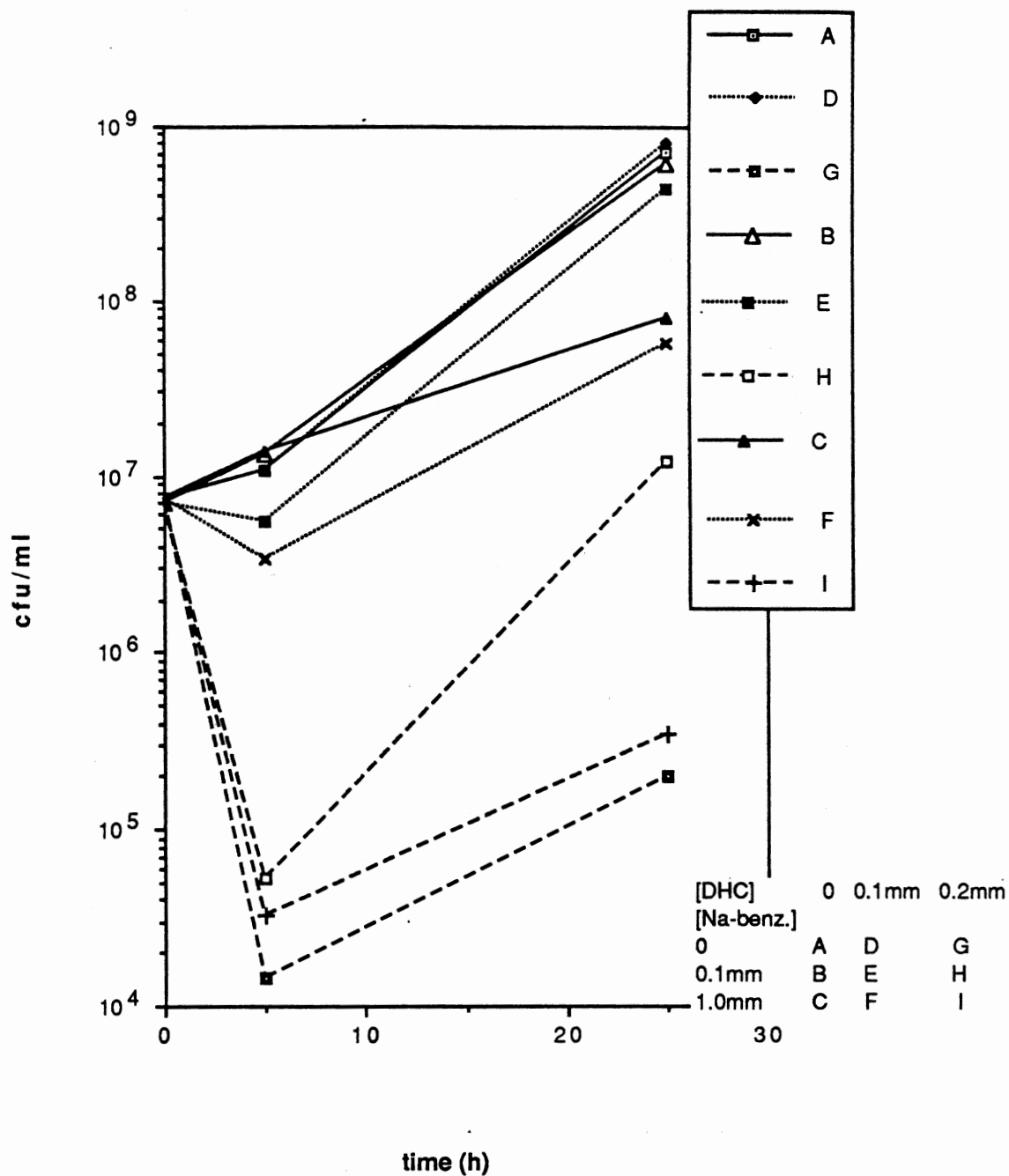
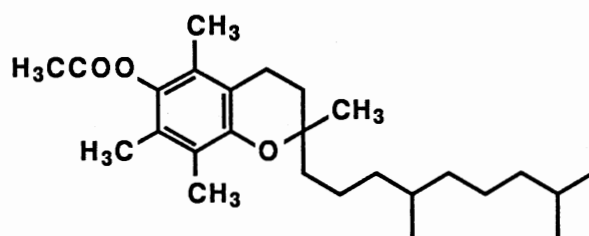


Fig. 14b Effect of Sodium Benzoate on Toxicity of DHC; Dark Conditions. Bioassay prepared and treated as in Fig.14a, except that samples were protected from light with foil throughout.

0.1 mM and 1.0 mM were used in combination with DHC. The 1.0 mM concentration of sodium benzoate was somewhat inhibitory toward Xcm in the control and 0.1 mM DHC conditions, and gave very slight protection from the toxicity of 0.2 mM DHC in the dark. Similarly, the 0.1 mM solution of sodium benzoate slightly inhibited Xcm growth relative to controls without the compound, except in the 0.2 mM DHC tubes, which indicated some protection.

SOD and Catalase. SOD, which catalyzes the conversion of the superoxide anion ($O_2^{\cdot-}$) to hydrogen peroxide; and catalase, which catalyzes the breakdown of hydrogen peroxide to water and oxygen, were assayed in a combined solution (Figs. 15a & 15b). This combination would be expected to interfere with toxicity due to either superoxide or peroxide. Since the enzymes, particularly SOD, are not stable for extended periods at bioassay conditions, these assays were terminated at 7.5 hours. The combined enzymes offered considerable protection against DHC toxicity in all conditions tested. SOD and catalase also appeared to slightly stimulate growth in controls without DHC.



α -tocopherol acetate

Vitamin E (α -tocopherol). Vitamin E is able to interact with several activated forms of oxygen. It both quenches and reacts with (scavenges) singlet oxygen, and can scavenge superoxide, peroxy radicals and other free radicals. Vitamin E and vitamin C (Na-

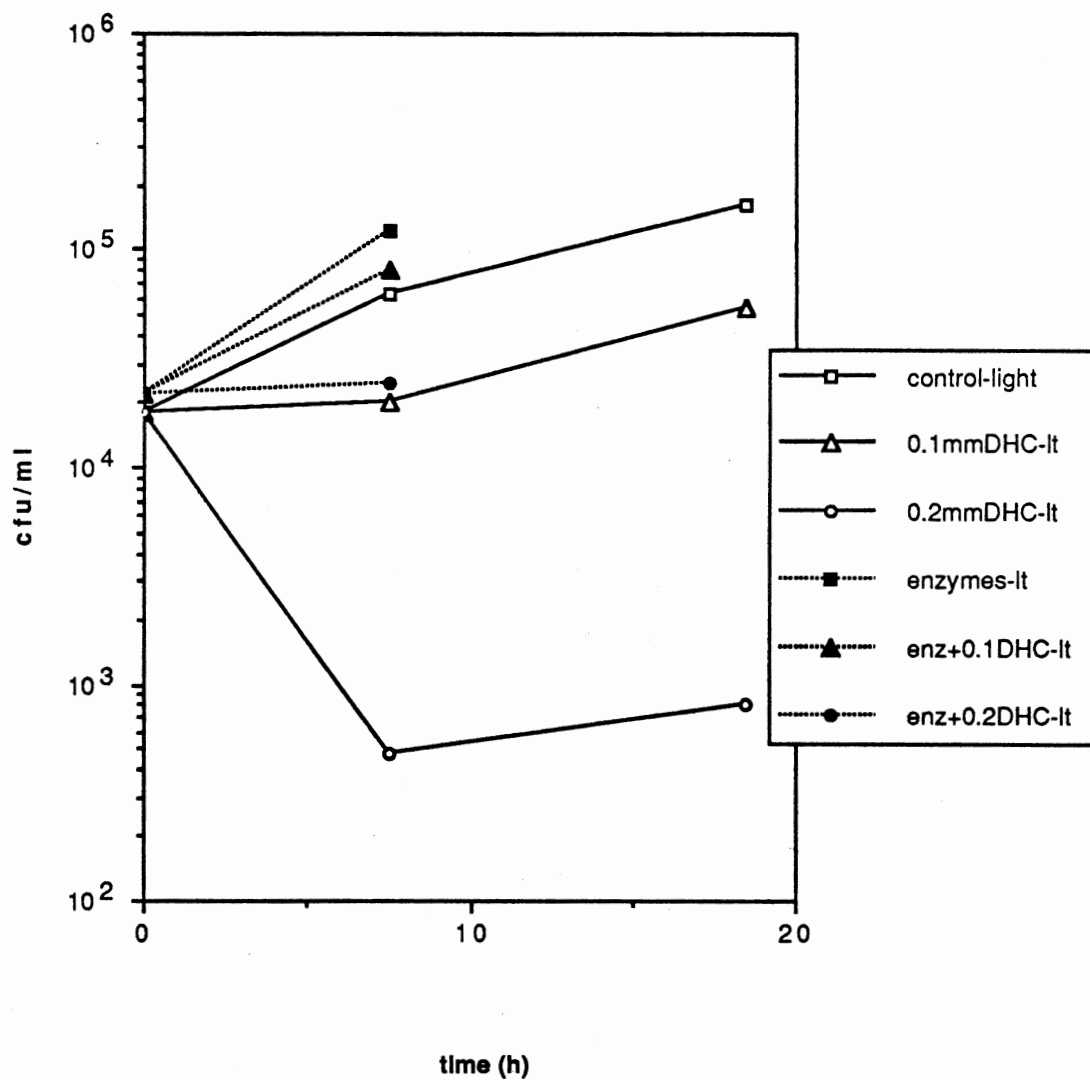


Fig. 15a Effect of SOD and Catalase on Toxicity of DHC; Light Conditions. DHC, at 0, 0.1, and 0.2 mM was dissolved in a suspension of Xcm in MOPS medium containing SOD (0.2 mg/ml, ~25.1 units/ml) and catalase (0.1 mg/ml, 100 units/ml) or without enzymes. The samples containing enzymes were plated at 7.5 hours; control samples at 7.5 and 18.5 hours. Bioassay method I.

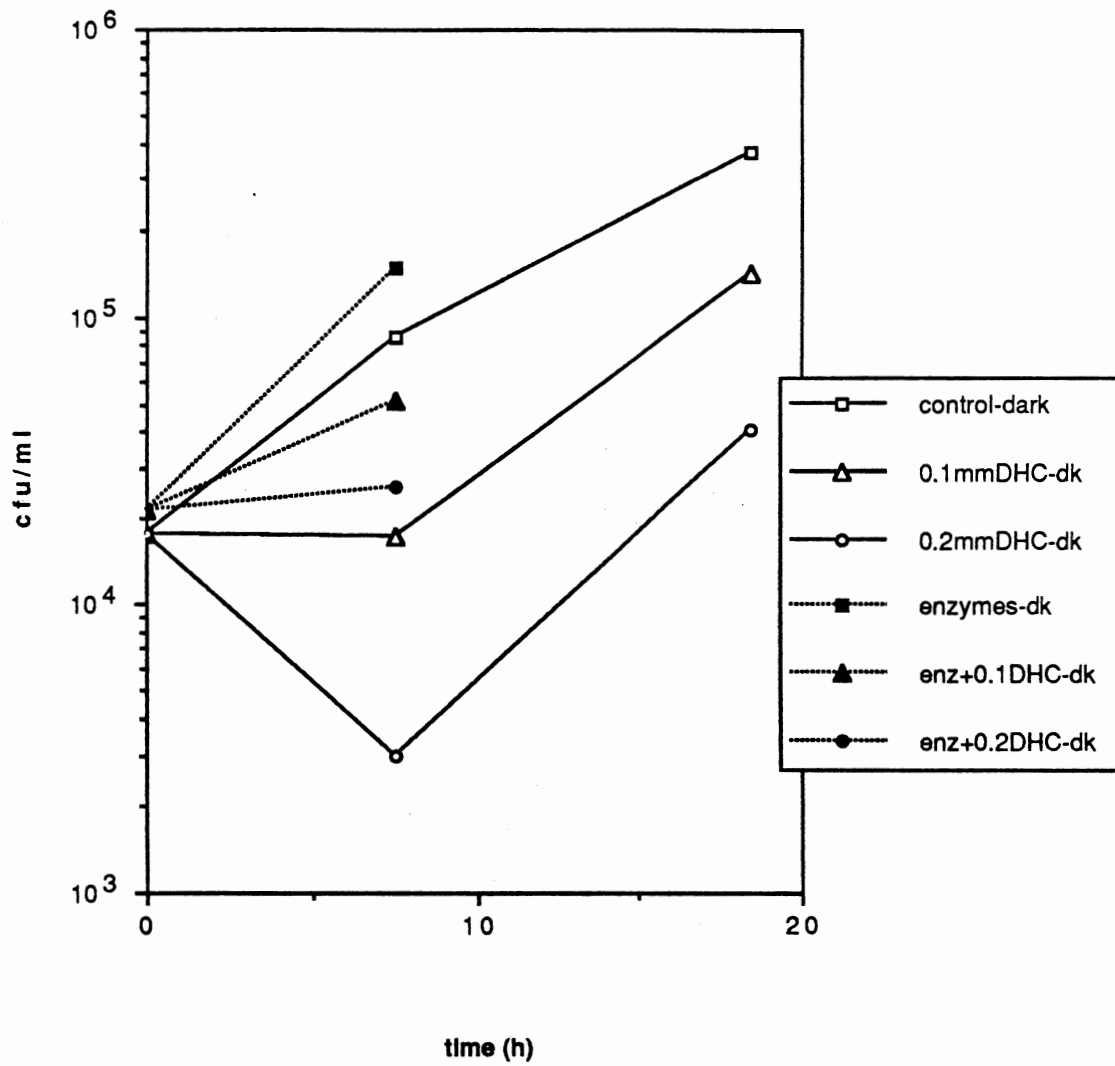


Fig. 15b Effect of SOD and Catalase on Toxicity of DHC; Dark Conditions. Bioassay prepared and treated as in Fig. 15a, except samples were protected from light with foil.

ascorbate) were both tested for toxicity toward Xcm (Figs. 16a & 16b). Vitamin E had very little toxicity toward the bacteria, and the concentration used was limited only by solubility. Vitamin C was toxic or inhibitory, although when vitamin C was combined with vitamin E, the toxic effect was decreased. To test the possible ability of vitamin E to interact with the toxic species in DHC inhibition, vitamin E and DHC were bioassayed in combination in both light and dark conditions (Figs. 17a & 17b). Vitamin E is quite insoluble in water, and was prepared for this experiment in ethanol, which was diluted to 1% in the bioassay tubes. Vitamin E, at 3 mM, provided no significant degree of protection in any of the conditions assayed, with the exception of the 0.1 mM DHC assay performed in the light. In this condition, a small protective effect by vitamin E was observed.

Sequestrene 138 and DTPA. Two compounds capable of chelating iron salts were assayed with DHC and Xcm to investigate the possible involvement of iron salts in generation of the toxic species in DHC inhibition. Since iron is an essential nutrient for Xcm, the chelators were themselves inhibitory toward Xcm growth. This effect was decreased either by lowering the chelator concentration, or by limiting the duration of the experiment.

Sequestrene 138 was assayed at concentrations shown not to inhibit Xcm (see toxicity test, Figure 18, and controls without DHC, Figs. 19a & 19b). In the presence of 0.2 mM DHC in the light, Sequestrene 138 appeared to exert a small protective effect. This effect was not seen at the lower DHC concentration (0.1 mM), or in the dark. (Figs. 19a & 19b).

DTPA was assayed at a concentration of 0.5 mM, with DHC, in the presence and absence of light. (Figs. 20a & 20b) At this concentration, the DTPA did not inhibit Xcm growth over the short bioassay period. In this assay, the Xcm + DTPA solution used for the DHC + DTPA condition was prepared separately and had a different initial Xcm

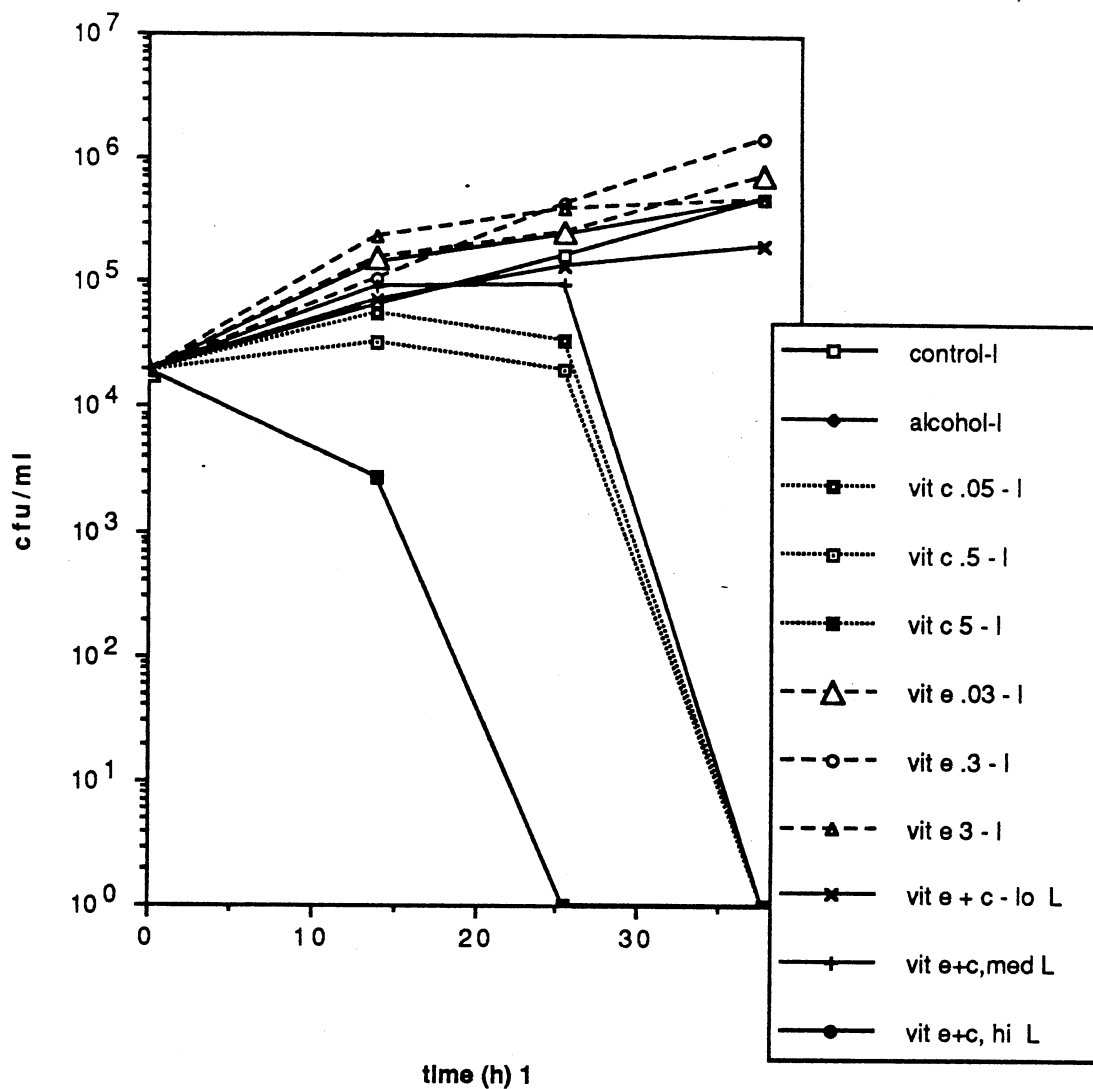


Fig.16a Toxicity of Vitamins E and C Toward Xcm; Light Conditions. Vitamin c in concentrations of 0.05, 0.5, and 5.0 mM; vitamin E, in concentrations of 0.03, 0.3, and 3.0 mM; and combinations of the two vitamins; "lo" (vitamin E, 0.03 mM and vitamin c 0.05 mM), "med" (vitamin E, 0.3 mM and vitamin C, 0.5 mM), and "hi" (vitamin E, 3 mM and vitamin C 5 mM) were added, to the stated final concentrations, to a suspension of Xcm in MOPS. Samples exposed to light; bioassay method I.

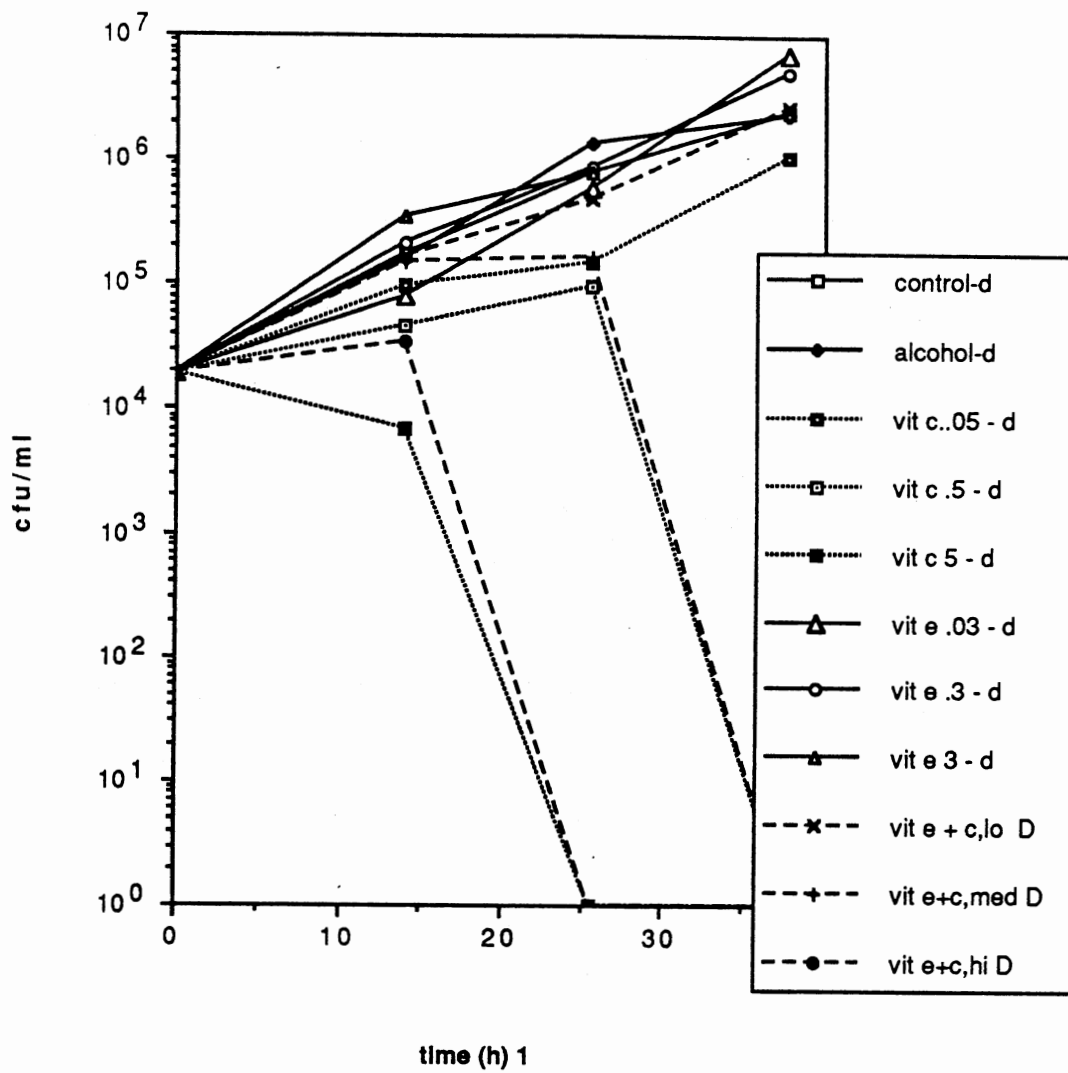


Fig. 16b Toxicity of Vitamins E and C Toward Xcm; Dark Conditions. Conditions as described for Fig. 16a, except all samples protected from light with aluminum foil.

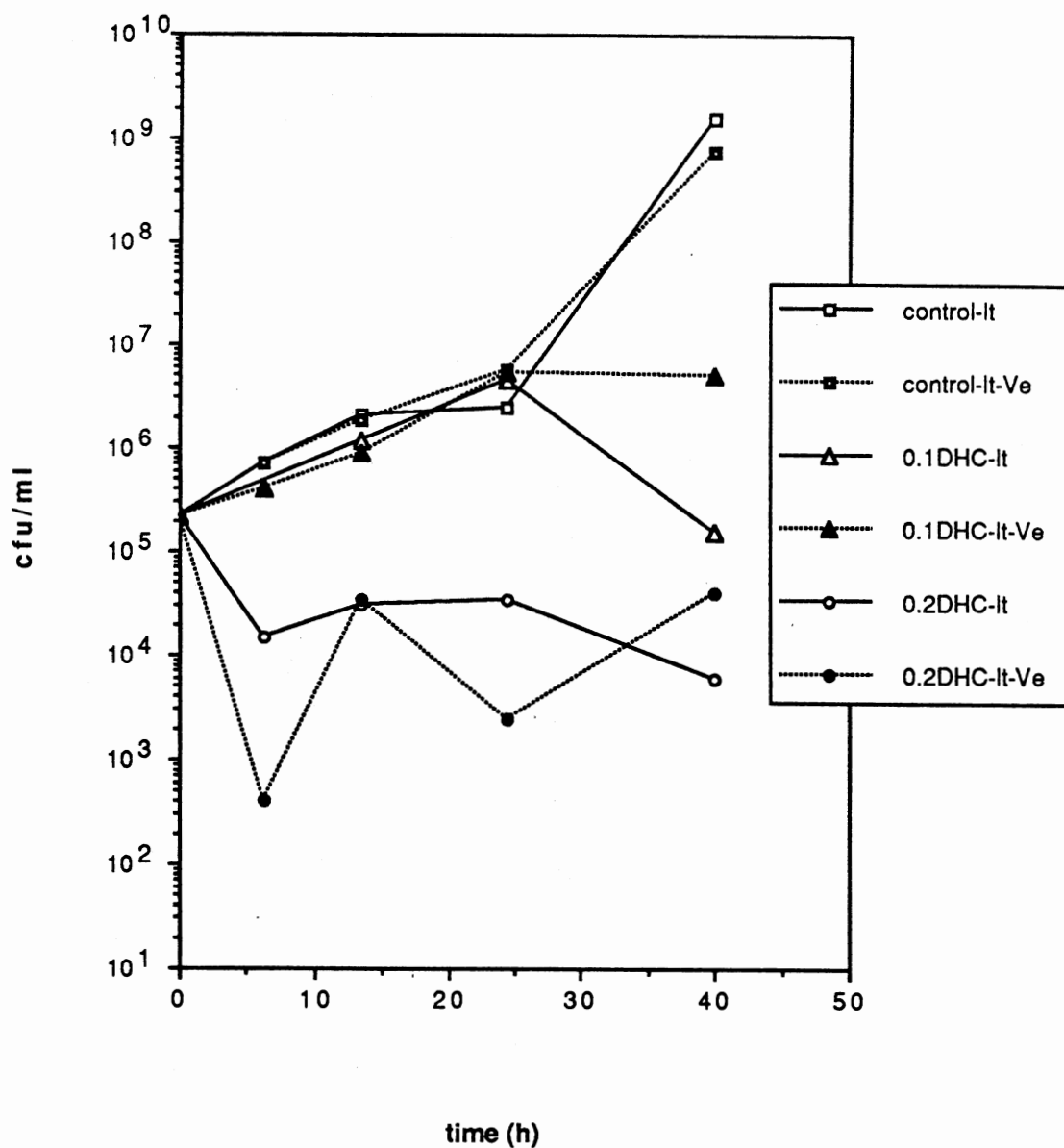


Fig. 17a Effect of Vitamin E on Toxicity of DHC; Light Conditions. DHC, (0, 0.1, and 0.2 mM) was dissolved in a suspension of Xcm in MOPS medium. Vitamin E (3 mM) was suspended in the indicated samples. All samples exposed to light; bioassay method I

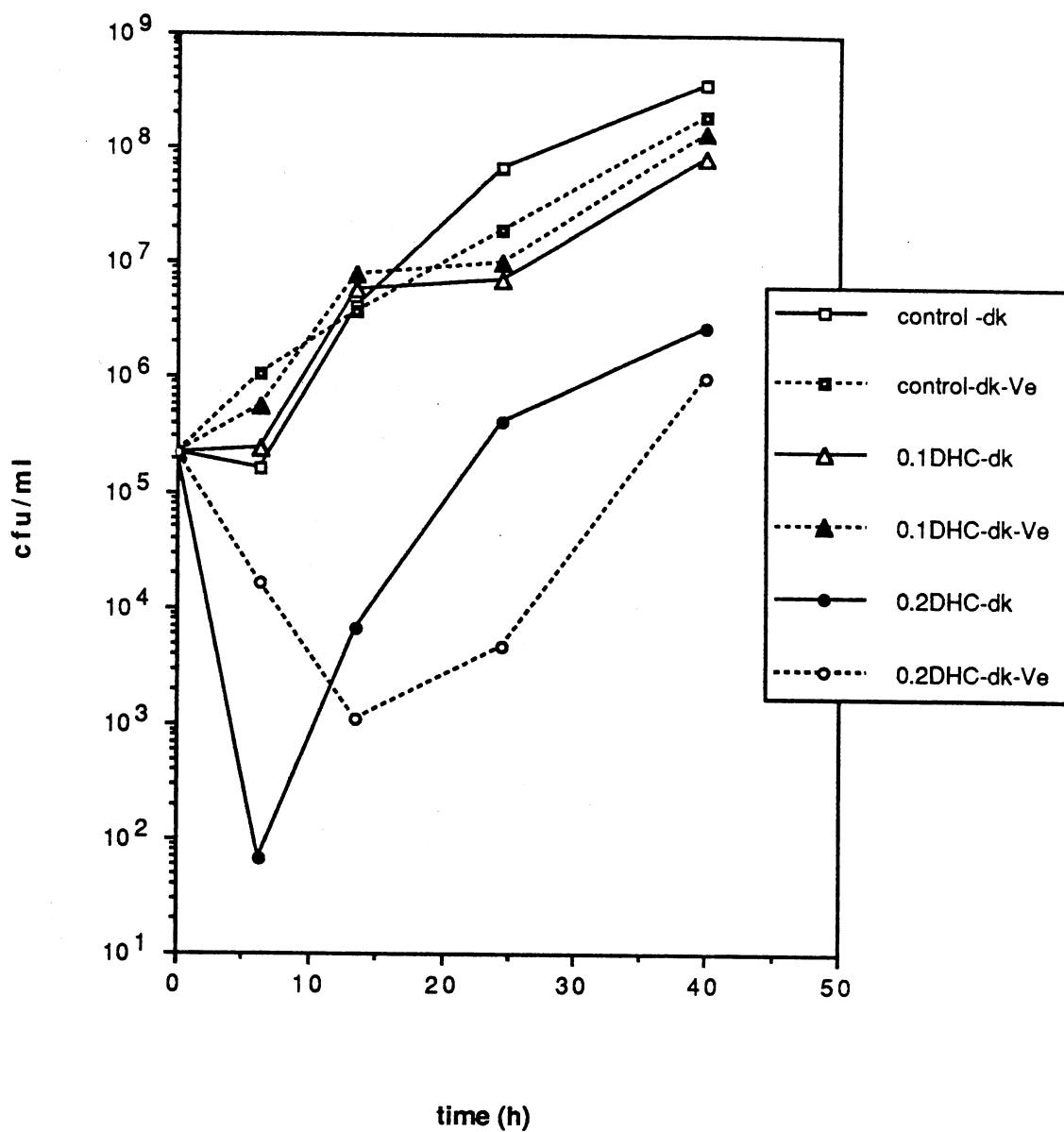


Fig. 17b Effect of Vitamin E on Toxicity of DHC; Dark Conditions. Bioassay handled concurrently with and as described in Fig. 17a, except all tubes were protected from light with foil.

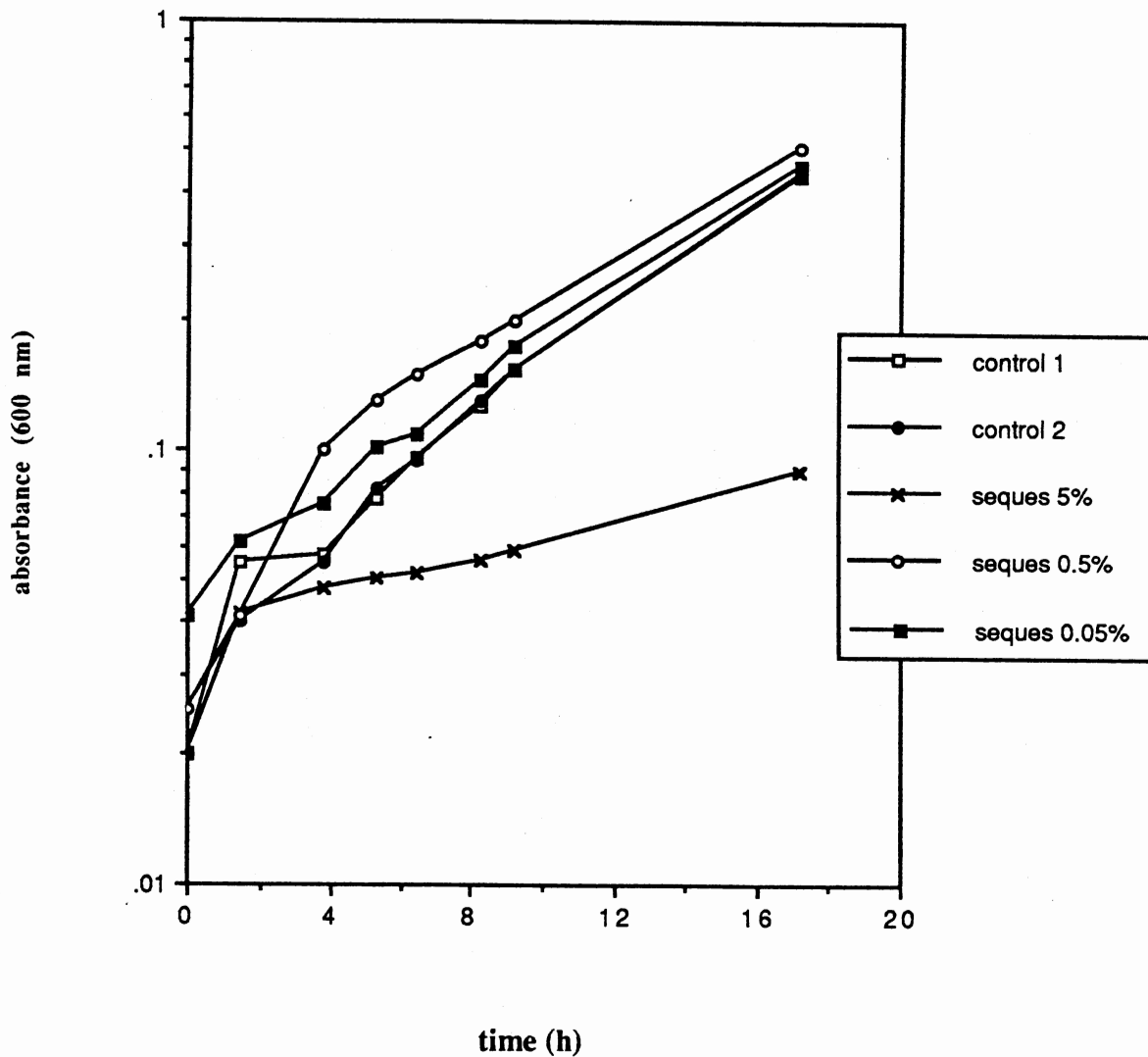


Fig. 18 Toxicity of Sequestrene 138 toward Xcm; Light Conditions. Growth curve of five log-phase cultures (10 ml each) of Xcm in MOPS medium; filter-sterilized sequestrene 138 was added to three cultures to final concentrations of 5, 0.5, and 0.05% (w/v). Bacterial concentration was estimated by monitoring A_{600} on a Coleman Jr. Spectrometer.

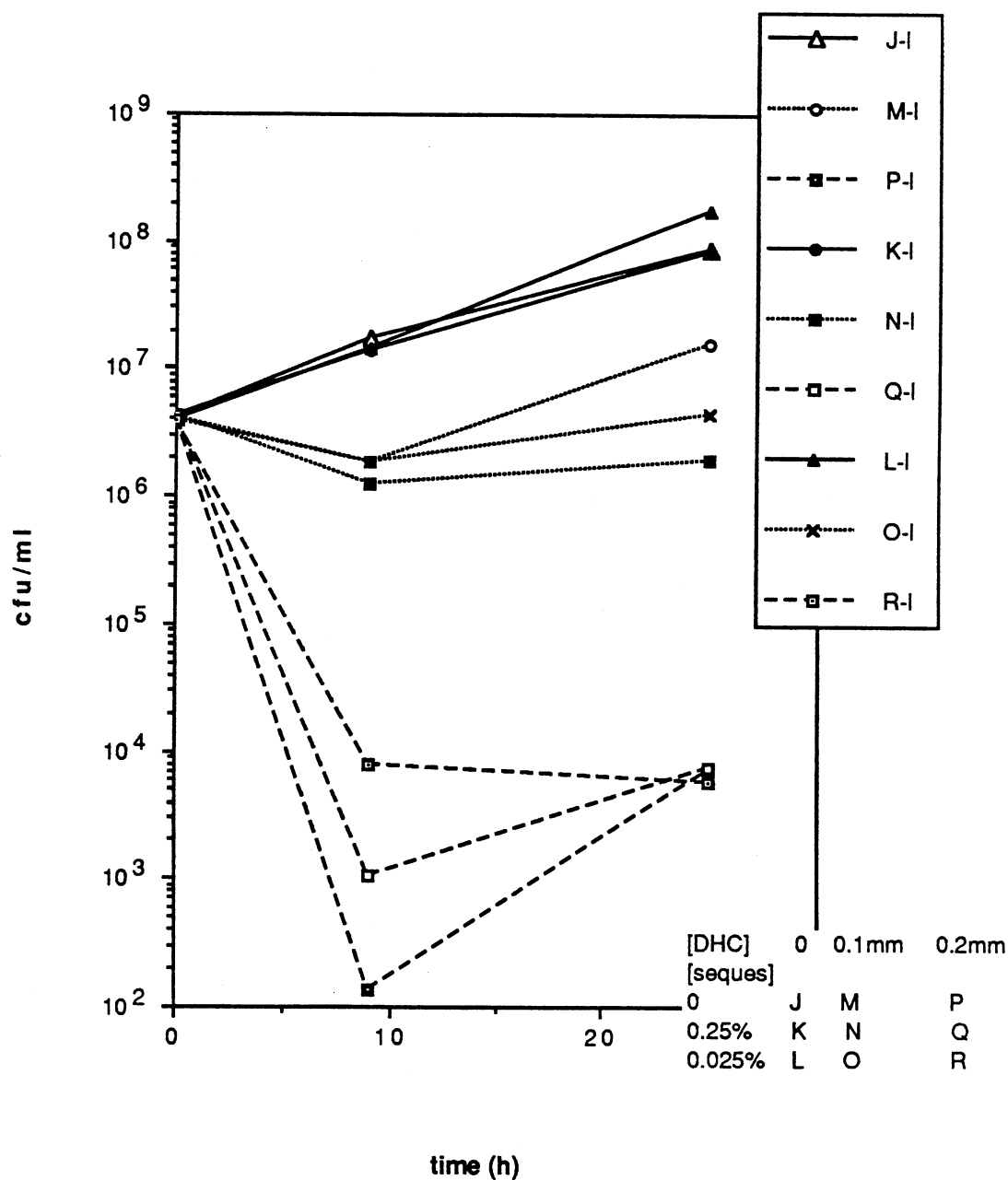


Fig. 19a Effect of Sequestrene 138 on Toxicity of DHC; Light Conditions. DHC (0, 0.1, and 0.2 mM) was dissolved in an Xcm suspensin in MOPS medium containing 0, 0.25 or 0.025% sequestrene 138. All samples exposed to light; bioassay method I.

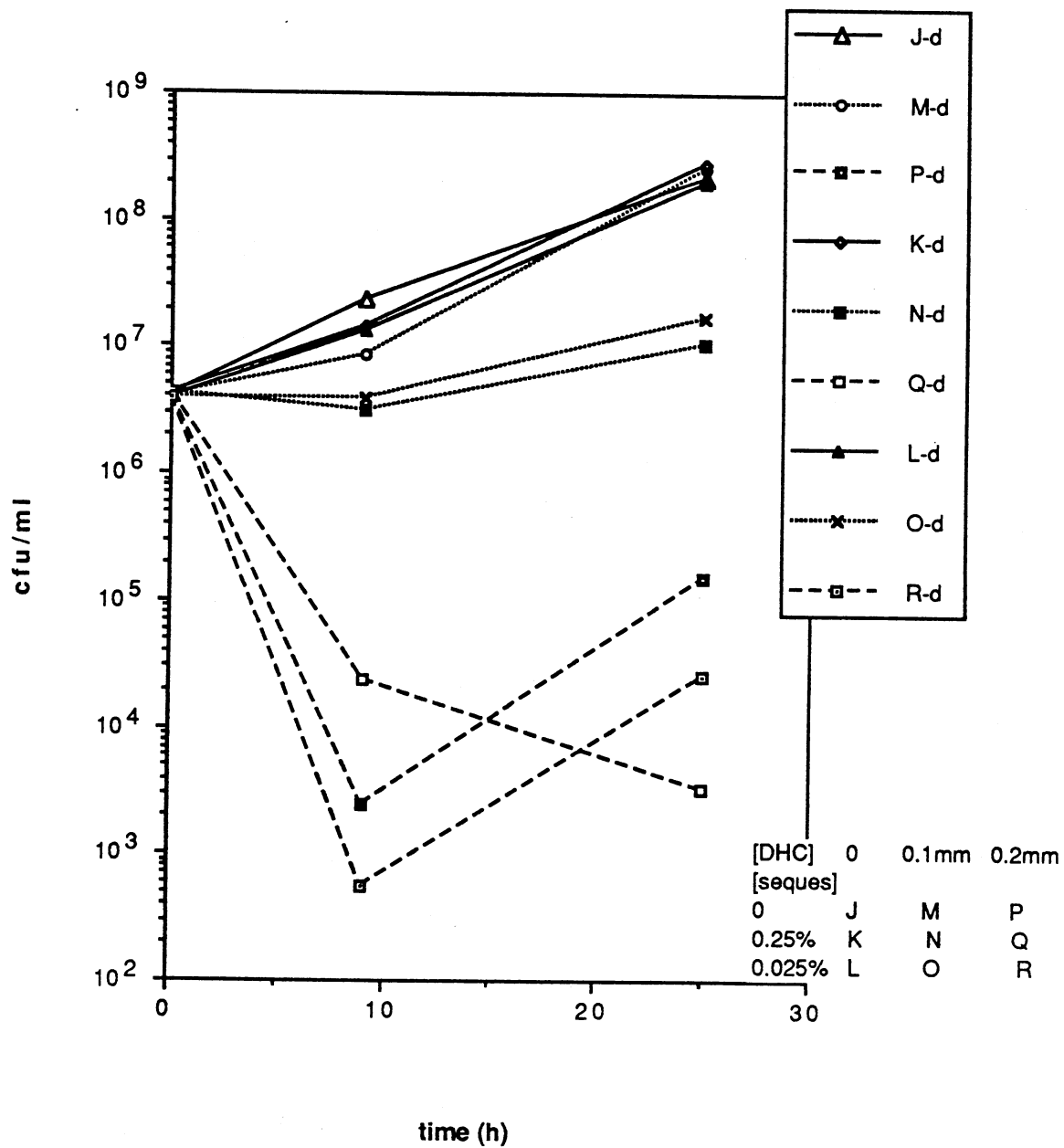


Fig. 19b Effect of Sequestrene 138 on Toxicity of DHC; Dark Conditions. Bioassay handled as described in Fig. 19b, and concurrently, except all samples protected from exposure to light with foil.

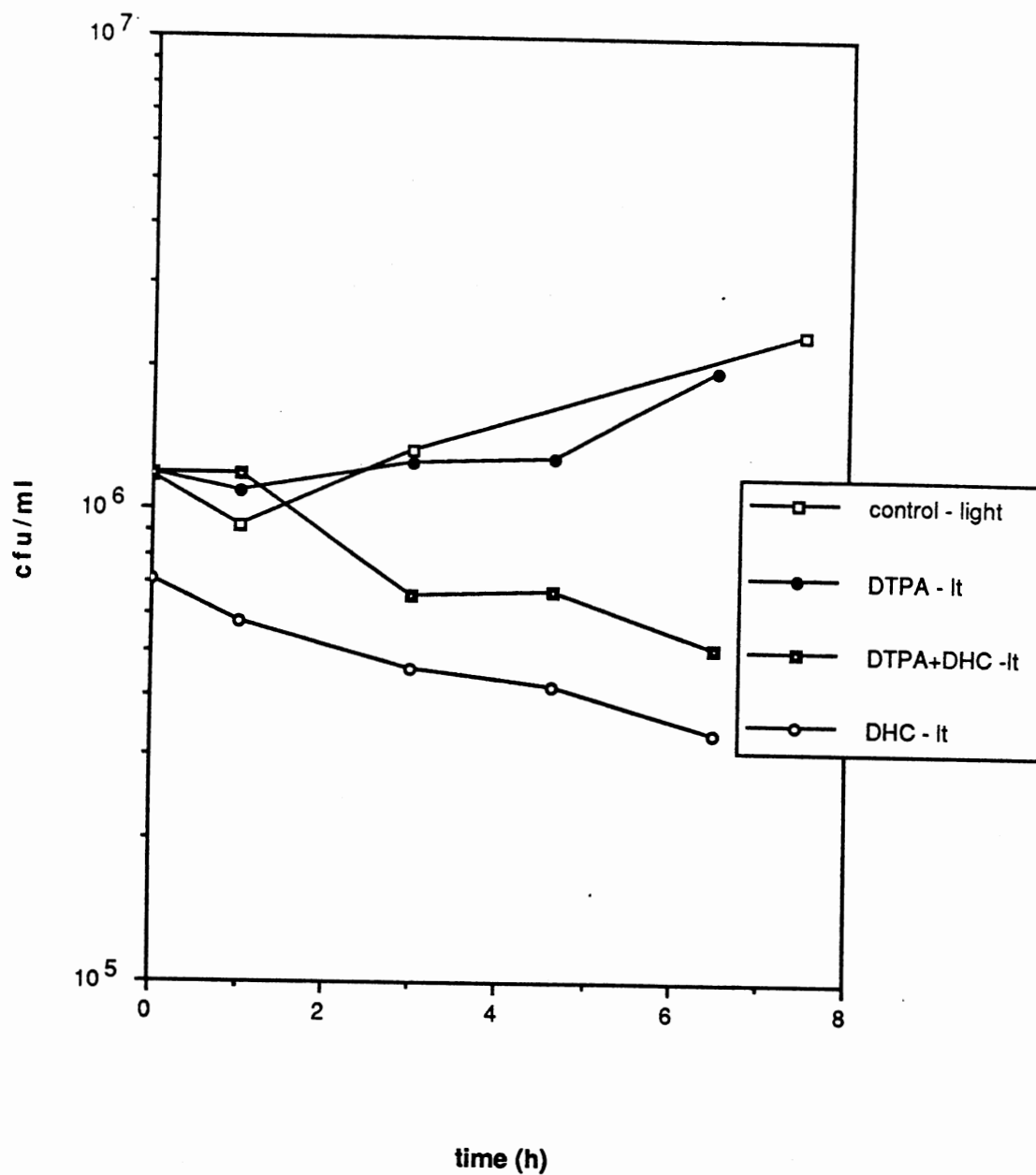


Fig. 20a Effect of DTPA on Toxicity of DHC; Light Conditions. DHC (0 or 0.15 mM) was dissolved in an Xcm suspension with DTPA (0 or 0.5 mM). Samples exposed to light; bioassay method II

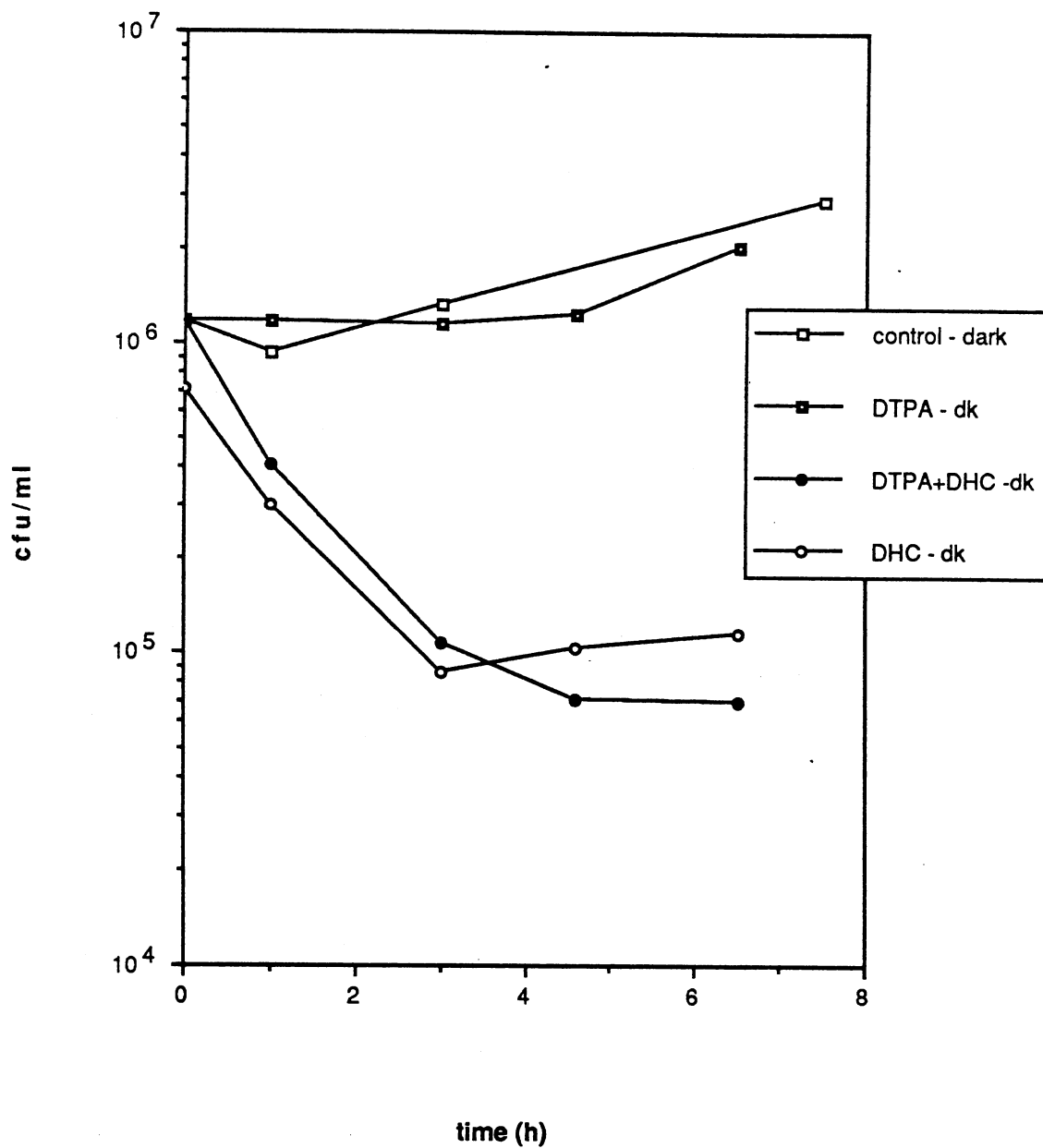


Fig. 20b Effect of DTPA on Toxicity DHC; Dark Conditions. Performed concurrently and under same conditions described in Fig. 20a, except all tubes were protected from light with foil.

concentration. No protection by DTPA against DHC toxicity was observed in either light or dark conditions.

DISCUSSION

The toxicity of DHC toward Xcm in these bioassays was considerably greater than that observed, using different bioassay conditions, by Essenberg *et al.* (1). The greater toxicity under the conditions used in this report was quite consistent. The plant-derived and synthetic preparations of DHC showed essentially identical toxicities, both in a dark assay, harvested at a single time (Fig. 1) and in a time-course assay with both light and dark conditions (Figs 2a & 2b). The bioassays shown in Fig. 3 were used to choose bioassay conditions which gave the best opportunity for observing effects on the light-activated toxicity of DHC. From these data, a starting bacterial concentration of 1×10^5 cfu/ml was chosen as giving the best separation of light and dark toxic effects at a DHC concentration of 0.1 mM.

Photo-activation of DHC to stimulate its toxicity toward bacteria has been previously reported (2) and was reproduced using the bioassay conditions described here. Exposure to intense light (300-700 nm), even with careful temperature control, was itself inhibitory to Xcm growth. The mechanism of this inhibition is not known, but a similar inhibition has been observed with *E.coli* (14). However, light exposure conditions were adjusted to produce no inhibition in a control sample (open diamonds, Fig. 4), yet show marked photo-stimulation of toxicity in the DHC-treated sample (open squares, Fig. 4).

Three other sesquiterpenoids isolated from resistant cotton lines inoculated with Xcm were tested for photo-activation of toxicity toward Xcm. This test was of interest, both for indicating the role of photoactivation in the disease response, and for the possible mechanistic information to be gained by comparisons among this group of highly structurally related compounds. Of the four sesquiterpenoids (DHC, LC, HMC and LCME), only DHC (Fig. 4) and LC (Fig. 5) showed photoactivation of toxicity. The

difference between the observed light and dark toxicity was even greater for LC than for DHC.

The LC assayed here was a racemic mixture prepared synthetically by oxidation of DHC. Plant-derived preparations of LC are strongly enriched in either the *R* or *S* enantiomer, depending on which cotton cultivar was used in isolation (1, 15). The *S* enantiomer is more toxic than the racemic mix, and the *R* form is much less toxic, in assays performed in the dark (1).

HMC, the 7-methyl ether of DHC, did not inhibit Xcm, either in the light or dark conditions used (Fig. 6). On the evidence to date, therefore, HMC cannot be considered to act as a phytoalexin in the cotton bacterial blight disease response. Since HMC is isolated in quantities comparable to, and often greater than, the other three sesquiterpenoids described here, its role in the disease response remains unexplained. It is possible that the very limited solubility of HMC under liquid-culture conditions does not reflect the conditions *in planta* particularly if the phytoalexins are associated with solubilizers or other carriers that aid their dispersion.

LCME showed a slight decrease in toxicity in the light (Fig. 7), in marked contrast to its close structural analog, LC (Fig. 5).

These results suggest a crucial role for the 7-hydroxy group in the photodynamic effect of these phytoalexins.

DHC is readily broken down in the presence of light and air. Since this degradation is almost certainly an ongoing process in the inoculated resistant cotton leaf, the properties of the degradation products are worthy of note.

An *ortho*-quinone structure has been tentatively assigned to a red product of DHC degradation under dark conditions. The toxicity of the proposed *ortho*-quinone toward Xcm, as assayed in the dark, is less than that of DHC, and is comparable to that of racemic LC. This compound has not been isolated from plant extracts, but may be present, at least transiently.

Fig. 9 compares the toxicity of DHC with that of its light degradation products. Degradation was allowed to proceed for 2 or 12 hours, and the assay was carried out in the light. The group of light products resulting from a 0.2 mM solution of DHC was sufficiently inhibitory toward Xcm to produce a bacteriostatic effect. The products of a 0.1 mM DHC solution (Fig. 9a) were less toxic.

Since these products are relatively stable in light, they may contribute to the long-term bacteriostatic effect observed in infected resistant leaves (Brinkerhoff & Essenberg, unpublished results).

The observation that DHC is degraded in the presence of light and/or air, coupled with the photo-stimulation of biological activity, suggests that DHC acts as a sensitizer in a photooxygenation reaction. Two general types of sensitized photooxygenations occur, as described by Foote *et al.* (16): Type I, in which the excited (triplet) sensitizer reacts directly with a substrate molecule to produce one or more free radical species, and Type II, in which the excited triplet-state sensitizer reacts with triplet (ground state) oxygen to produce singlet oxygen. Both types of reactions may occur in a single system, if the rates of reaction are comparable, and both groups of immediate products probably interact with other compounds to give a variety of possible end products.

Two compounds classified as singlet oxygen quenchers were used to probe the possible involvement of singlet oxygen in the photo-sensitization of DHC: DABCO, a tertiary aliphatic amine, and bixin, a water-soluble analog of β -carotene.

DABCO gave a partial protection against the light-activated toxicity of DHC. This effect was apparently only possible when DABCO was present in large (100X) excess to DHC. No protection was observed in the accompanying dark bioassay.

The requirement for an excess of DABCO might be explained by assuming that the DABCO is consumed in the reaction. However, Oannes and Wilson (10) in their report of singlet oxygen quenching by DABCO, assert that the DABCO is not oxidized. This is supported by Foote *et al.* (17). However, M. Daub, in experiments with the

photosensitizer cercosporin, reports data which can most readily be explained by consumption of DABCO during interaction with photo-activated cercosporin (12). It should be noted that later reports indicated the production of superoxide anion by the photoactivated cercosporin, as well as singlet oxygen, which may have contributed to consumption of DABCO (18).

If DHC acts as a Type II photosensitizer, it would not be consumed in the energy transfer which generates singlet oxygen. One DHC molecule could, therefore, potentially generate many singlet oxygen molecules, necessitating an excess concentration of DABCO for adequate quenching. Since reactions which cause degradation do occur to DHC under these conditions (described in Ch. 4 this work), the effective amount of DHC present and capable of generating singlet oxygen would decrease over time. Therefore, even if the DABCO present was consumed, the decrease in DHC concentration would probably help to maintain the relative DABCO excess.

It is also fairly probable that DHC is adsorbed onto the cell surface or even inserted into the cell membrane during the toxic interaction. Some phytoalexins exert their toxicity by disrupting membrane order (19). If DHC generates singlet oxygen under such conditions, only extremely prompt quenching could prevent biological damage. A high concentration of quencher might be the only means to ensure an appreciable frequency of collisions between the quencher and singlet oxygen under these conditions. If the DHC is partly or wholly buried in the membrane, accessibility of the singlet oxygen to DABCO would impose limits to the protection possible.

As with most compounds which interact with a reactive oxygen species, DABCO and β -carotene interact to at least some degree with other reactive oxygen species. DABCO and β -carotene have been reported to quench a highly reactive peroxy radical (20). Packer *et al.* also noted that DABCO was capable of quenching $\text{OH}\cdot$. Inhibition of the toxicity of DHC by DABCO, cannot, therefore, be considered sufficient evidence for the presence of singlet oxygen in the toxic interaction.

Bixin, which gave no protection to Xcm from DHC toxicity in the light, has been proposed as a singlet oxygen quencher based on its structural analogy to β -carotene; see structures, page 51. Foote *et al.* (21) reported that carotenoid quenching of singlet oxygen, which parallels its biological protection, is a sensitive function of the length of the conjugated polyene chain. Bixin, which differs from β -carotene in the substituents at the chain ends, has a 22-carbon chain with 9 double bonds, identical to that of β -carotene. M. Daub has shown that bixin quenches the photodynamic action of cercosporin, which generates singlet oxygen (12) and superoxide anion (18).

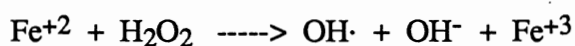
Bixin inhibited Xcm growth in the light, but not in the dark. In the dark, bixin provided partial protection to Xcm from the toxic effect of DHC. The dark reaction of DHC with Xcm is unlikely to involve singlet oxygen, since the known systems for non-photochemical generation of singlet oxygen utilize strong oxidizing species or an endoperoxide. DHC decomposes in the dark under bioassay conditions to LC and other products, as yet unidentified, (Chapter V, this work). If this reaction, a 2-electron oxidation, involves an intermediate free radical, bixin may interact with this free radical to produce a less toxic species, giving the protection shown in Fig. 13b.

Sodium benzoate was slightly inhibitory toward Xcm in both light and dark conditions. Unlike the effect of bixin, the inhibitory effect of sodium benzoate did not appear to be photodynamic. In combination with 0.1 mM DHC, which was only slightly inhibitory at this bacterial concentration, sodium benzoate exerted only a slight inhibition, comparable to that seen in the control solutions (light and dark conditions, Figs. 14a and 14b). When sodium benzoate was combined with a bactericidal concentration of DHC (0.2 mM), a partial protection was observed in the dark. No significant effect was exerted by sodium benzoate in the light with this concentration of DHC. The specificity of sodium benzoate for $\text{OH}\cdot$ (13), suggests that some of the toxicity of the DHC interaction in the dark is due to this activated species.

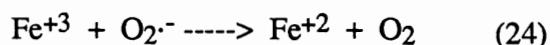
SOD and catalase, when assayed in combination with DHC, provided a quite marked protection to Xcm. This result, however, must be interpreted with consideration of the reaction between either of these enzymes and DHC reported in Chapter V, this work. In this observed reaction, SOD catalyzed the very rapid conversion of DHC to LC (or a compound spectrally identical to LC). Catalase promoted the same reaction, but more slowly. Since LC requires much higher concentrations to exert a toxic effect than does DHC, this conversion would have the effect of detoxifying the DHC treatment. Since this conversion of DHC to LC by SOD and catalase almost certainly occurred during the bioassay, no conclusion can be drawn about the presence or absence of superoxide or hydrogen peroxide in this system.

Vitamin E is able to interact with a variety of activated oxygen species in non-aqueous systems, but is chiefly described in aqueous biological systems as inhibiting membrane lipid peroxidation (22). With a negligible solubility in water, vitamin E, at 3 mM (the bioassay concentration) is probably adsorbed to the cell surfaces or the walls of the bioassay tube, or taken up into the cell membrane. Vitamin E uptake into the cell membrane is a necessary prerequisite to effective quenching of lipid peroxidation (23). The slight apparent protection of Xcm from 0.1 mM DHC in the light (Fig. 17a) may be an indication of involvement of lipid peroxidation, but is not conclusive. Since the vitamin E cannot be assumed to have reached the cell membrane, its target protection site, the failure of this scavenger to provide substantial protection is not conclusive evidence against lipid peroxidation by DHC.

The ability of ferrous ion to catalyze the formation of $\text{OH}\cdot$ has drawn attention to the role of iron salts in activated oxygen toxicity. If superoxide anion is present, Fe^{+2} catalyzes the following reaction:



Ferrous ion can then be regenerated:



Two chelators for iron salts were tested for inhibition of toxicity. DTPA, in particular, has been reported to prevent the redox reactions of Fe^{+3} . Fe^{+3} bound to EDTA, by contrast, is more readily reduced than unchelated Fe^{+3} (25). Very small concentrations of iron salts may suffice to catalyze the Fenton reaction. High concentrations of either chelator, which would be presumed to completely scavenge the iron salts from the medium, were toxic to Xcm, and could not be used. The chelator concentrations used almost certainly left some Fe^{+3} in the medium, permitting Xcm growth (Figs. 19 and 20). The lack of effect on DHC toxicity by iron chelators cannot be interpreted as eliminating the involvement of a Fenton-type reaction in DHC toxicity.

The series of scavengers and quenchers of reactive oxygen species used to probe the toxic interaction of DHC with Xcm did not conclusively identify a single species as the toxic agent. This should not be surprising, as most systems in which one type of activated oxygen has been identified, have been found to have other species present as well. (26)

The quenching protection by DABCO strongly suggests the involvement of O_2^1 as part, but not all, of the photo-dynamic toxicity. Since the quenched DHC photo-toxicity in this assay was still greater than that observed in the absence of light, another photo-activated species may be present.

Since both sodium benzoate and bixin provided some protection from toxicity in the dark, a free radical species, possibly $\text{OH}\cdot$, may be involved in the dark toxicity of DHC. The incompleteness of this protection suggests that either the radical is not free in solution [a ferryl (27) or "crypto-hydroxyl" (28) radical] and thus cannot efficiently be scavenged by the agents used, or the free radical may represent only one of a plethora of toxic effects exerted by DHC and its products.

REFERENCES

1. Essenberg, M., Doherty, M., Hamilton, B., Henning V., Cover, E., McFaul, S., and Johnson, W. (1982) Identification and effects on *Xanthomonas campestris*

- pv. *malvacearum* of two phytoalexins from leaves and cotyledons of resistant cotton. *Phytopathology* **72**, 1349-1356
2. Sun, T., Essenberg, M., and Melcher, U. Photactivated DNA cleavage, enzyme inactivation, and bacterial inhibition by sesquiterpenoid phytoalexins from cotton. Manuscript submitted.
 3. Spikes, J.D. (1977) Photosensitization. in *The Science of Photobiology*, ed. K.C. Smith, Plenum Press, New York, 87-112
 4. Towers, G.H.N. (1980) Photosensitizers in plants and their photodynamic action. *Progress in Phytochemistry* **6**, 183-202
 5. Morgham, A., Richardson, P., Essenberg, M., and Cover, E. (1988) Effects of continuous dark upon ultrastructure, bacterial populations and accumulation of phytoalexins during interactions between *Xanthomonas campestris* pv. *malvacearum* and bacterial blight susceptible and resistant cotton. *Physiological and Molecular Plant Pathology* **32**, 141-162
 6. Teresa, J., Mateos, A. and Gonzalez, R. (1982) The synthesis of 2-hydroxy-4-isopropyl-7-methoxy-1,6-dimethyl naphthalene, "chemical precursor" of the byssinotic agent from cotton. *Tetrahedron Letters*. **23**, 3405-3406
 7. Niedhardt, F., Bloch, P. and Smith, D. (1974) Culture medium for enterobacteria. *Journal of Bacteriology* **119**,736-747
 8. McNally, K., Gabriel, D. and Essenberg, M. (1984) Useful minimal media for *Xanthomonas campestris* pv. *malvacearum*. *Phytopathology* **74**, abstract #A685, p.875
 9. Mohan, K., Knight, W., Chen, K., Lewin, I., and Heinisch, R. (1980) *Health and Human Services Publication* FDA 81-8136, p.174
 10. Oannes, C. and Wilson, T. (1968) Quenching of singlet oxygen by tertiary aliphatic amines. Effect of DABCO. *Journal of the American Chemical Society* **90**, 6257-6258
 11. Foote, C. and Denny, R. (1968) Chemistry of singlet oxygen VIII. Quenching by β -carotene. *Journal of the American Chemical Society* **90** 6233-6235
 12. Daub, M. (1982) Cercosporin, a photosensitizing toxin from *cercospora* species. *Phytopathology* **72**, 370-374
 13. Winston, G. and Cederbaum, A. (1985) Decarboxylation of 7-¹⁴C-Benzoic Acid, in *CRC Handbook of Methods for Oxygen Radical Research*. Ed., R. Greenwald, CRC Press, Boca Raton, FA, 169-175
 14. Davis, B.D., Dolbecco, R., Eisen, H.N., Ginsberg, H.S., Wood, W.B., and McCarty, M. (1973) *Microbiology*, Second Ed. Harper & Row, Hagerstown, MD.p. 237
 15. Stipanovic, R., McCormick, J., Schlemper, E., Hamper, B., Shinmyozu, T., and Pirkle, W. (1986) Corroboration of techniques for assigning absolute

configuration: lacinilene C methyl ether as an exemplary study. *Journal of Organic Chemistry* **51**, 2500-2504

16. Foote, C. (1976) Photosensitized oxidation and singlet oxygen: consequences in biological systems., in *Free Radicals in Biology, Vol II*, Ed., W. Pryor, Academic Press, New York, 85-93
17. Foote, C., Shook, F. and Abakerli, R. (1984) Characterization of singlet oxygen. in *Methods in Enzymology, Vol. 105*, Ed., L. Packer, Academic Press, Orlando, FA., 36-47
18. Daub, M. and Hangarter, R. (1983) Light-induced production of singlet oxygen and superoxide by the fungal toxin, cercosporin. *Plant Physiology* **73**, 855-857
19. Weinstein, L. and Albersheim, P. (1983) Host-pathogen interactions. XXIII. The mechanism of the antibacterial action of glycinol, a pterocarpan phytoalexin synthesized by soybeans. *Plant Physiology* **72**, 557-563
20. Packer, J., Mahood, J., Mora-Arellano, V., Slater, T., Willson, R., and Wolfenden, B. (1981) Free radical and singlet oxygen scavengers: reaction of a peroxy-radical with b-carotene, diphenyl furan and 1,4-diazobicyclo (2,2,2)-octane. *Biochemical and Biophysical Research Communications* **98**, 901-906
21. Foote, C., Chang, Y. and Denny, R. (1970) Chemistry of singlet oxygen. X. Carotenoid quenching parallels biological protection. *Journal of the American Chemical Society* **92**, 5216-5219
22. Buttriss, J. and Diplock, A. (1984) High performance liquid chromatography methods for vitamin E in tissues. in *Methods in Enzymology, Vol. 105*, Ed. L. Packer, Academic Press, Orlando, FA. 131-138
23. Tinberg, H.M., and Barber, A. A. (1970) Studies on vitamin E action: peroxidation inhibition in structural protein-lipid micelle complexes derived from rat liver microsomal membranes. *Journal of Nutrition* **100**, 413-418
24. Halliwell, B. (1978) Superoxide-dependent formation of hydroxyl radicals in the presence of iron chelates. *FEBS Letters* **92**, 321-326
25. Butler, J. and Halliwell, B. (1982) Reaction of iron-EDTA chelates with the superoxide radical *Archives of Biochemistry and Biophysics* **218**, 174- 178
26. Singh, A. (1982) Chemical and biochemical aspects of superoxide radicals and related species of activated oxygen. *Canadian Journal of Physiological Pharmacology* **60**, 1330-1345
27. Imlay, J. A., Chin, S.M. and Linn, S. (1988) Toxic DNA damage by hydrogen peroxide through the Fenton reaction *in vivo* and *in vitro*. *Science* **240**, 640-642
28. Moorhouse, C., Halliwell, B., Grootveld, M. and Gutteridge, J. (1985) Cobalt (II) ion as a promoter of hydroxyl radical and possible 'crypto-hydroxyl' radical formation under physiological conditions. Differential effects of hydroxyl radical scavengers. *Biochimica et Biophysica Acta* **843**, 261-268

CHAPTER V

TWO REACTIONS OF DHC UNDER BIOASSAY CONDITIONS: A PHOTO-ACTIVATED GENERATION OF A FREE RADICAL, AND AN FE^{+3} -DEPENDENT OXIDATION TO FORM LACINILENE C

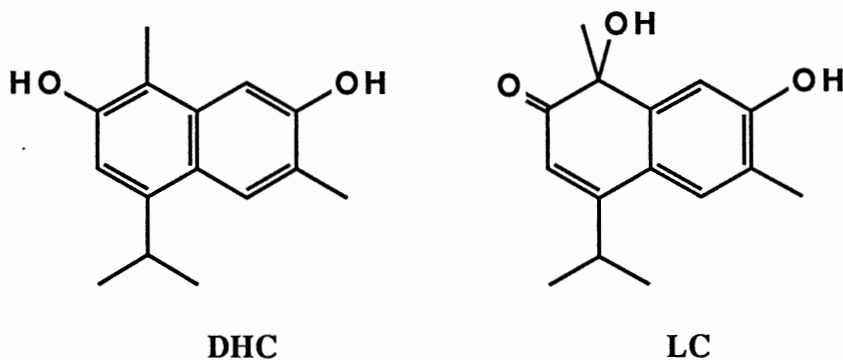
Joy Steidl¹, E. J. Eisenbraun² and Margaret Essenberg¹

¹Department of Biochemistry, and ²Department of Chemistry, Oklahoma State University, Stillwater, Oklahoma, U.S.A., 74078

Abbreviations used: DHC, 2,7-dihydroxycadalene; LC, lacinilene C; LCME, lacinilene C 7-methyl ether; HMC, 2-hydroxy, 7-methoxycadalene; Xcm, *Xanthomonas campestris* pv. *malvacearum*, SOD, superoxide dismutase; DABCO, diazobicyclo (2,2,2) octane; DTPA, diethylenetriamine pentaacetic acid; MOPS, 3-(N-morpholino) propanesulfonic acid; AET, S,2-aminoethyl-isothiuronium bromide hydrobromide; MEG, 2-mercaptoethyl guanidine hydrobromide; GED, bis(2-guanidinoethyl) disulfide; OH·, hydroxyl radical; O_2^1 singlet oxygen; O_2^- , superoxide anion; PBN, phenyl *t*-butylnitron; and DMPO, 5,5-dimethylpyrroline N-oxide.

ABSTRACT

DHC, a phytoalexin produced by cotton against bacterial leaf blight, has antibacterial activity which is markedly stimulated by light. DHC undergoes two distinctly different degradation reactions: a light-dependent reaction blocked by AET and inhibited by crocin; and an Fe^{+3} -dependent reaction which occurs in the dark and produces LC as a major product. DHC generated or was converted to a free radical in the light which was trapped by PBN, with $A_N = 15.24$ and $A_H = 3.53$ G. Both the splitting constants and the broadened appearance of the spectrum suggested the presence of more than one trapped species.



INTRODUCTION

Lines of Upland cotton resistant to bacterial leaf blight initiate a rapid response following inoculation by the causative agent of the disease, *Xanthomonas campestris* pv. *malvacearum* (Xcm). Part of this response is *de novo* synthesis of a group of sesquiterpenoids, including 2,7-dihydroxycadalene (DHC), lacinilene C (LC), and their 7-methyl ethers (HMC, and LCME, respectively) (1).

DHC, LC, and LCME inhibit the growth of Xcm in liquid culture (*ibid*) and the toxicity of DHC and LC is markedly stimulated by exposure to light (2).

The mechanism of toxicity of DHC (the most potent phytoalexin in this group) is unknown. The use of several scavengers and quenchers of reactive oxygen species produced no definitive conclusions about the mechanism of light activation or the inhibition in the dark (Chapter IV), perhaps because the toxic reactions occur inside the bacterial plasma membrane or in the cytoplasm, or because several toxic reactions are involved.

To characterize the chemical reactions of DHC under bioassay conditions, the investigation was carried out in a simplified system, using the bioassay medium (MOPS medium), but omitting the bacteria. The concentration of DHC was monitored by its intense UV absorption, and reactions in light/dark conditions, in the presence and absence of iron salts (Fe^{+2} and Fe^{+3}), under anaerobic conditions, and in the presence of DABCO, crocin, Na-benzoate, mannitol, several metallo-proteins, AET and PBN were carried out.

RESULTS

Effect of Fe and Light on DHC Degradation

When DHC was exposed to light under conditions identical to those applied during bioassays of DHC with Xcm, the DHC was rapidly degraded. The progress of this reaction was observed using UV-visible spectroscopy. As shown in Fig. 1, the absorption spectrum of DHC has an intense peak at 237 nm ($\epsilon = 7.26 \times 10^4 \text{ M}^{-1}\text{cm}^{-1}$). The absorption spectrum of the degradation products of a sample of DHC exposed to light until the reaction had apparently gone to completion is shown in Fig. 2. The light products of DHC had no sharply defined peak but showed an absorption at 237 nm which was 21% that of the fresh sample (average of seven degradations). Subsequent separation of a degradation product mixture by HPLC showed that no DHC was present in a sample with the typical spectrum seen in Fig. 2.



Fig. 1 UV-visible Absorption Spectrum of DHC, 10.3 μM in MOPS Medium; Scanned with MOPS Medium Blank.

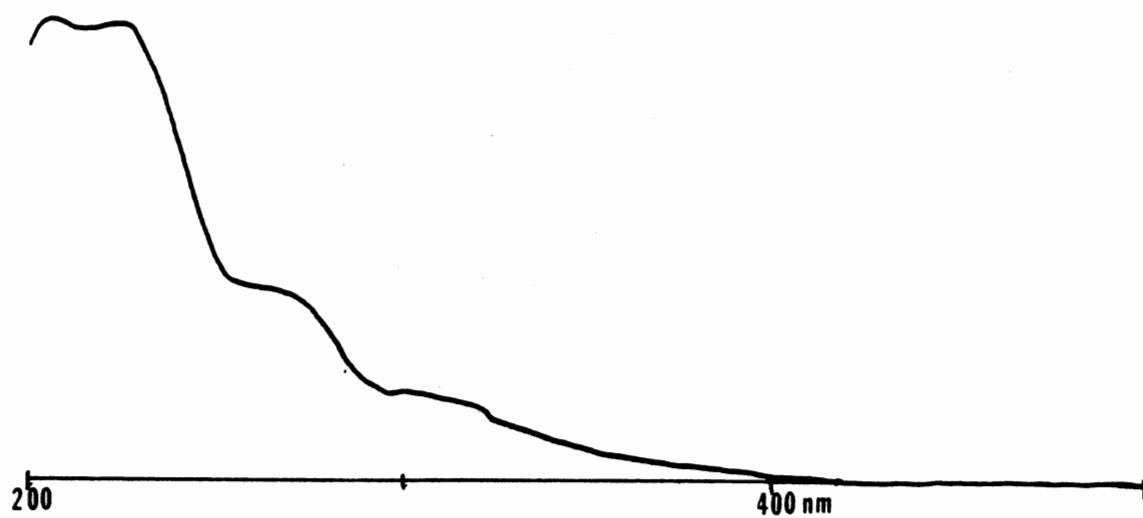


Fig. 2 UV-visible Absorption Spectrum in MOPS Medium of an Equal Sample from DHC solution Shown in Fig. 1, after Exposure to Light for 7 h.

DHC mixed with the bioassay medium (MOPS medium) and protected from exposure to light was also degraded. A typical spectrum of these degradation products is shown in Fig. 3. This spectrum has marked similarities to that of LC (Fig. 4), suggesting that one of the major degradation products is LC. LC has been previously observed to be generated as an oxidation product of DHC (3). Unlike DHC and the light products of DHC, the dark degradation products showed a significant absorption at 343 nm. Although the 250 nm absorption of the degradation products is more intense than the 343 band, the appearance of the 343 nm absorbance was chosen as the most specific monitor for the progress of the dark degradation reaction because both DHC and its light-degradation products have significant absorption at 250 nm and none at 343 nm.

In order to test the possible involvement of iron salts in the rapid degradation of DHC observed in bacterial bioassay conditions, MOPS medium, in which the studies were carried out, was prepared without added iron salts. (Iron salts of unknown or unspecified oxidation state present in these experiments will be referred to simply as 'Fe'. No metallic Fe was used in these studies.) MOPS medium usually contains $10\mu\text{M}$ Fe, added as $\text{FeSO}_4 \cdot 7\text{H}_2\text{O}$, which is probably spontaneously oxidized to Fe^{+3} . Fig. 5a shows the degradation of DHC, monitored by UV spectroscopy, in the presence and absence of added Fe, and in both light and dark conditions. The absence of Fe had a greater effect on the degradation of DHC in the dark, markedly inhibiting this reaction. However, the light-activated degradation was also slowed by the omission of Fe from the reaction medium. These experimental data when replotted with a semilog scale in Fig. 5b, gave approximately straight lines, indicating that the degradation reaction proceeded with first-order or pseudo-first-order kinetics. The appearance of LC during the dark degradation of DHC is shown in Fig 5c, as a semilog plot. The appearance of product is also a linear function in this reaction, again indicating first-order or pseudo-first-order kinetics.

When an Fe chelator, DTPA, was added to the MOPS medium prepared without Fe, inhibition of the degradation of DHC in the dark was even more marked (Fig. 6). Under

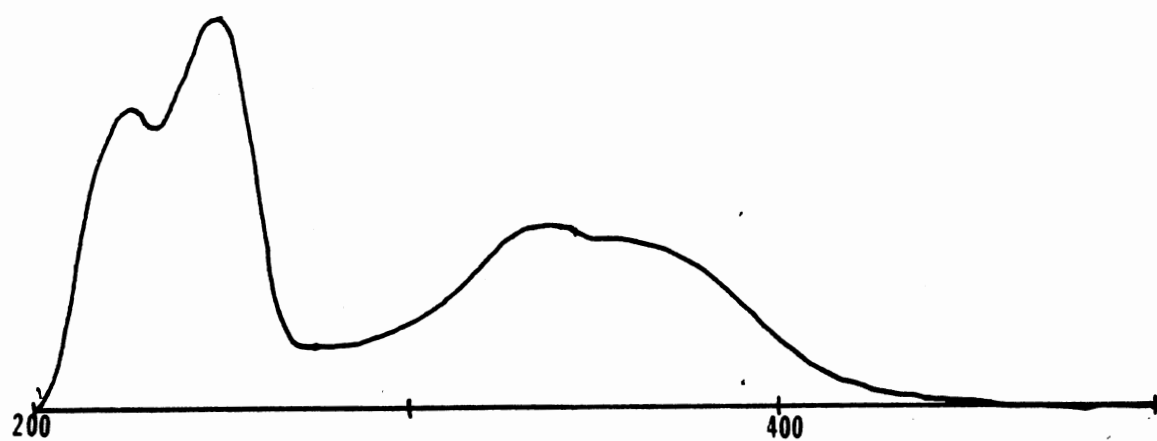


Fig. 3 UV-visible Absorption Spectrum in MOPS Medium of Degradation Products of 10.9 μM DHC, 12 h in Dark, in MOPS Medium.

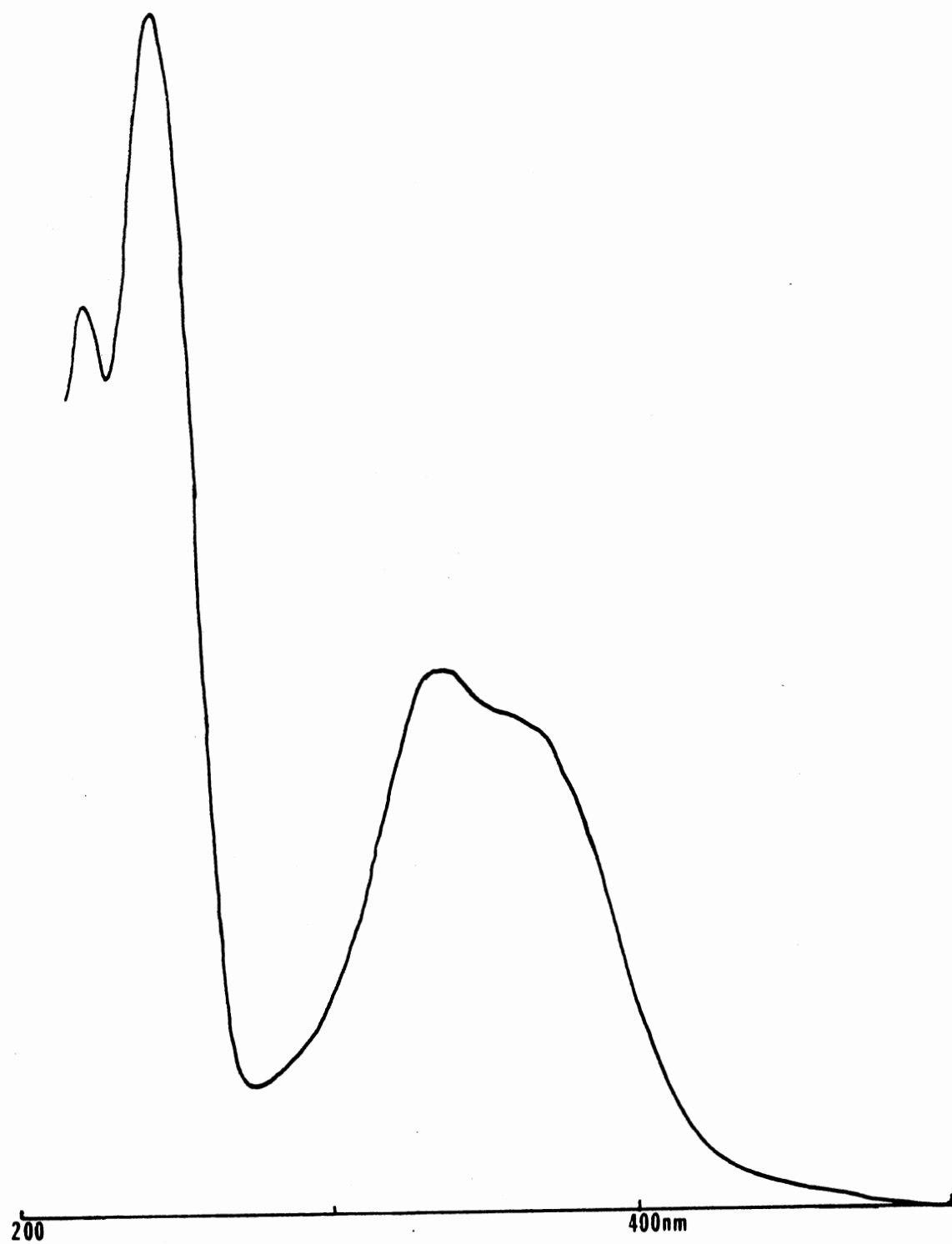


Fig. 4 UV-visible Absorption Spectrum of LC, 85.4 μM LC, in MOPS Medium.

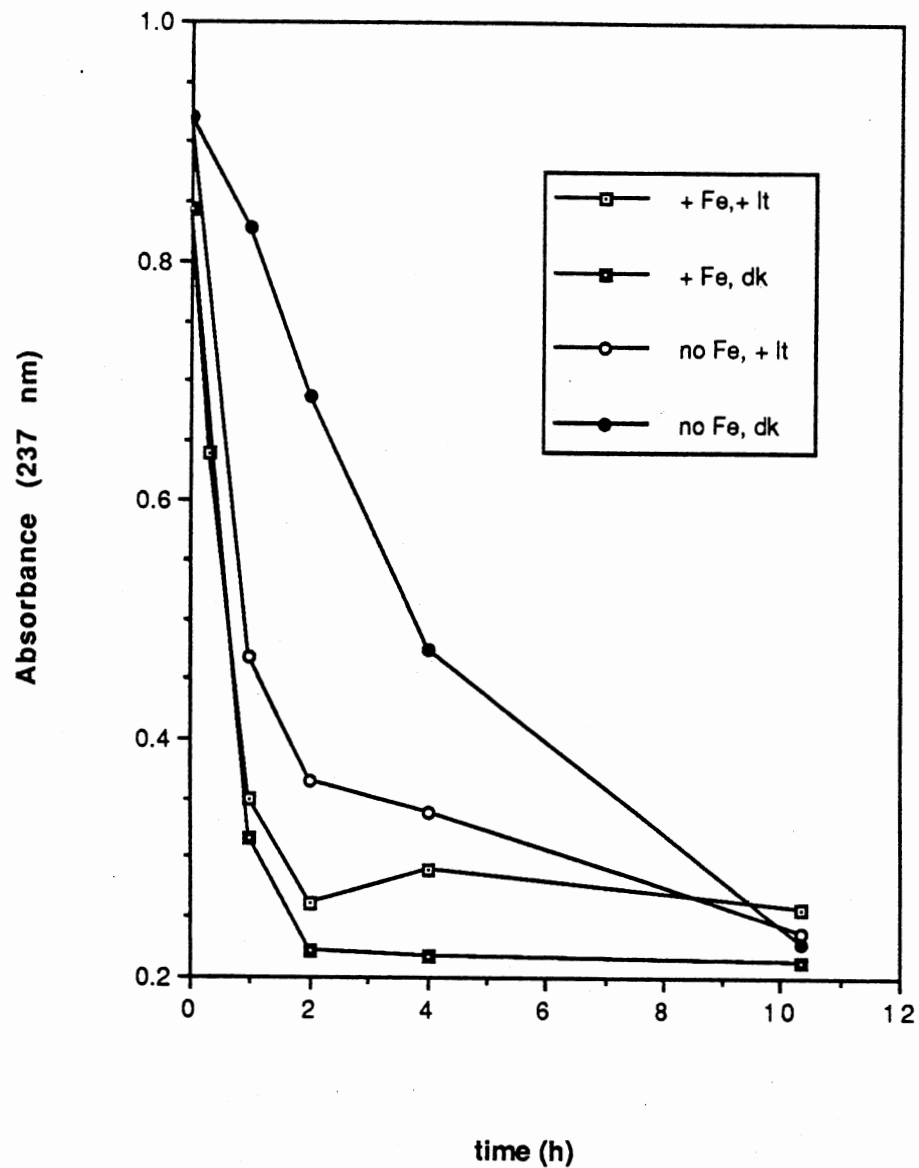


Fig. 5a Effect of Fe and Light on Degradation of DHC. DHC ($0.374 \mu\text{M}$) was dissolved in MOPS medium prepared with or without Fe (Fe concentration in MOPS medium = $10 \mu\text{M}$). Samples were withdrawn and diluted, and absorption spectra were taken at indicated times.

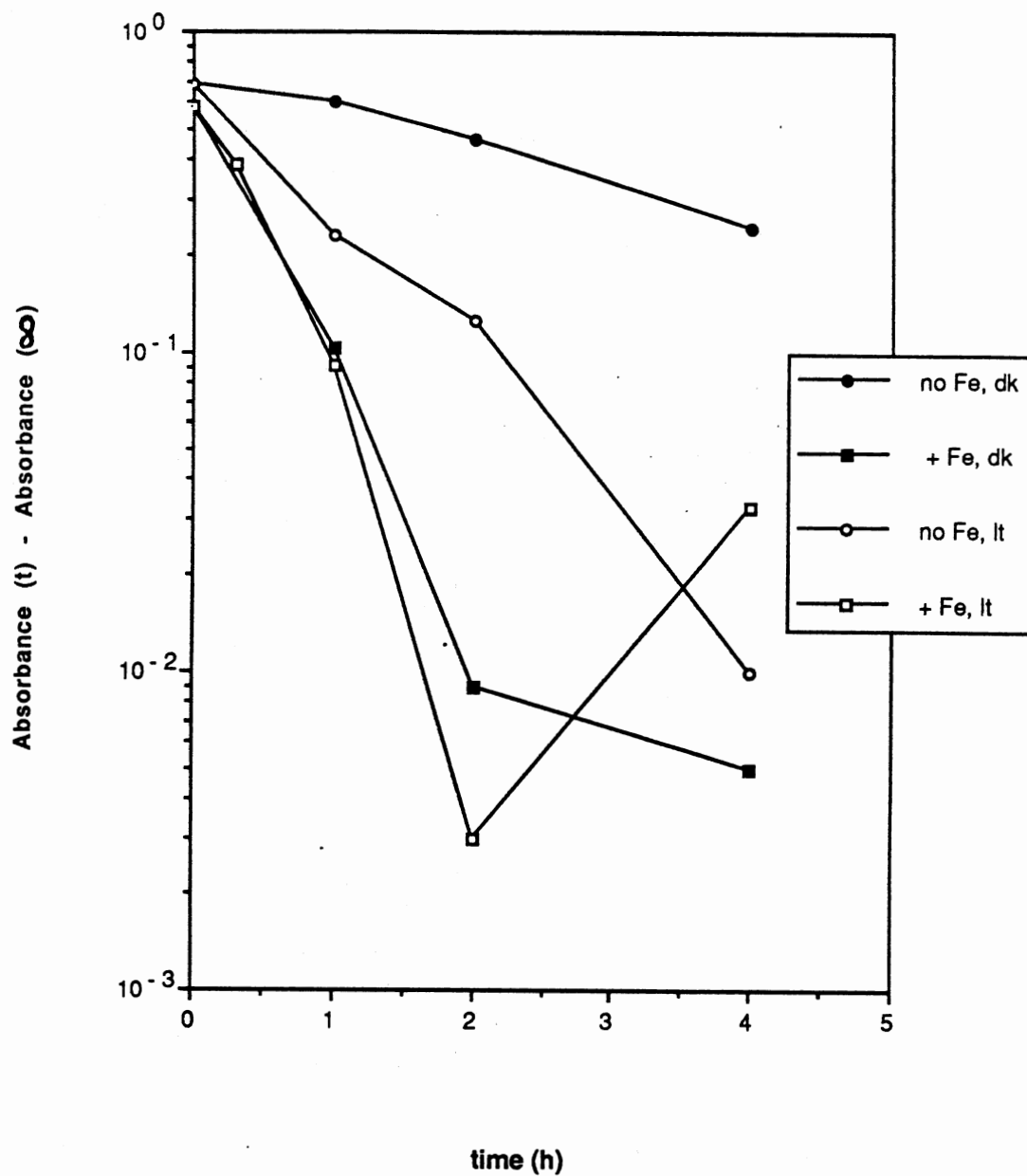


Fig. 5b Rate of DHC Degradation with/without Fe or Light; Semilog Plot. Data from experiment shown in Fig. 5 replotted. A_{237} at infinity was estimated from two successive time points which exhibited no further decrease in A_{237} .

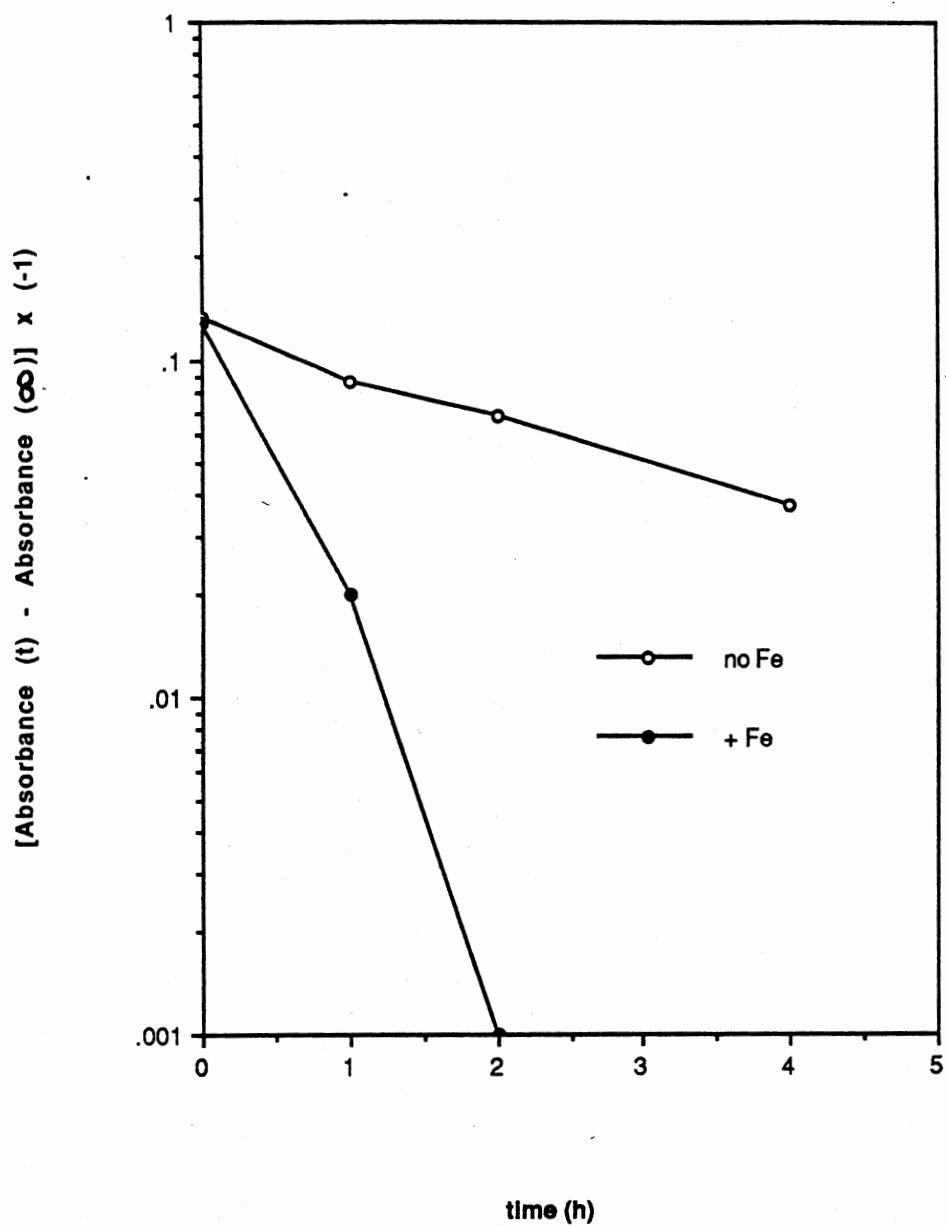


Fig. 5c Effects of Fe on Rate of Appearance of DHC Degradation Products; Dark Conditions. A_{343} at infinity was estimated from a time point at which the reaction had gone to completion.

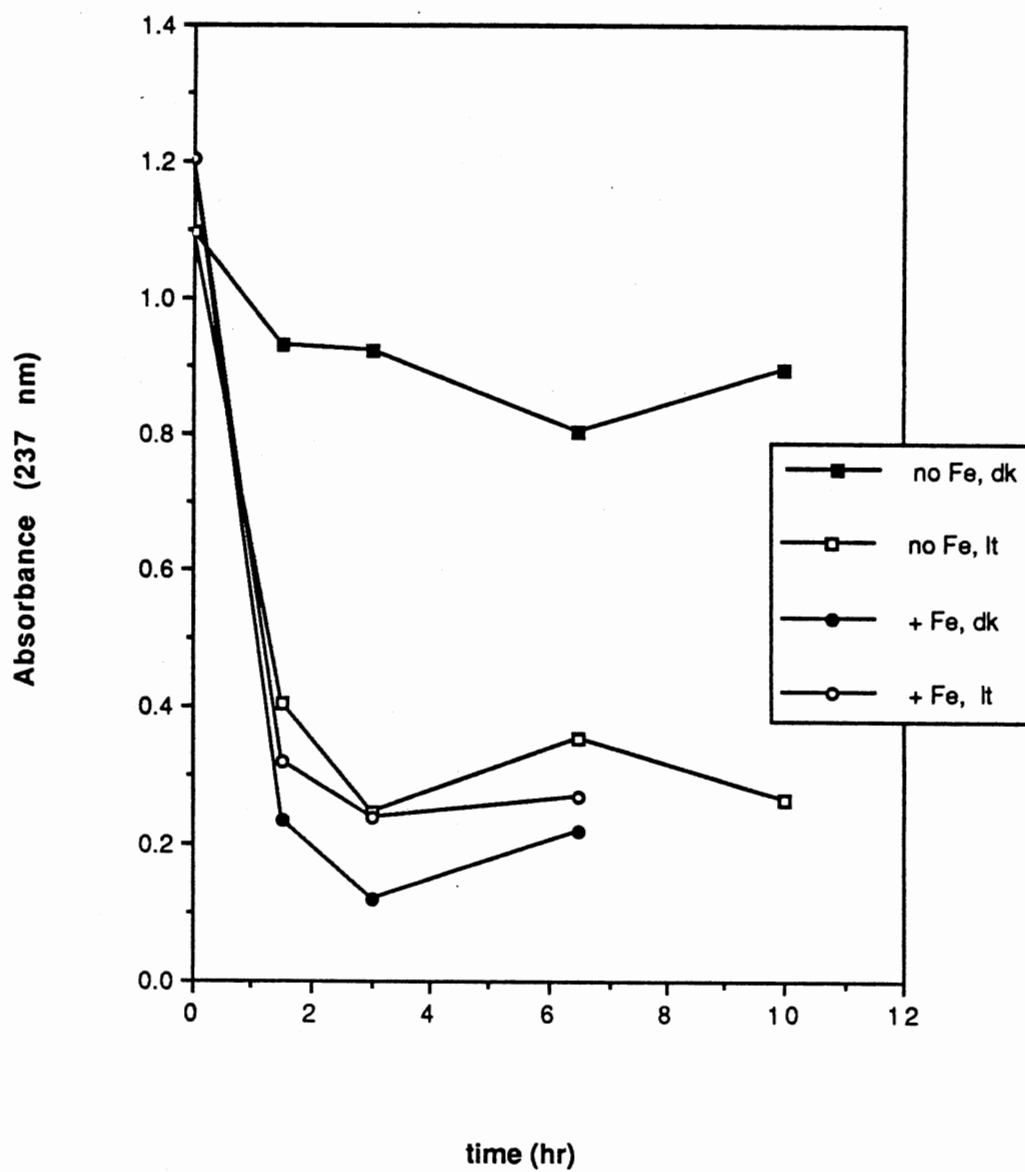


Fig. 6 Effect of Fe on Degradation of DHC; DTPA Used to Remove Fe. Experiment performed as in Fig. 5, except MOPS medium prepared without Fe contained 13 mM DTPA.

these conditions, the degradation of DHC was almost completely blocked. The reactions of DHC in the dark with and without DTPA are replotted in Fig. 7. As the degradation of DHC in the dark proceeded, the broad peak at 343 nm appeared. Appearance of the 343 nm peak during dark degradation was blocked by DTPA and slowed by omission of Fe from the medium. (Fig. 8) A semilog plot of these reactions is shown in Fig. 8a.

The Fe in MOPS growth medium was added in the ferrous form ($\text{Fe SO}_4 \cdot 7\text{H}_2\text{O}$, 10 μM). However, MOPS medium is buffered at pH 7.4, and contains phosphates, conditions which are reported to promote rapid oxidation of Fe^{+2} to Fe^{+3} (4). In clean water, below pH 7, Fe^{+2} has been reported to be relatively stable (*ibid*). The effects of Fe^{+2} and Fe^{+3} on DHC in the absence of light were compared in an experiment shown in Fig. 9. Since H_2SO_4 is used to dissolve the Fe salts, a low-pH control was included. Both Fe salts were present in large excess (113X) to DHC, and, under these conditions, Fe^{+2} very effectively protected DHC from degradation. Fe^{+3} stimulated the degradation. DHC in both water controls and in the Fe^{+3} sample was degraded more slowly than in the previous experiment in MOPS medium (Figs. 5a & 6).

In a separate experiment, using Fe/DHC ratios of approximately 20 and 1.0, the appearance of LC and the disappearance of DHC during the degradation of DHC in the dark were monitored by extracting the reaction mixture with CHCl_3 and separating the products by HPLC (Fig. 10). For all time points, DHC and LC were the major extractable products seen on HPLC (monitored at 254 nm). The reaction mixtures through 6 hours showed virtually no other UV-absorbing compounds present. At 24 hours, some small peaks eluting before LC were visible in the Fe^{+3} and 0.1 mM Fe^{+2} treatments. In Fig. 10, DHC is shown as estimated fractions of the sum of the LC and DHC present. Details of the method used for estimation are given in the Experimental section. Both excess and stoichiometric amounts of Fe^{+3} promoted the oxidation of DHC to form LC, relative to the control samples. A stoichiometric amount of Fe^{+2} stimulated the disappearance of DHC and the appearance of LC at a rate and to an extent comparable to

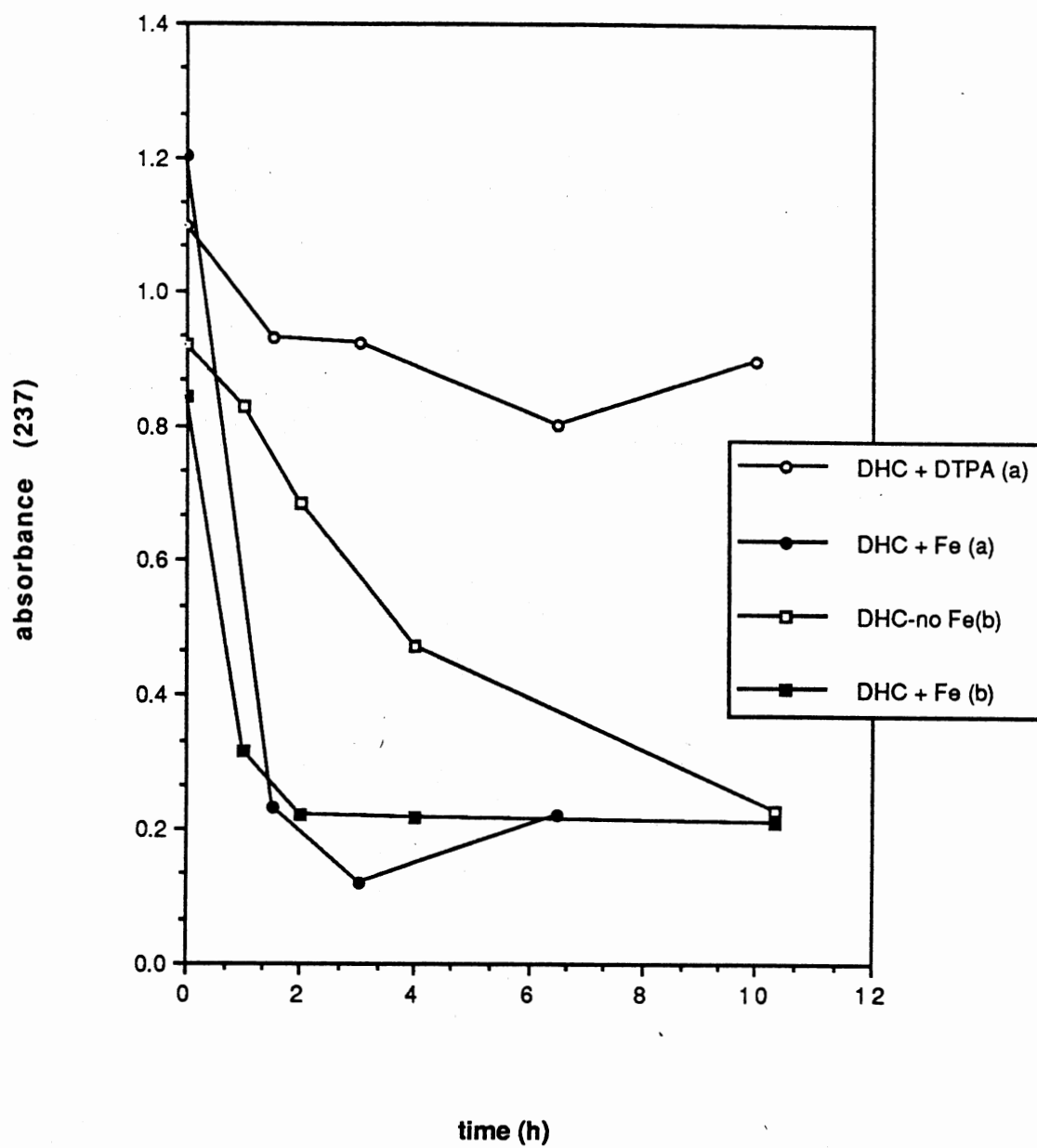


Fig. 7 Effect of DTPA and Fe on Degradation of DHC; Dark Conditions. Data (A237) from dark conditions shown in Figs. 5 & 6 replotted. a) Dark experiment from Fig. 6, and b) dark experiment, Fig. 5.

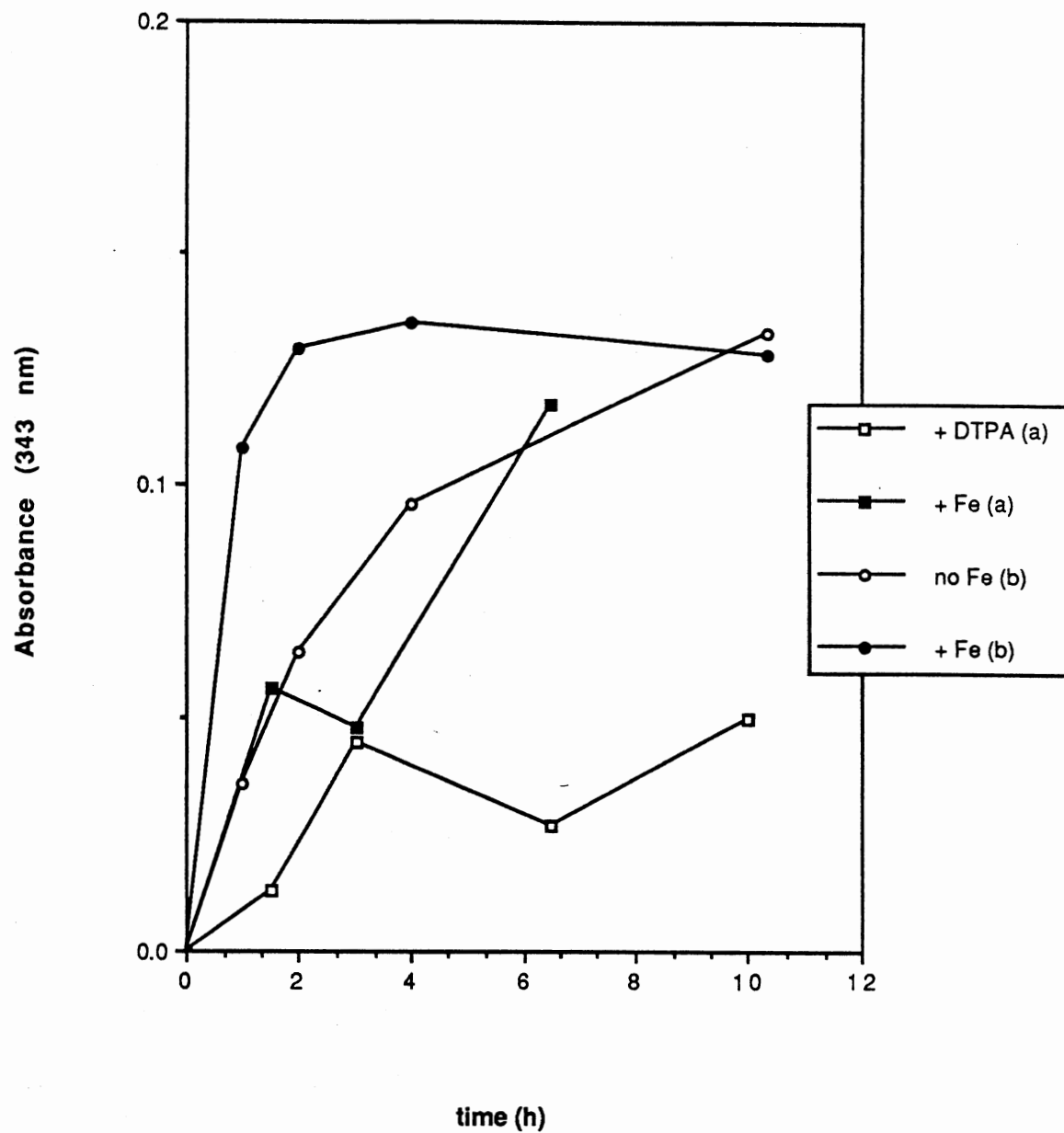


Fig. 8 Effects of DTPA and Fe on Appearance of DHC Degradation Products; Dark Condiitons. Data (A343) from dark conditions shown in Fig. 5 & 6; a) dark exp., Fig. 6, and b) dark exp. Fig. 5a.

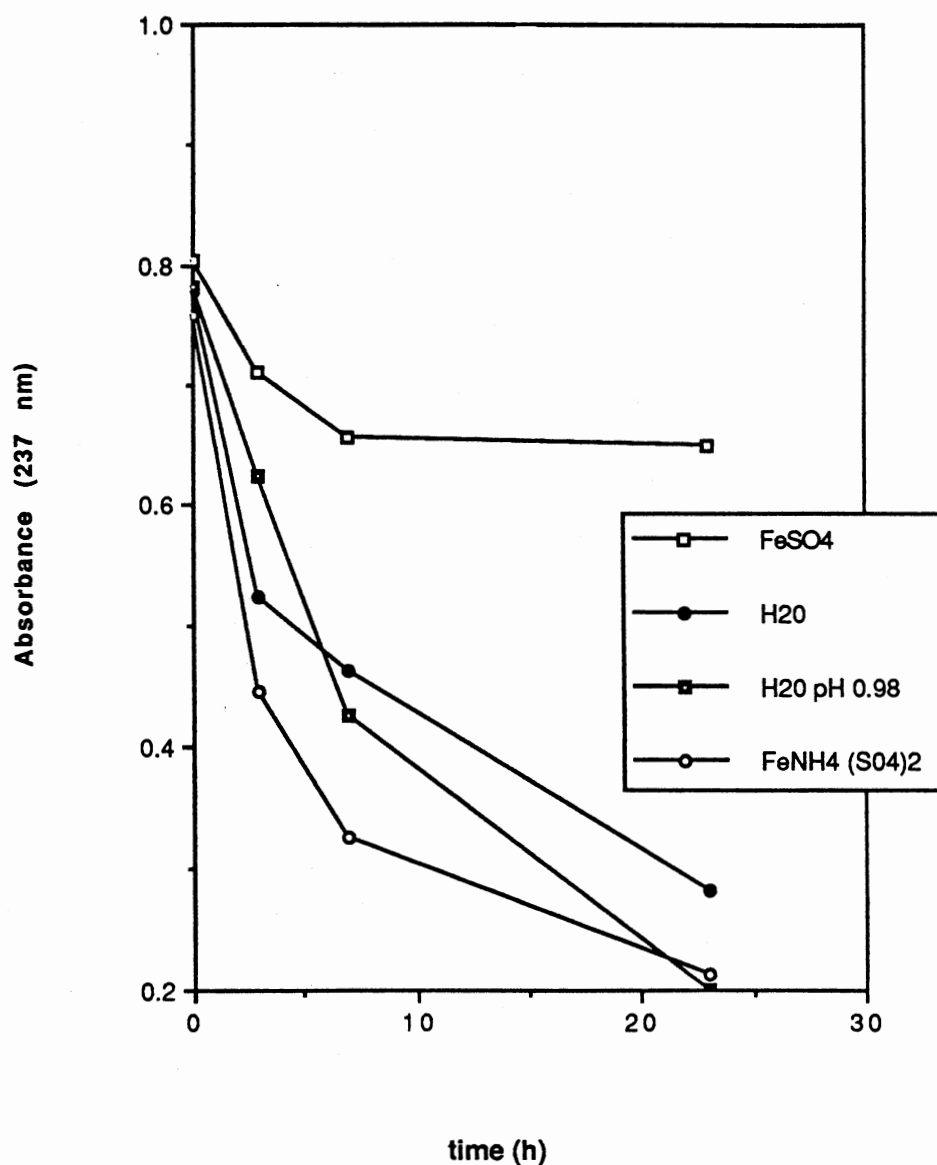


Fig. 9 Effects of Excess Fe⁺² and Fe⁺³ on DHC Degradation; Dark Conditions. FeSO₄·7H₂O and FeNH₄(SO₄)₂·12H₂O were dissolved in glass-distilled water, using H₂SO₄ to achieve solvation. Solutions of 2 mM Fe and 17.1 μM DHC in water were agitated at 30°C in the dark, and samples were withdrawn at the indicated times, extracted 3X with CHCl₃, evaporated, dissolved in 550 μl methanol and scanned on the spectrophotometer.

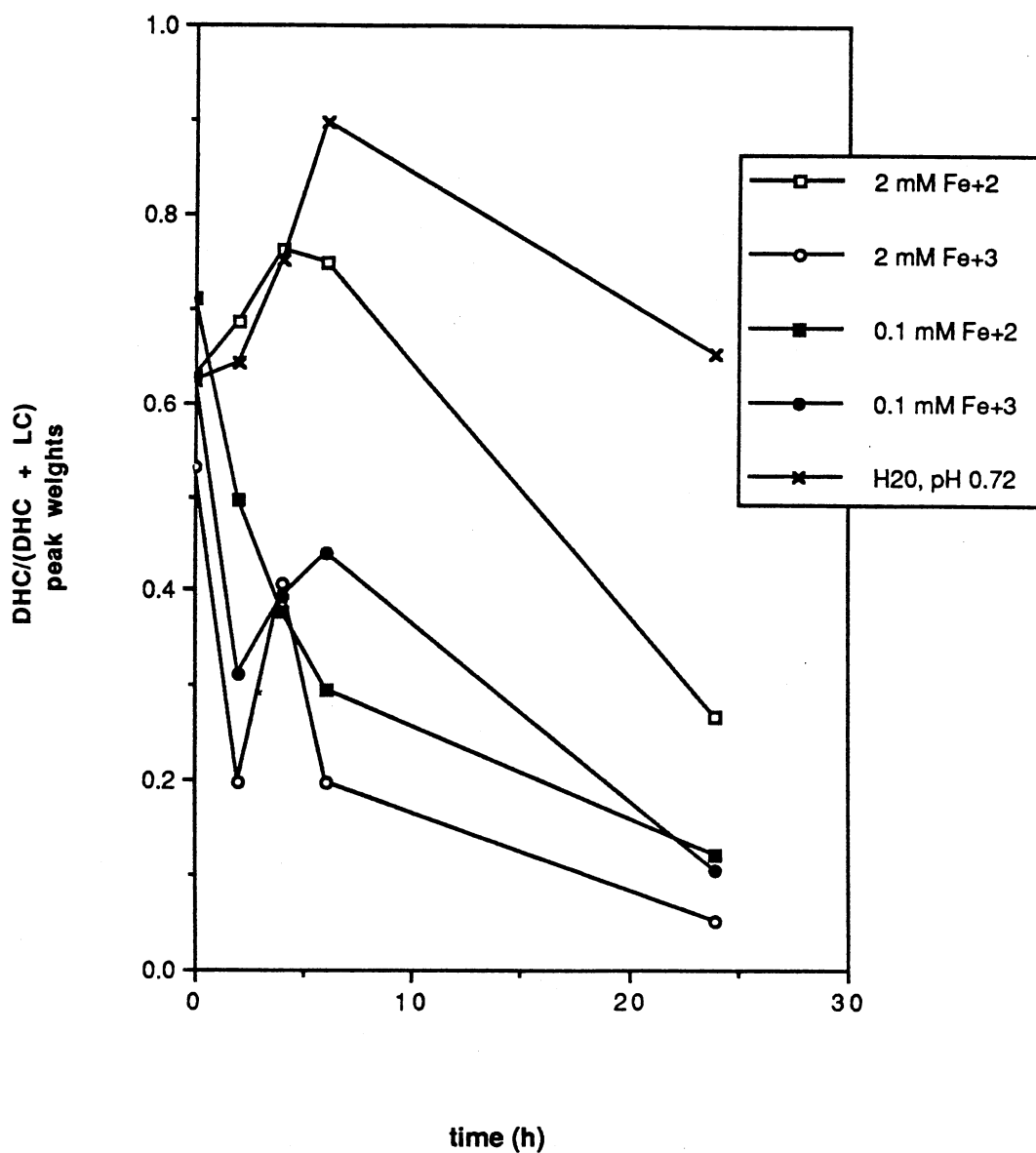


Fig. 10 Effects of Fe²⁺ and Fe³⁺ on Disappearance of DHC in the Dark. Fe²⁺ and Fe³⁺ were prepared as in Fig. 9. Solutions of 2 mM and 0.1 mM Fe with 0.108 mM DHC in distilled H₂O were agitated at 30°C in the dark, and samples were withdrawn at the indicated times and extracted as in Fig. 9. The extracts were dissolved in methanol/H₂O : 60/40, v/v. and subjected to HPLC. The peaks corresponding to DHC and LC were cut and weighed, and DHC is expressed here as a fraction of the sum of peak weights.

the reaction in the presence of stoichiometric Fe^{+3} . The excess Fe^{+2} treatment (2 mM) provided no protection and caused no acceleration of degradation of DHC, up to about 4 hours. After that time, the DHC samples treated with excess Fe^{+2} degraded much more rapidly than did the control samples.

Effect of Fe on LC Degradation

The stability of LC toward Fe and light was tested under the same conditions used for DHC in Fig. 6, and is shown in Fig. 11. The progress of this degradation was monitored by the absorption at 250 nm, although some inaccuracy is introduced by the fact that the light-degraded samples displayed an increasing absorption at 270 nm as the reaction progressed. This complication could not, with the available data, be compensated for, since the degradation of LC is so slow that none of the reactions proceeded to completion. LC was lost most rapidly in the presence of both Fe ($10\mu\text{M Fe}^{+3}$, in MOPS) and light. In the dark, the presence of Fe^{+3} appeared to stabilize LC relative to the dark treatment performed with an excess of chelator (DTPA).

Effects of Selected Enzymes on DHC Degradation

The ability of catalase or SOD to interfere with the reaction which degrades DHC in the presence of light was tested (Fig. 12). Also included were two other proteins having no catalytic activity toward activated oxygen species (BSA and lysozyme). The progress of the degradation in this experiment, monitored spectrally as in the previous experiments, is expressed as the difference between the absorbances at 237 and 220 nm. This method was chosen because the proteins, particularly catalase and lysozyme, absorbed significantly at 220 nm, and the absorbance at this wavelength increased markedly during the course of the experiment. Therefore, although the shape of the DHC A_{237} peak disappeared in these samples, the actual absorption at 237 nm did not decrease accordingly. The difference ($A_{237} - A_{220}$) reflected the loss of this identifying peak.

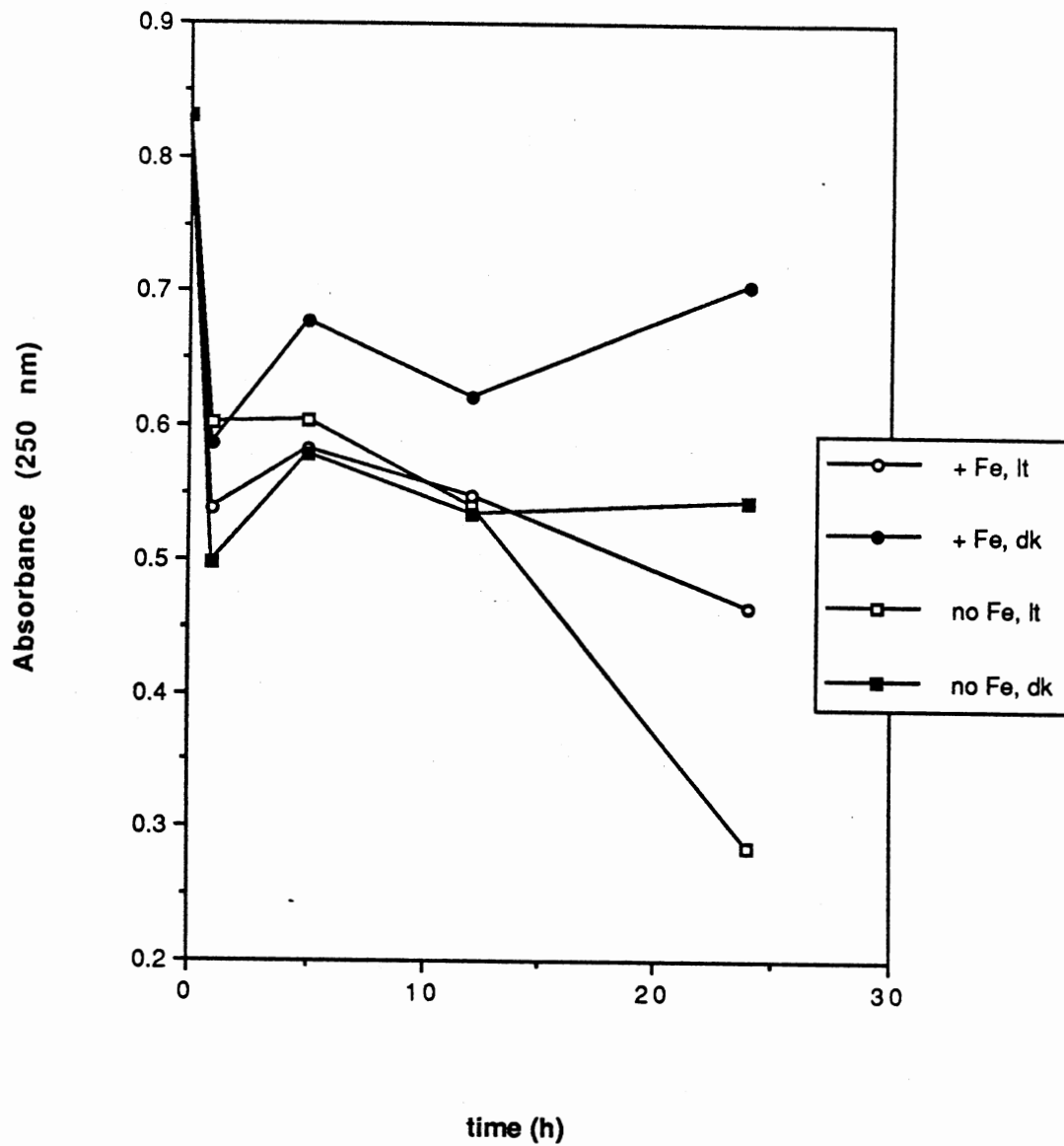


Fig. 11 Effects of Fe and Light on Degradation of LC. LC (85.4 μ M) was dissolved in MOPS medium which was prepared with and without Fe (+ 13 mM DTPA), and treated as in Figs. 5 & 6.

SOD, catalase and lysozyme were quite ineffective in preventing the photo-degradation of DHC, and even appeared to accelerate the reaction to a small extent. BSA alone provided quite significant protection against the degradation of DHC in the presence of light.

A fresh preparation of SOD was obtained, and mixed with DHC in the dark, preparatory to starting a light degradation reaction. This concentration of SOD (10 times greater than that used in Fig. 12) caused a degradation of DHC in the dark which proceeded so rapidly that $t=0$ data was difficult to obtain. Fig. 13 shows the rapid disappearance of DHC (monitored by the 237nm peak) and the concomitant appearance of LC (343 nm). The rate of this reaction was markedly inhibited by KCN (Fig. 14), which inhibits the Cu/Zn types of SOD. (5)

In addition to catalase and SOD, two other metalloproteins were added to DHC to test their effects on DHC in the dark reaction (Figs. 15 & 16). Peroxidase exerted only a slight effect on the degradation, but all three other metalloproteins tested markedly stimulated the oxidation of DHC to LC. The rate and extent of both the disappearance of DHC and appearance of LC were stimulated in the presence of SOD, catalase and cytochrome c , relative to those of a control sample prepared in the same buffer used with the proteins.

Inhibition of the Degradation of DHC Under Anaerobic Conditions

The degradation of DHC which occurs in the dark in MOPS medium was significantly inhibited by the application of rigorously anaerobic conditions, but the light degradation was not (Figs. 17 & 18).

The light reactions shown in Fig. 17 showed a rapid and complete destruction of DHC in the light when O_2 was present. The anaerobic treatment slightly inhibited the apparent initial rate of this degradation, but allow rapid degradation.

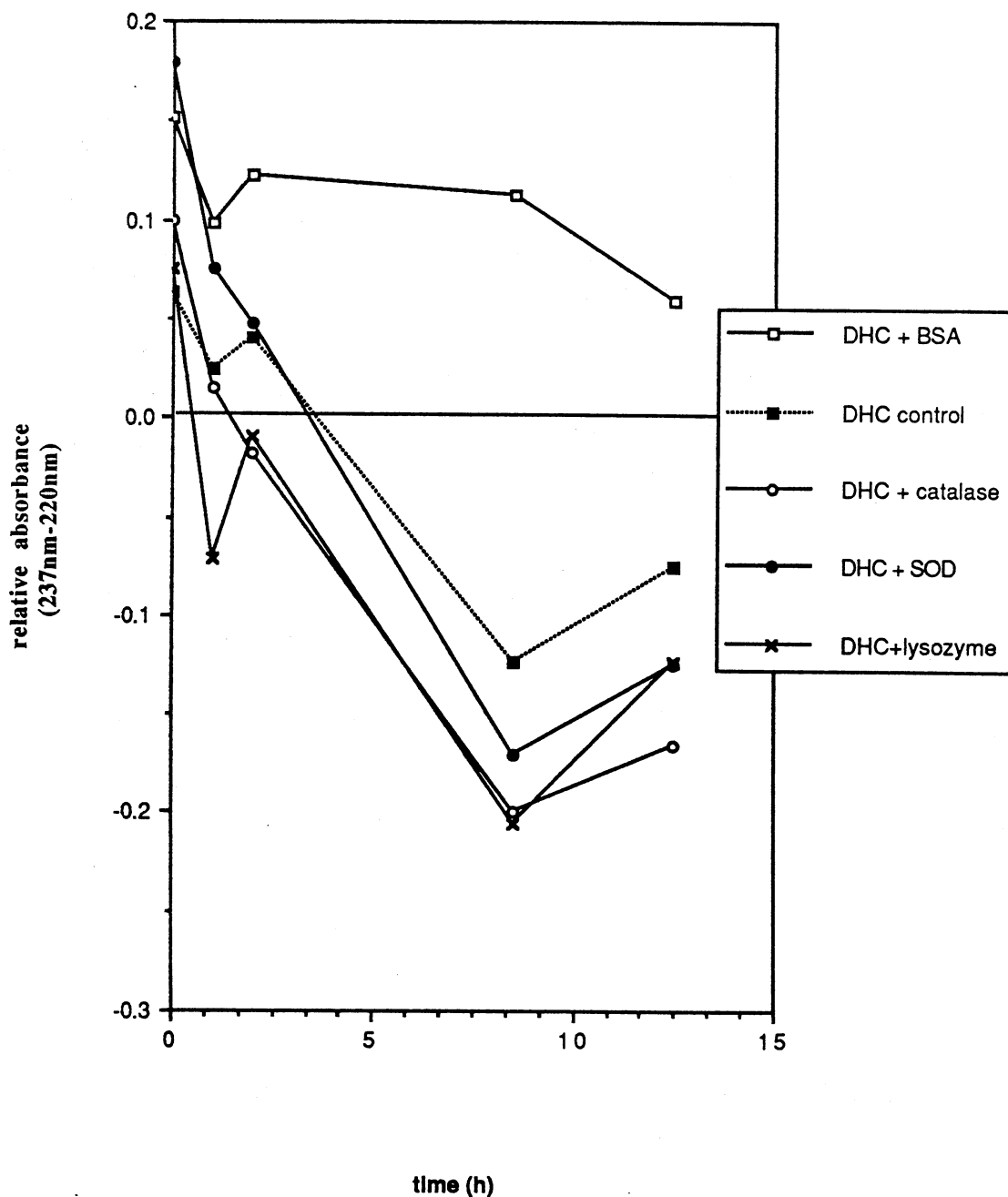


Fig. 12 Effects of Some Proteins on Light Degradation of DHC. Solutions of four proteins in 50 mM K-PO₄ buffer, pH 7.8, were dissolved with 0.7 mM DHC : BSA, 0.5 mg/ml (7.4 μ M); catalase, 0.5 mg/ml (185 units/ml, 2 μ M); SOD, 1 μ g/ml, (~3.1 units/ml, ~ 16.1 μ M) and lysozyme, 0.5 mg/ml (35.7 μ M). The solutions were agitated in the light, as in bioassays, and samples were withdrawn, diluted and scanned in the spectrophotometer at the indicated times. Relative DHC concentration was estimated using the difference $A_{237} - A_{220}$.

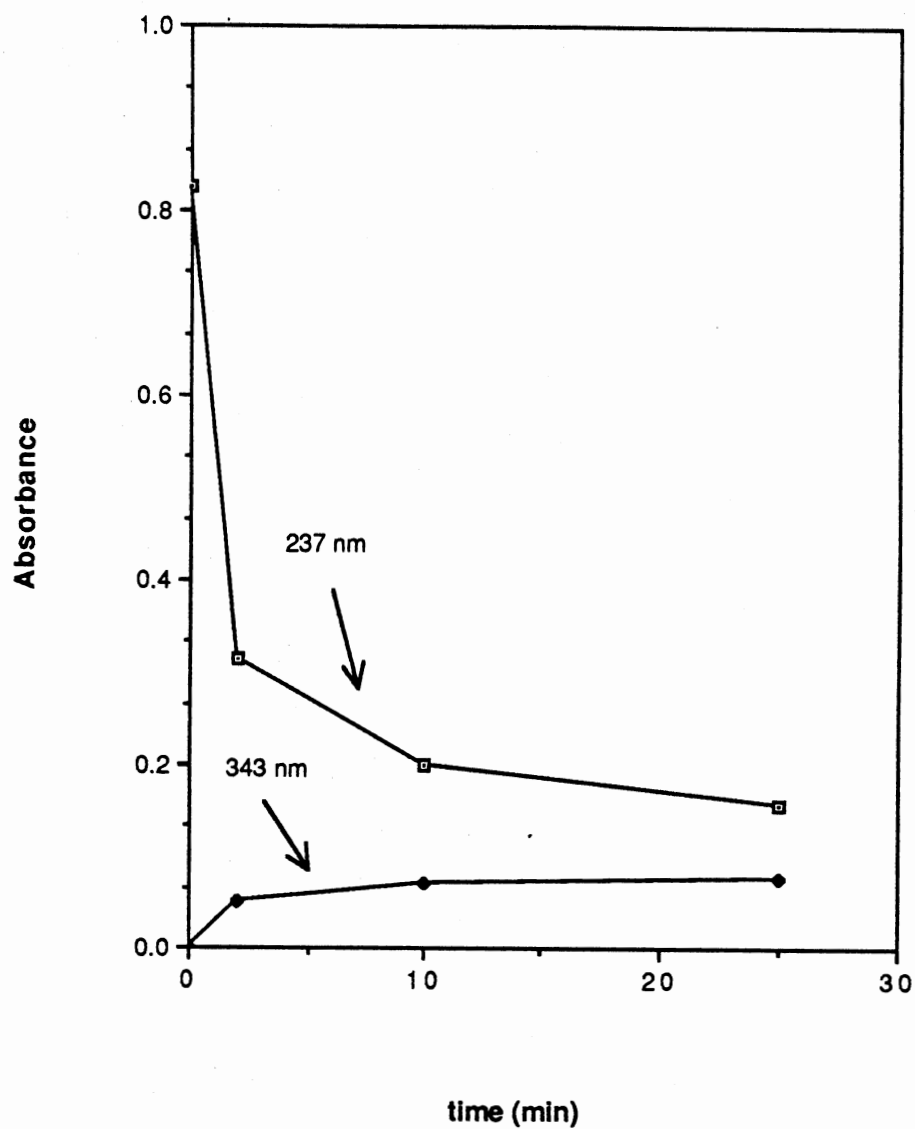


Fig. 13 Effect of SOD on DHC Degradation in the Dark. A solution of DHC ($99.8 \mu\text{M}$) was prepared in 50 mM K-PO₄ buffer, pH 7.8, with 0.1 mM EDTA in the dark, and scanned on the spectrophotometer ($t = 0$). SOD was added to a final concentration of 10 $\mu\text{g/ml}$ (~ 31 units/ml) and mixed. Samples were withdrawn, diluted and scanned at 2, 10 and 20 minutes.

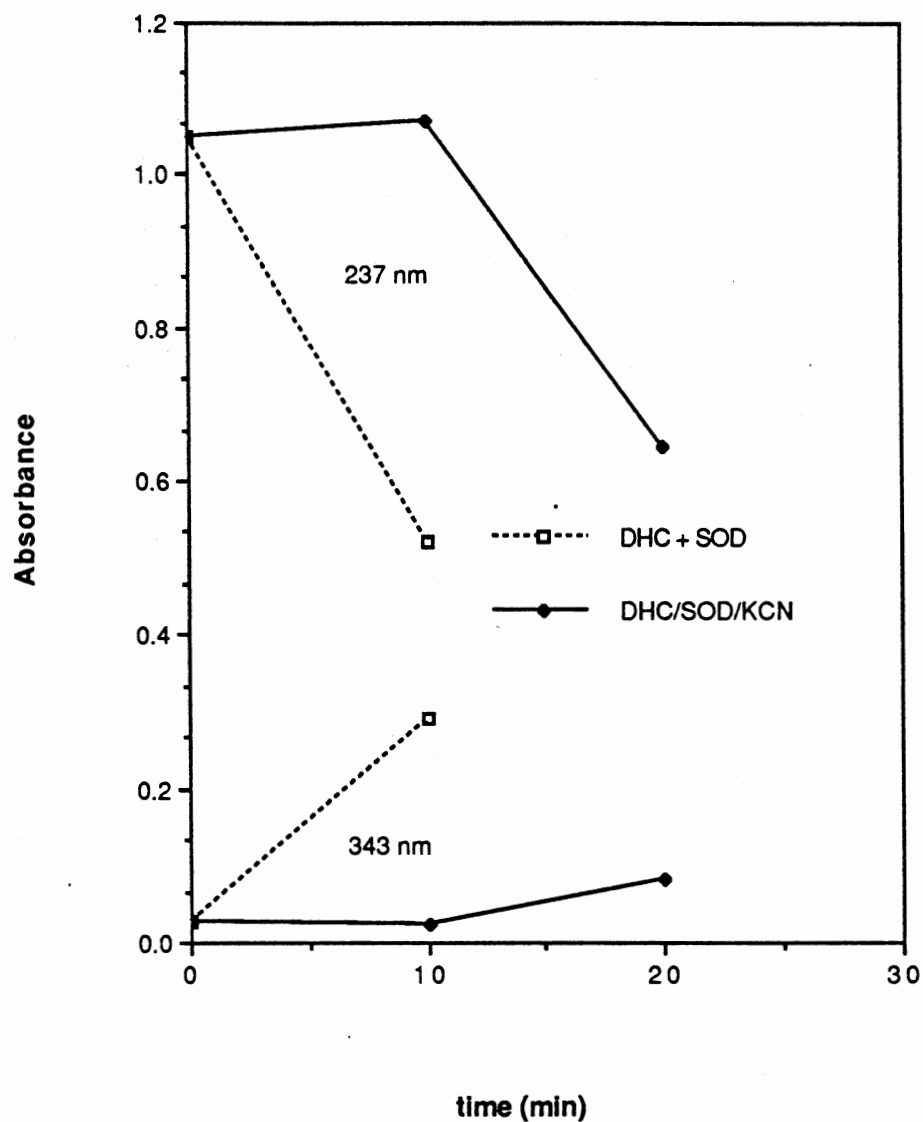


Fig. 14 Effect of KCN on the Degradation of DHC by SOD in the Dark. Solutions of DHC were prepared and scanned as for Fig. 13. SOD (10 $\mu\text{g/ml}$) and SOD + KCN (1mM) were added, and samples were withdrawn, diluted and scanned at 10 and 20 minutes.

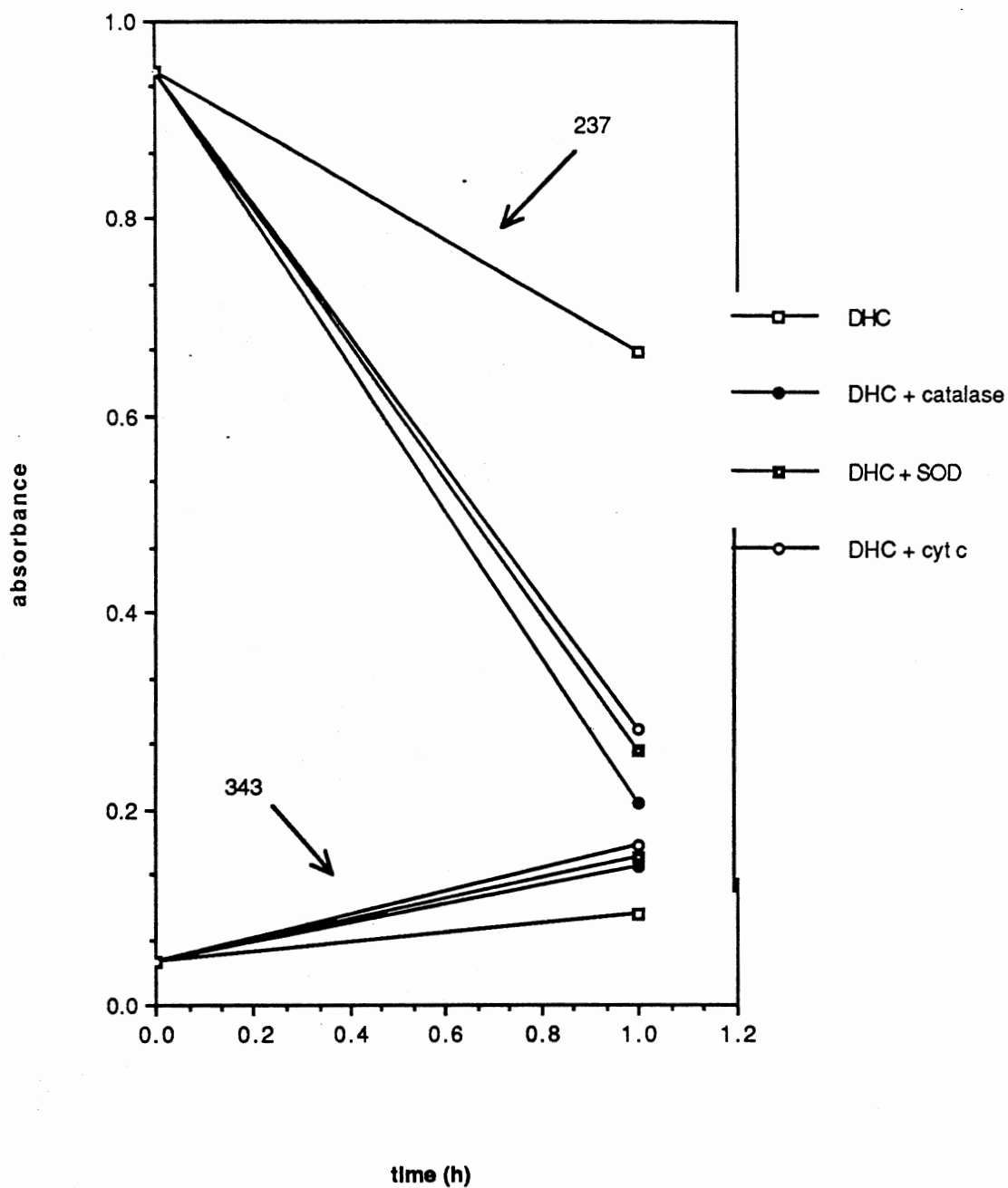


Fig. 15 Effect of SOD, Catalase and Cytochrome c on Degradation of DHC; Dark Conditions. Solutions of DHC (99.8 μM) and proteins in MOPS were prepared : SOD, ~ 31 units/ml (~ 161 μM); catalase, 0.48 mg/ml (1.9 μM , 108 units/ml); and cytochrome c 62 $\mu\text{g/ml}$ (50 μM). A sample of the control solution was scanned at $t = 0$, and absorption spectra of all solution were taken at 1 hour.

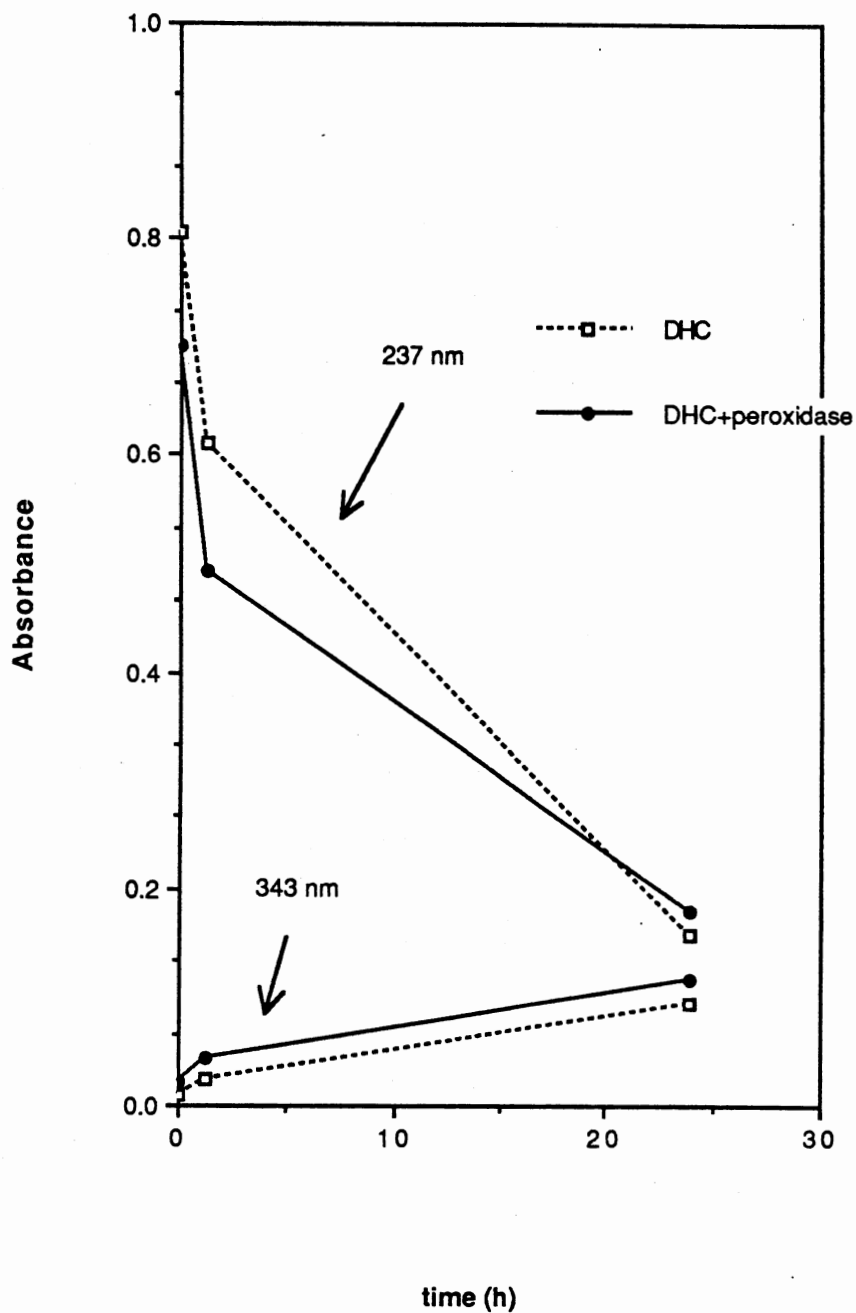


Fig. 16 Effect of Peroxidase on the Degradation of DHC; Dark Conditions. DHC (0.4 mM) was prepared in MOPS medium, with peroxidase (0.1 mg/ml, 2.5 μ M). Samples were withdrawn and absorption spectra taken at $t = 0, 1$ h, and 24 h.

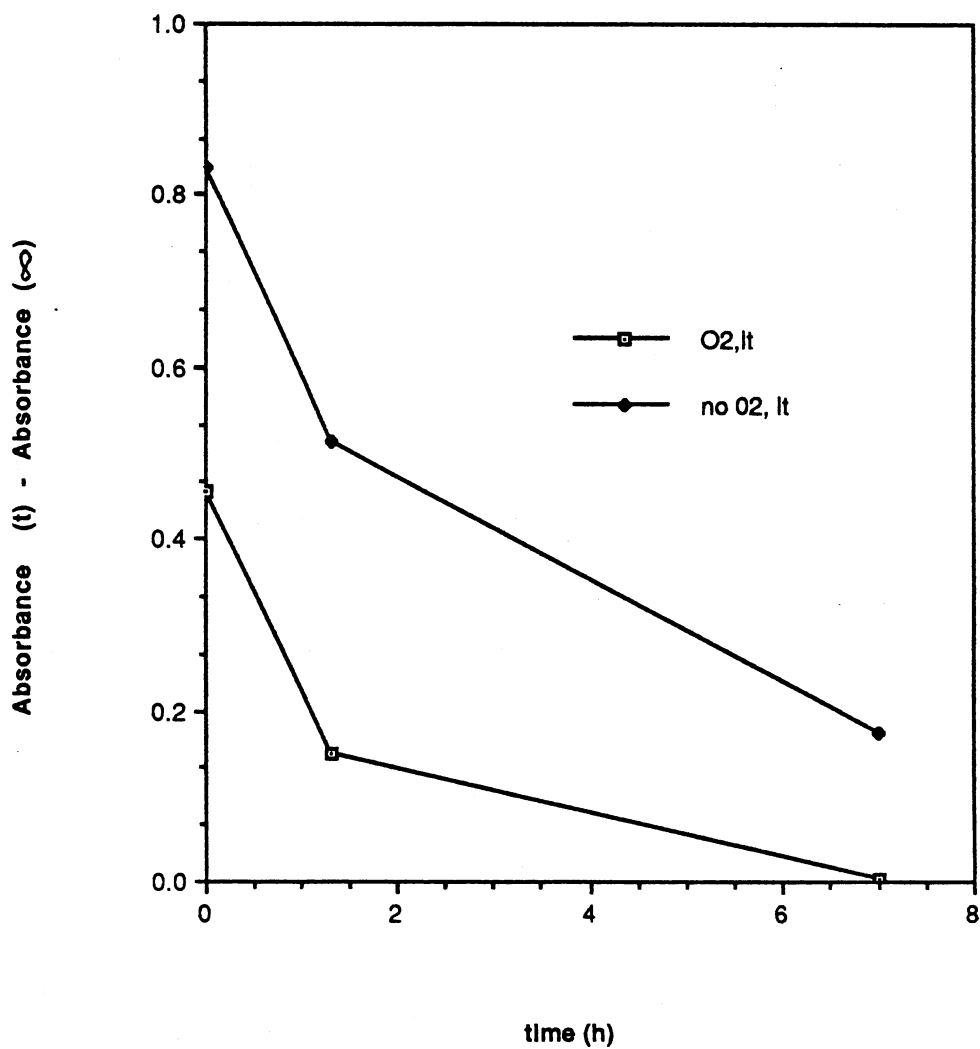


Fig. 17 Effect of Anaerobic Conditions on Degradation of DHC; Light Conditions. MOPS was deaerated at very low pressure, and transferred via syringe to conical plastic 1.5 ml tubes covered with septa, with constant argon flushing. DHC was transferred with a syringe, 0.0217 mM in O₂ treatments, 0.0396 mM in anaerobic treatments. Samples were withdrawn via syringe at indicated times, diluted, and absorption spectra taken.

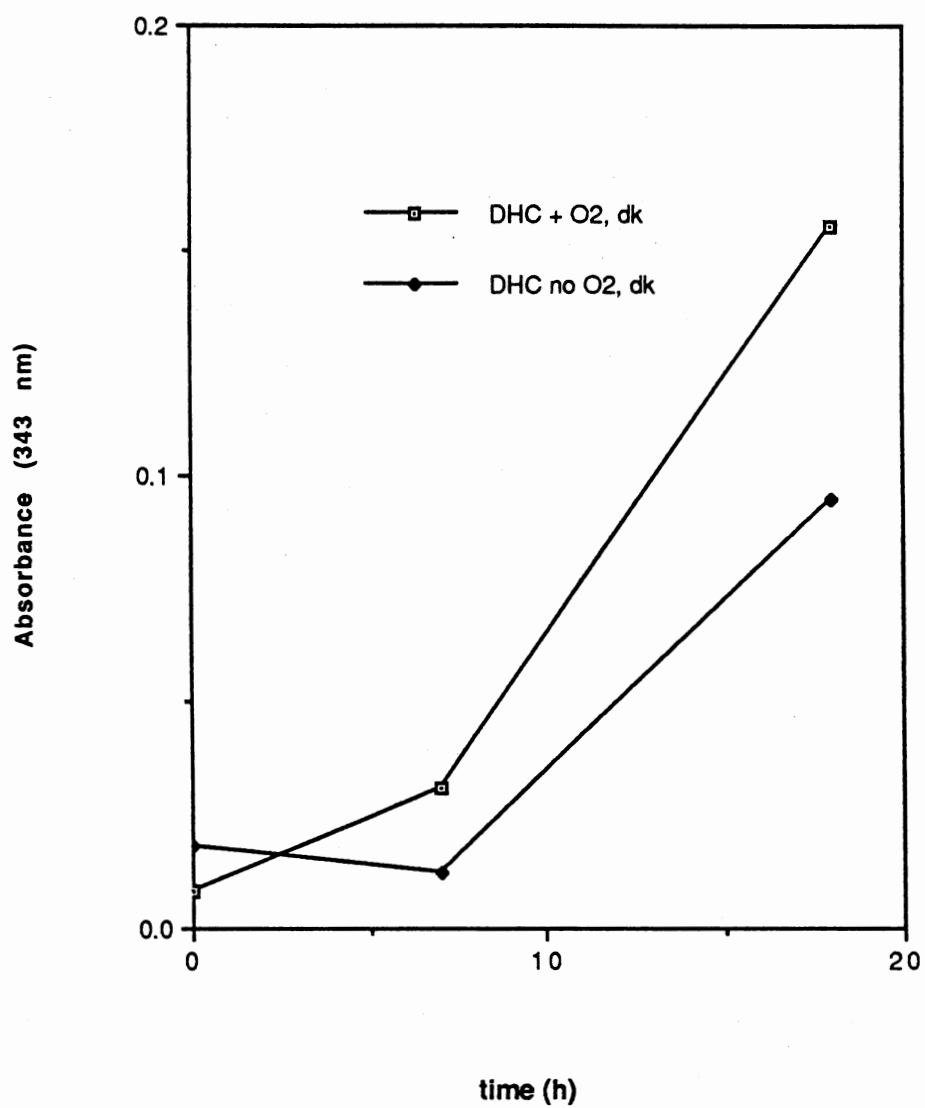


Fig. 18 Effect of Anaerobic Conditions on Appearance of DHC Degradation Products; Dark Conditions. MOPS prepared, and DHC handled as in Fig. 18, except that samples were protected from exposure to light.

The progress of the dark reaction, and the appearance of LC, was monitored at 343 nm as seen in Fig. 18. The DHC treated in MOPS medium without Fe with O₂ in the dark produced LC as expected. The corresponding anaerobic treatment markedly inhibited LC production, particularly during the first 7.5 h, in which the maintenance of anaerobic conditions was probably more rigorous than in the latter part of the experiment

*Effect of Selected Scavengers or Quenchers
of Activated Oxygen*

Crocin, a water-soluble carotenoid pigment isolated from saffron, is reported to react with free radicals, specifically bleaching its absorption band at 440 nm (6). When crocin was added to DHC in H₂O in a 2/1 ratio to DHC and the mixture was exposed to light, the crocin provided partial protection from degradation for the DHC (Fig. 19). In this experiment both a crocin control solution in water and the crocin mixed with DHC were bleached at the 440 nm band to some extent, but the DHC-treated crocin was considerably more bleached than was the water control. The bleaching specifically attributed to the DHC treatment was calculated to represent 16% of the original (t=0) 440nm absorption.

In a dark treatment of DHC with crocin in MOPS medium, crocin provided no protection from degradation to DHC, and the bleaching of the crocin 440 nm absorption was not significantly different in the presence or absence of DHC.

The effects of Na-benzoate, which scavenges the hydroxyl radical (OH·) (7) and of DABCO, which quenches singlet oxygen (O₂¹) were tested in the light-induced degradation of DHC (Fig. 19). Neither compound protected DHC from photo-degradation; indeed, both appeared to very slightly stimulate the loss of DHC in the light.

Mannitol is reported to scavenge free radicals, including OH· (8). AET is widely used to protect against damage from radioactivity, and is proposed to scavenge the highly reactive free radicals generated by radiation (9). These two compounds were added to DHC in the light, and the concentration of DHC present was monitored by UV

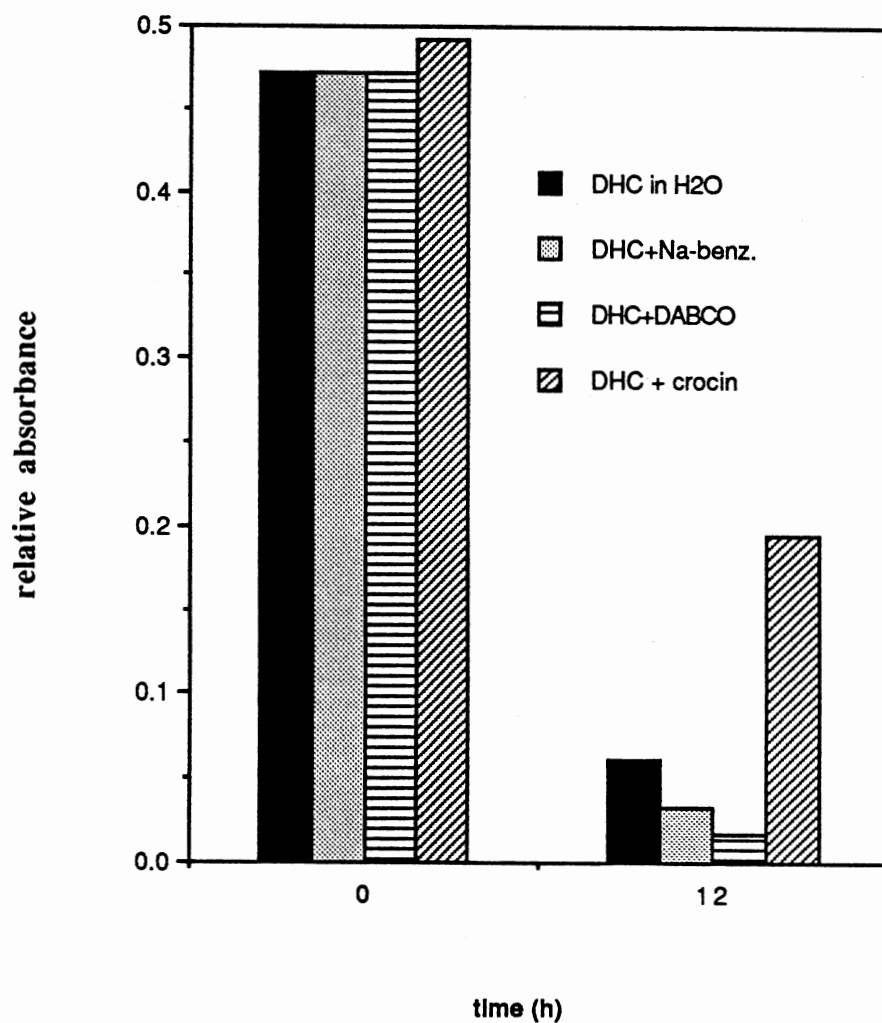


Fig. 19 Effect of Crocin, Na-benzoate and DABCO on Light Degradation of DHC. DHC ($8.4 \mu\text{M}$ in MOPS medium) was mixed with crocin ($\sim 17.3 \mu\text{M}$), DABCO (100 mM) or Na-benzoate (100 mM) and exposed to light for 12 hours. Samples were diluted and scanned on a spectrophotometer.

spectroscopy (Fig. 20). Mannitol provided only very slight protection to DHC, but AET almost completely inhibited the photo-degradation reaction. These data are replotted with a semilog scale in Fig. 20a. As in Fig. 5a, the semilog plot indicates first-order or pseudo-first-order kinetics for the uninhibited reactions.

Three ratios of AET to DHC concentrations were tested for protection (Fig. 20b). A 6.7-fold excess provided some protection in the earliest times tested, but permitted complete degradation of DHC in approximately 12 hours. The DHC treated with a 66.7-fold excess of AET was highly protected from degradation.

The effect of AET on the degradation of DHC in MOPS medium in the absence of light is shown in Figure 21. AET almost completely blocked the destruction of DHC and the formation of LC, when present in large excess (66.7-fold).

Photo-degradation of HMC

HMC (structure 9, page 13), whose structure differs from DHC only in the presence of a methoxy group at the 7-carbon on the cadalene ring system, was exposed to light to test the possibility that it undergoes a degradation analogous to that of DHC (Fig. 22). The reaction was carried out in methanol due to the low water solubility of HMC. Under these conditions, DHC was degraded more slowly than in clean water or MOPS medium, but gave a product mixture with UV absorption spectral traits identical to those produced in water or MOPS medium. HMC was degraded under these conditions, but its degradation proceeded more slowly than did that of DHC. HMC and DHC have almost identical UV-visible spectra, and their respective light-degradation mixtures were spectrally indistinguishable.

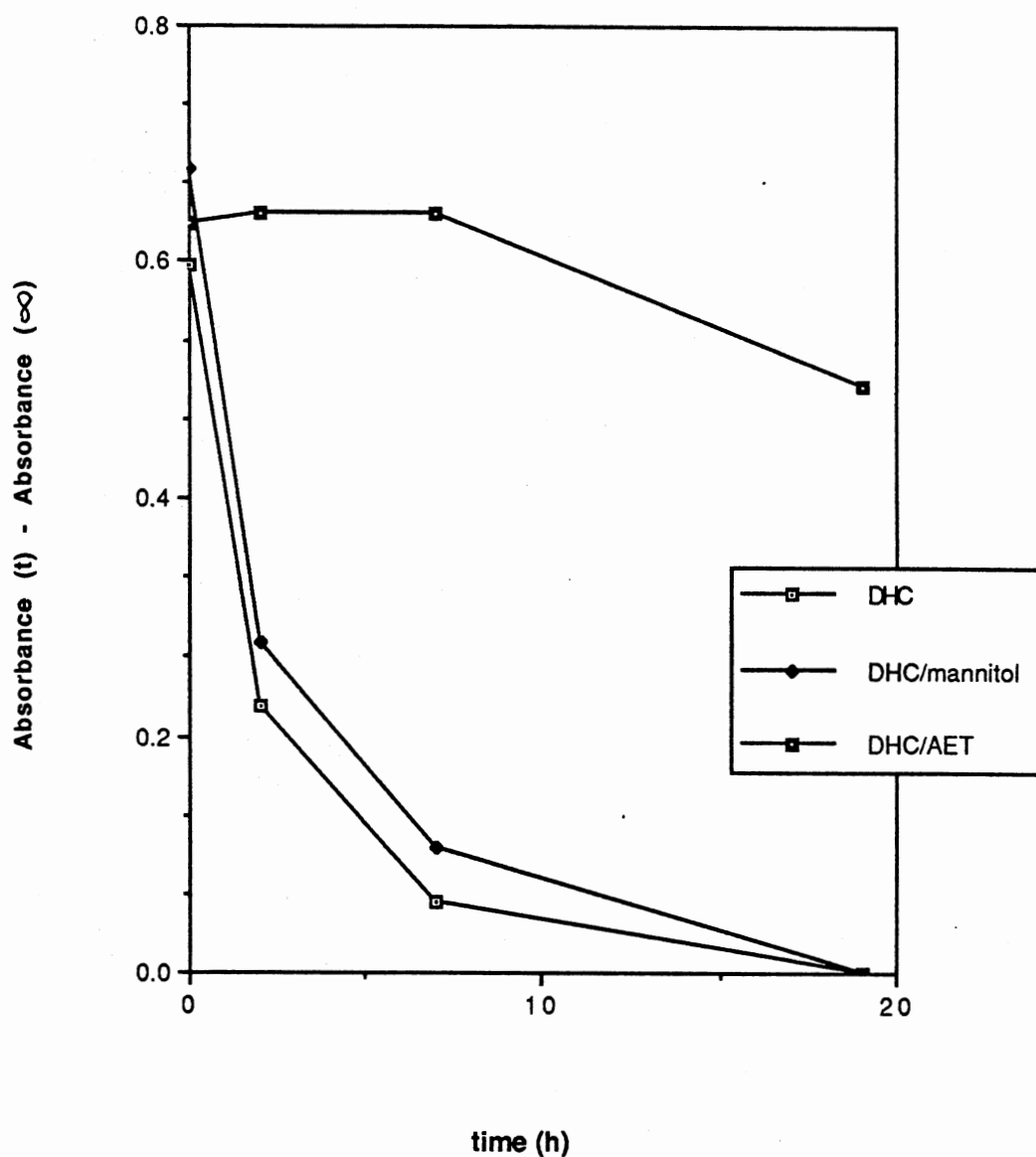


Fig. 20 Effect of Mannitol and AET on Light Degradation of DHC. DHC (0.40 mM, in MOPS medium) was mixed with mannitol (0.22 M) or AET (12.1 mM) and exposed to light. Samples were withdrawn, diluted, and absorption spectra taken at the indicated times.

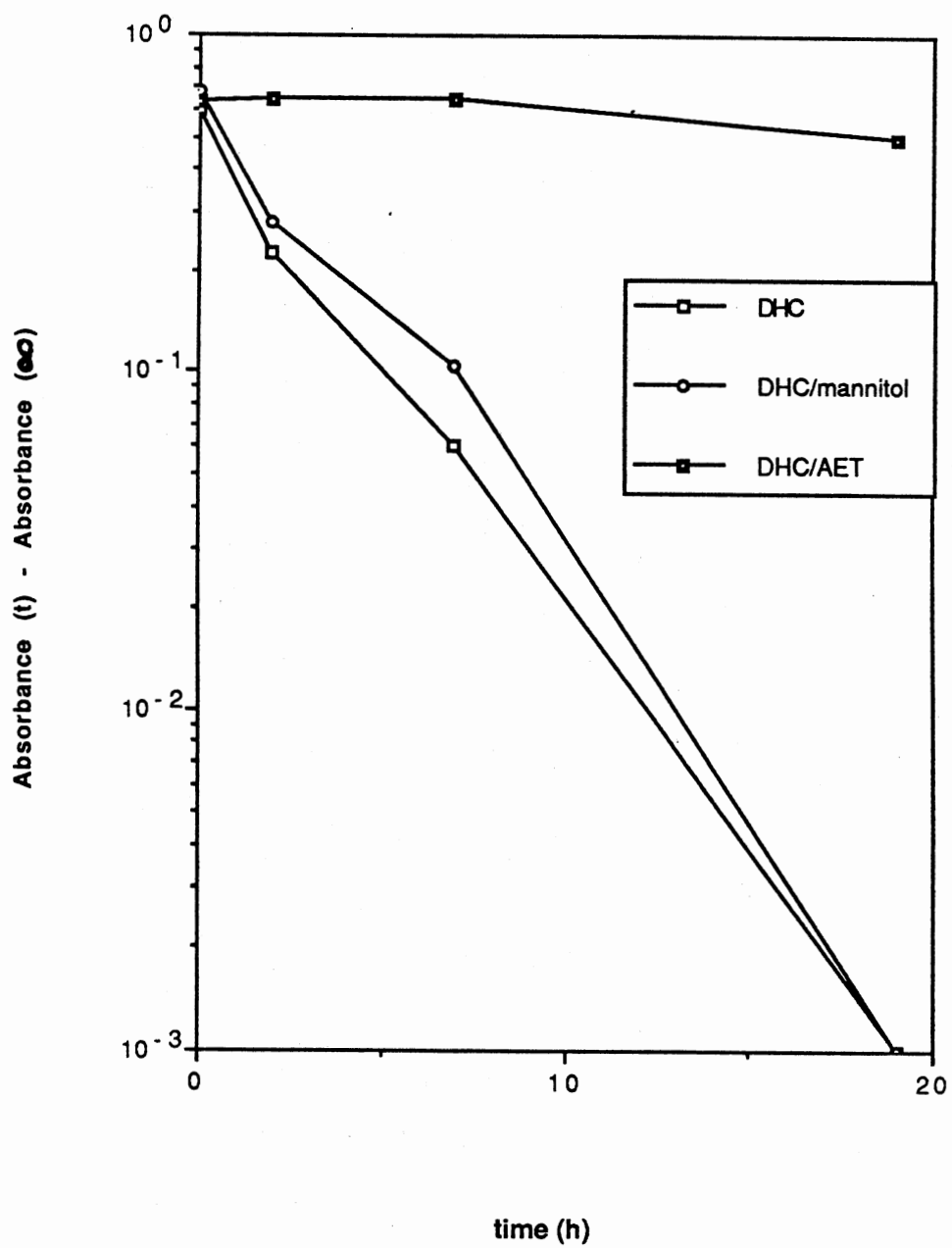


Fig. 20a Effect of Mannitol and AET on Rate of Light Degradation of DHC; Semilog Plot. Data (A_{237}) from experiment shown in Fig. 20 plotted on semilog scale.

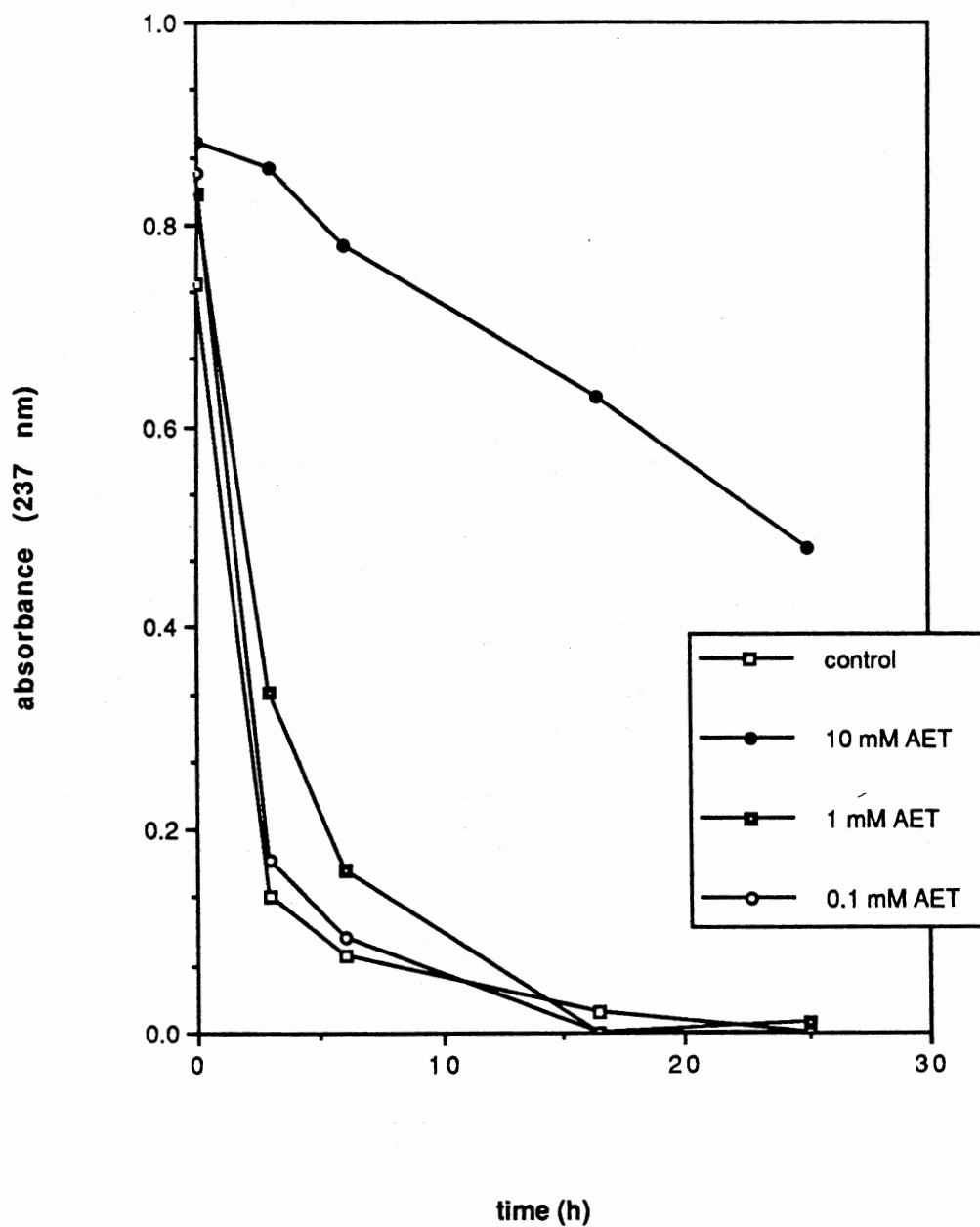


Fig. 20b Effect of AET Concentration on Degradation of DHC; Light Conditions. DHC (0.15 mM) was mixed with MOPS medium containing 0, 0.1, 1.0 or 10 mM AET. Solutions were exposed to light, and samples were withdrawn, diluted and scanned on the spectrophotometer at the stated times.

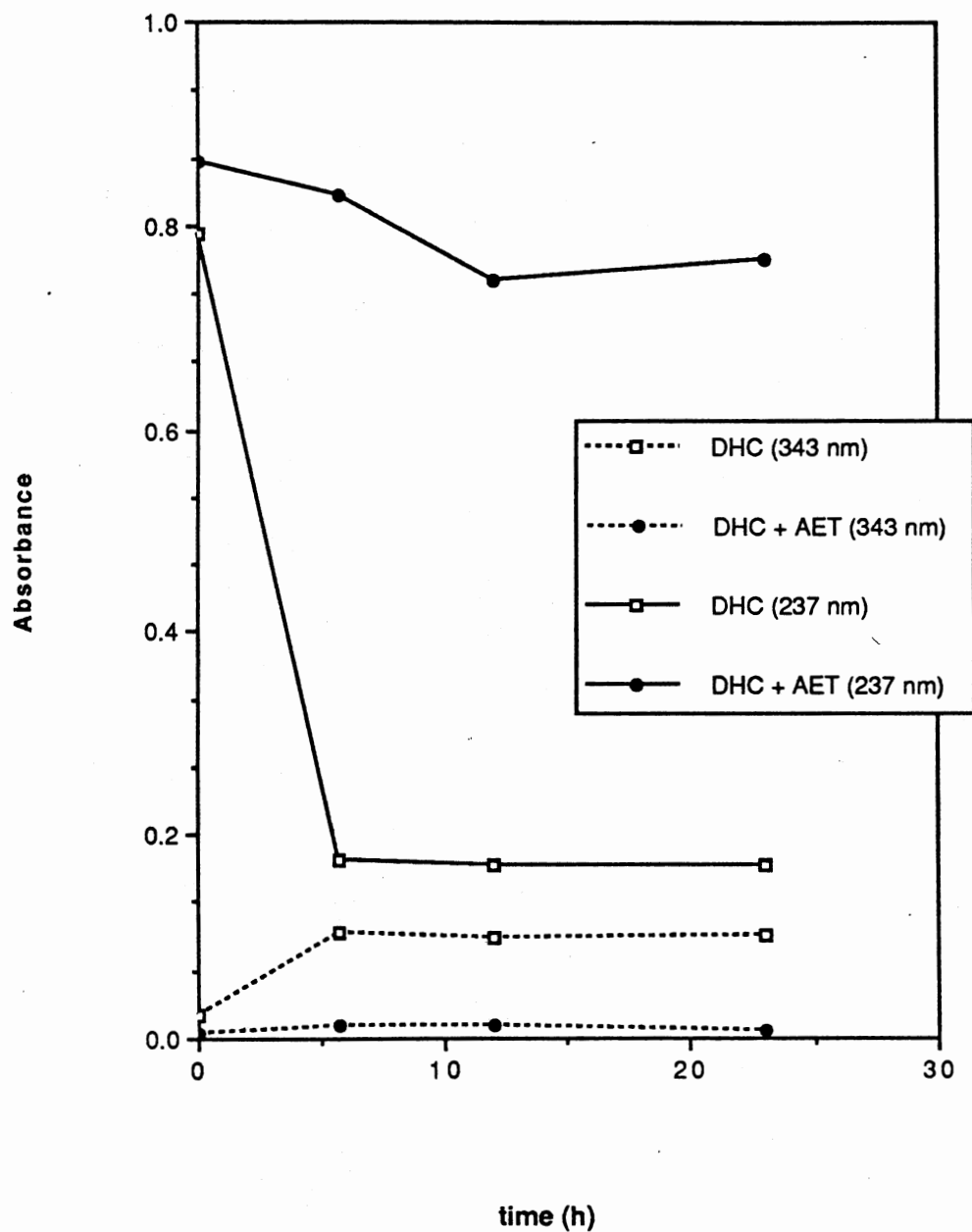


Fig. 21 Effect of AET on Degradation of DHC; Dark Conditions. DHC (0.15 mM in MOPS medium) was mixed with AET (10 mM). Samples were withdrawn at indicated times, diluted, and absorption spectra were taken.

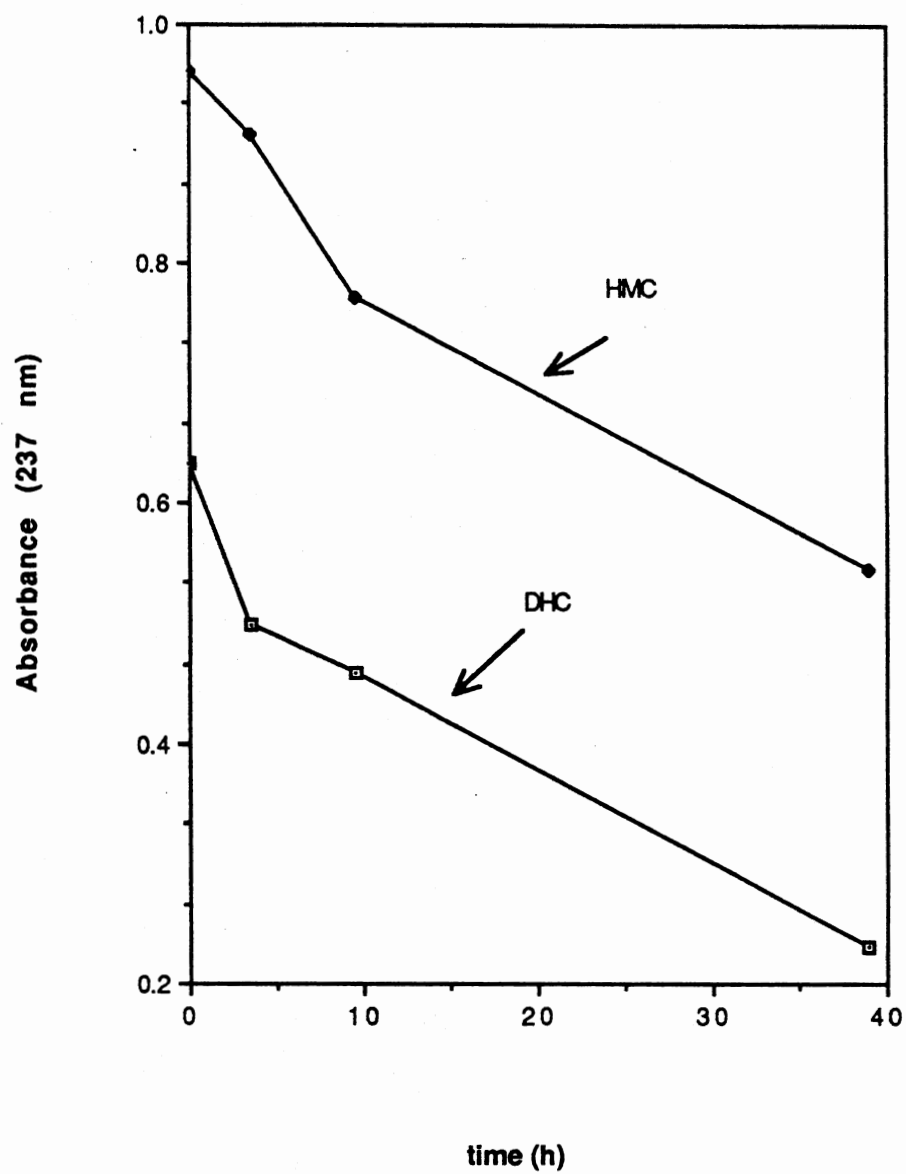


Fig. 22 Light Degradation of DHC and HMC in Methanol. DHC ($17.4\mu\text{M}$) and HMC ($32.3\mu\text{M}$) were dissolved in methanol and exposed to light. Samples were withdrawn at indicated times, diluted in methanol and absorption spectra were taken.

*Spin Trapping of a Free Radical Produced
by DHC in the Light*

In order to test the hypothesis that the photo-degradation of DHC involves a free radical species, at least transiently, DHC was mixed with PBN, a spin-trapping compound, and exposed to light for 2 hours. Shorter time exposures were tested, and gave very low signal yield. These conditions produced a free-radical nitrene signal from the PBN, which was observed by EPR (Fig 23). A barely detectable signal was generated by PBN and DHC in the dark (middle spectrum, Fig. 23). PBN alone, when exposed to light, generated a small signal (bottom spectrum, Fig. 23).

Separation of Degradation Products of DHC

In order to begin characterization of the products of both the light and dark degradation reactions of DHC, preparative samples of DHC were degraded in MOPS medium under conditions duplicating the dark and light degradation reactions carried out in this study. Both reaction mixtures were extracted with CHCl_3 , and reverse-phase HPLC was used to separate the products present in each.

The dark reaction products were a complex mixture with 3 major UV-absorbing peaks: LC, recovered DHC, and a third compound with a UV-visible spectrum very similar to that of LC (Fig. 24).

The light reaction products were separated, giving 5 major peaks in the HPLC conditions used. The UV-visible spectra of these 5 compounds are shown in Figure 25.

DISCUSSION

DHC undergoes a reaction or series of reactions when exposed to light, degrading to form a group of unidentified products. In the absence of light, DHC is degraded by a different reaction, dependent on Fe, and giving LC as a major product, as well as some unidentified products. The two reactions appear to be entirely separate and independent

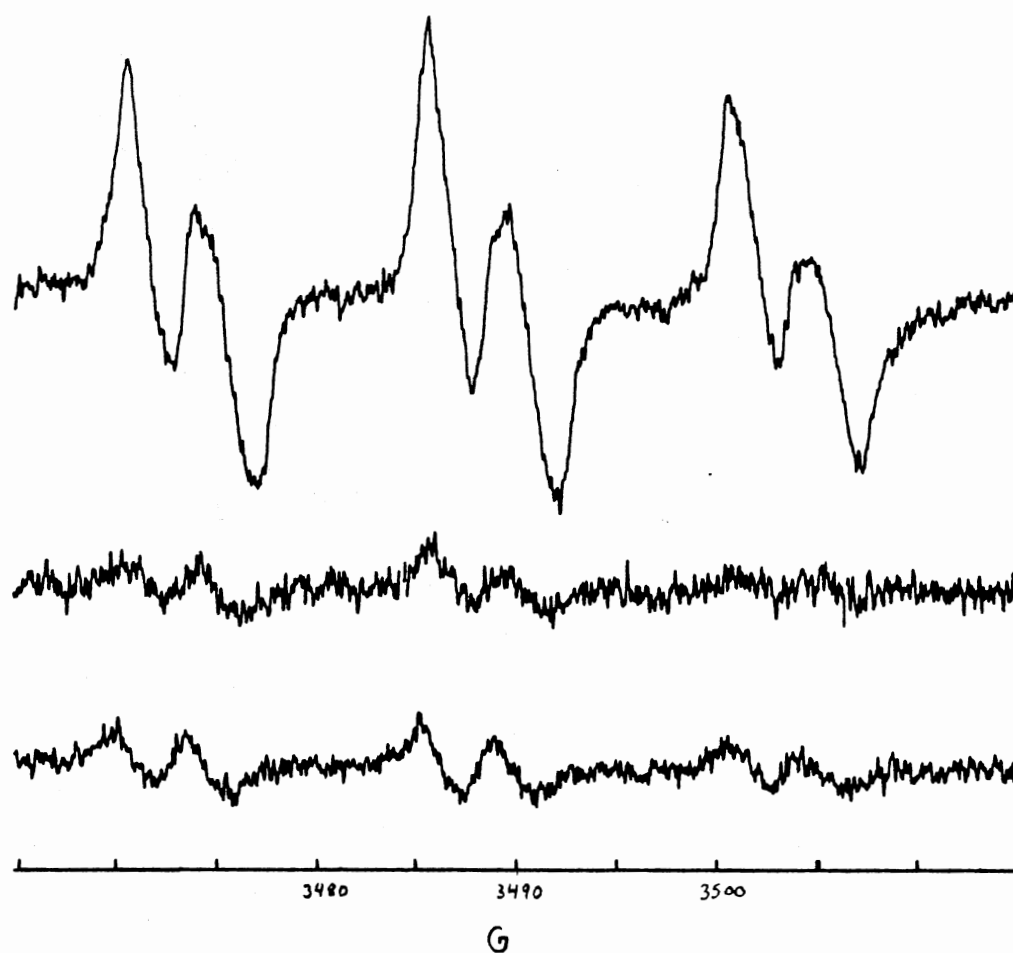


Fig. 23 Spin Trapping by PBN of a Free Radical Produced by DHC in the Light. PBN was diluted in water to 0.1M, and DHC (0.1mM) was added. Sample 1 (top spectrum) was exposed to light, 2 hours. Sample 2 (middle spectrum) was agitated in the dark, 2 hours. Sample 3 (bottom spectrum) PBN alone, was exposed to light 2 hours.

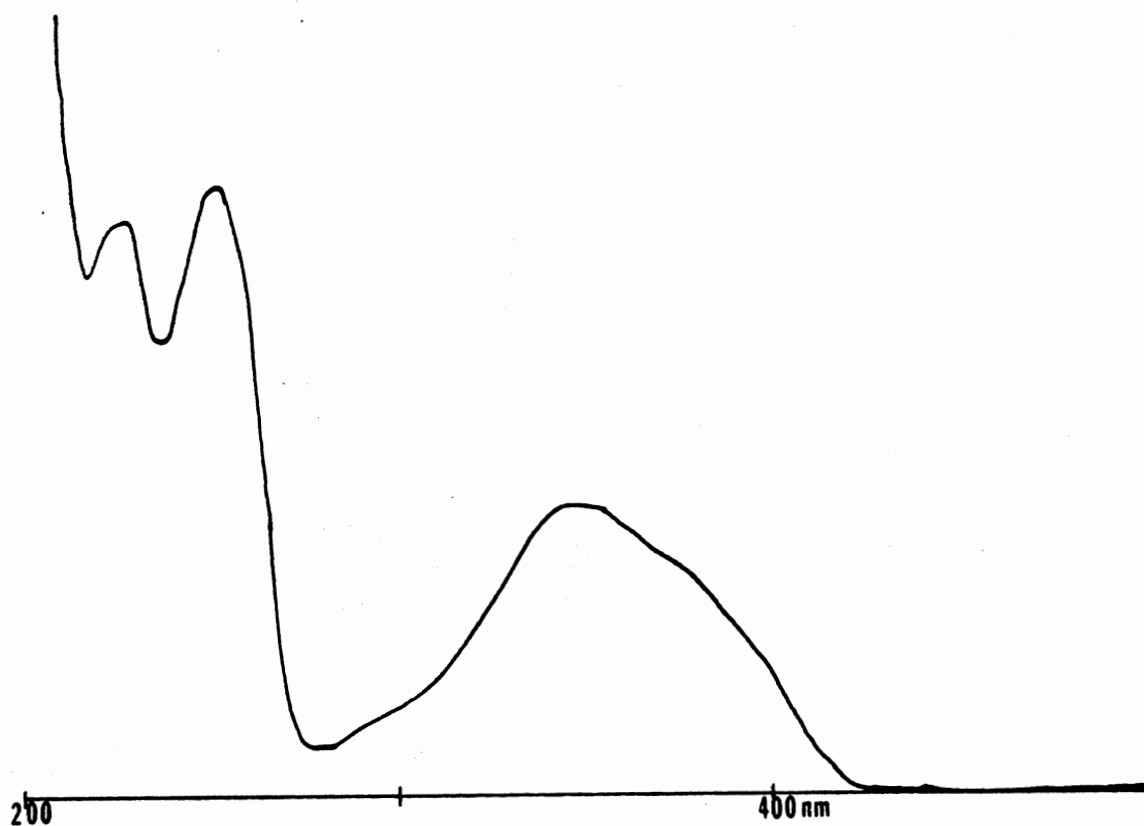


Fig. 24 UV-visible Absorption Spectrum of a Degradation Product of DHC; Dark Conditions. DHC was degraded 24 hours in a mixture of MOPS, Fe^{+3} , and water. The products were separated on HPLC and collected. Peak 3 (spectrum shown here) eluted at 25.5 minutes.

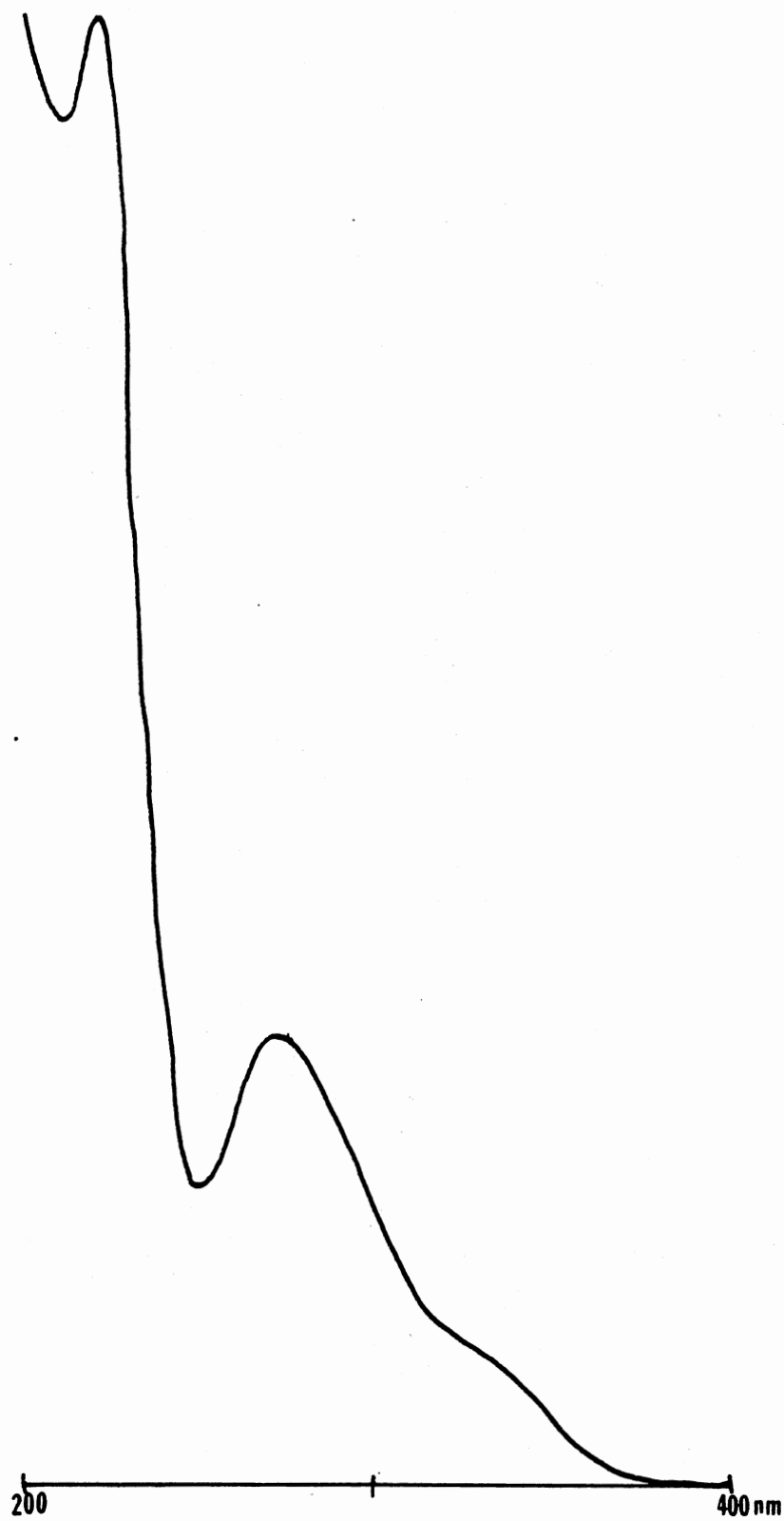


Fig. 25a - e UV-visible Spectra of Light Degradation Products of DHC. DHC (in MOPS) was degraded 24 hours, the products were separated on HPLC and collected. Spectra in 100% methanol of products with elution times: a) 9.9 minutes, b) 15.3 minutes, c) 17.9 minutes, d) 21.7 minutes and e) 25.6 minutes.

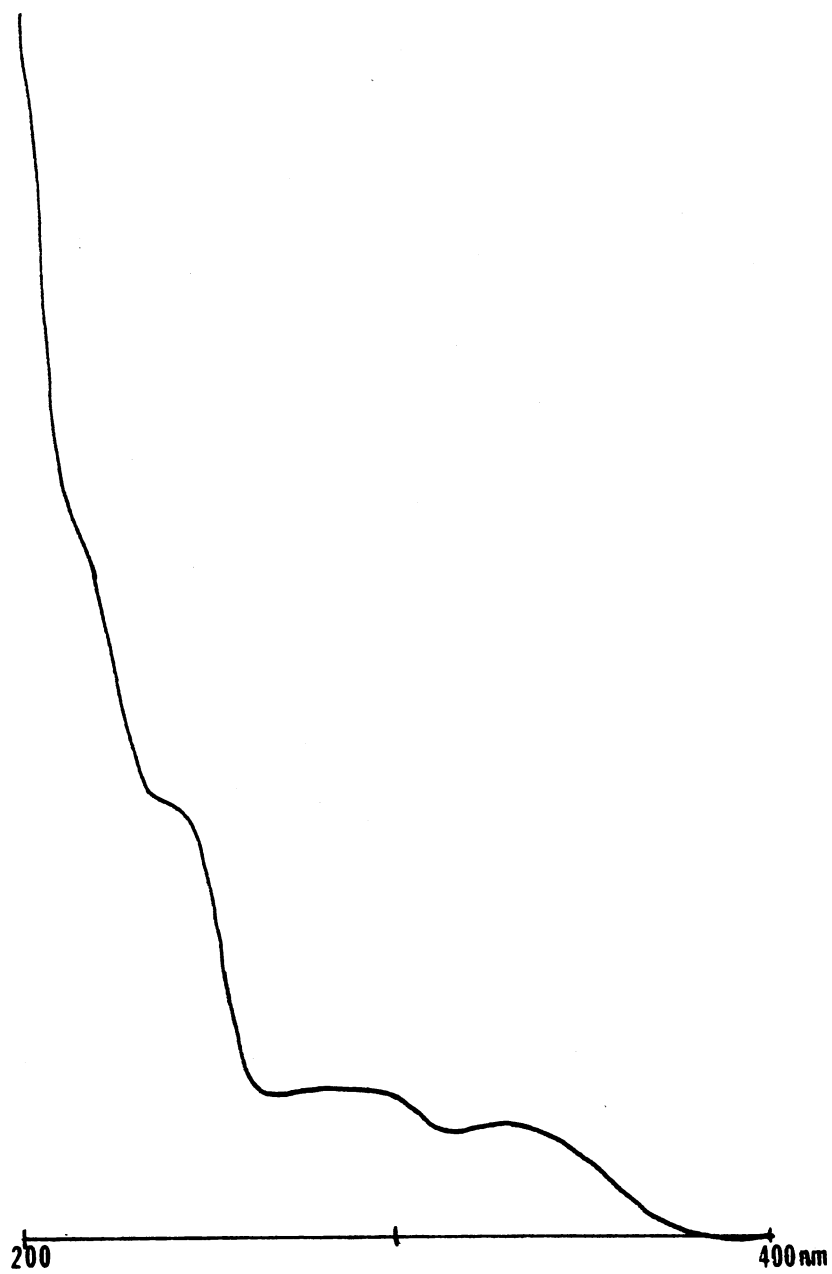


Fig. 25b

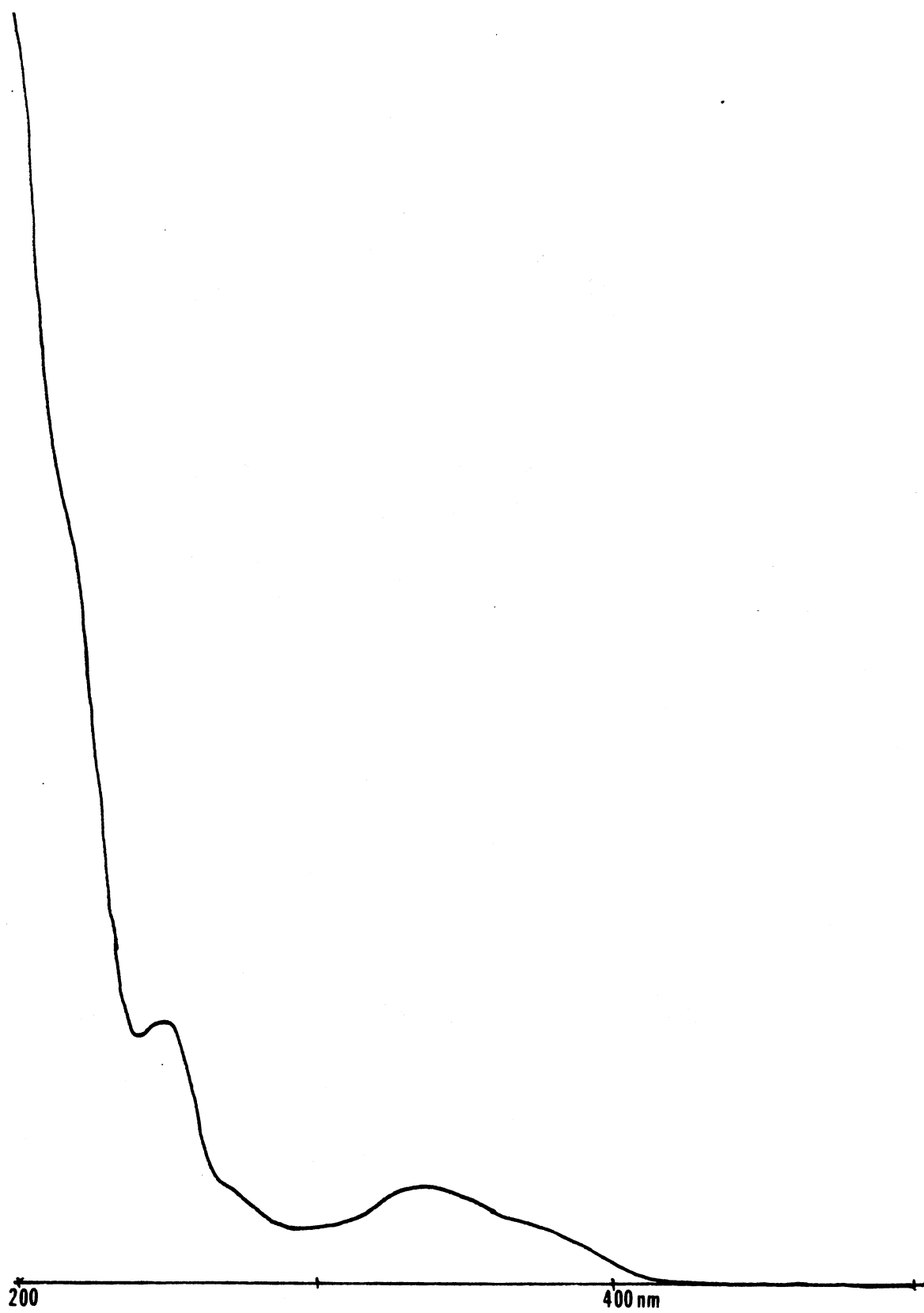


Fig. 25c

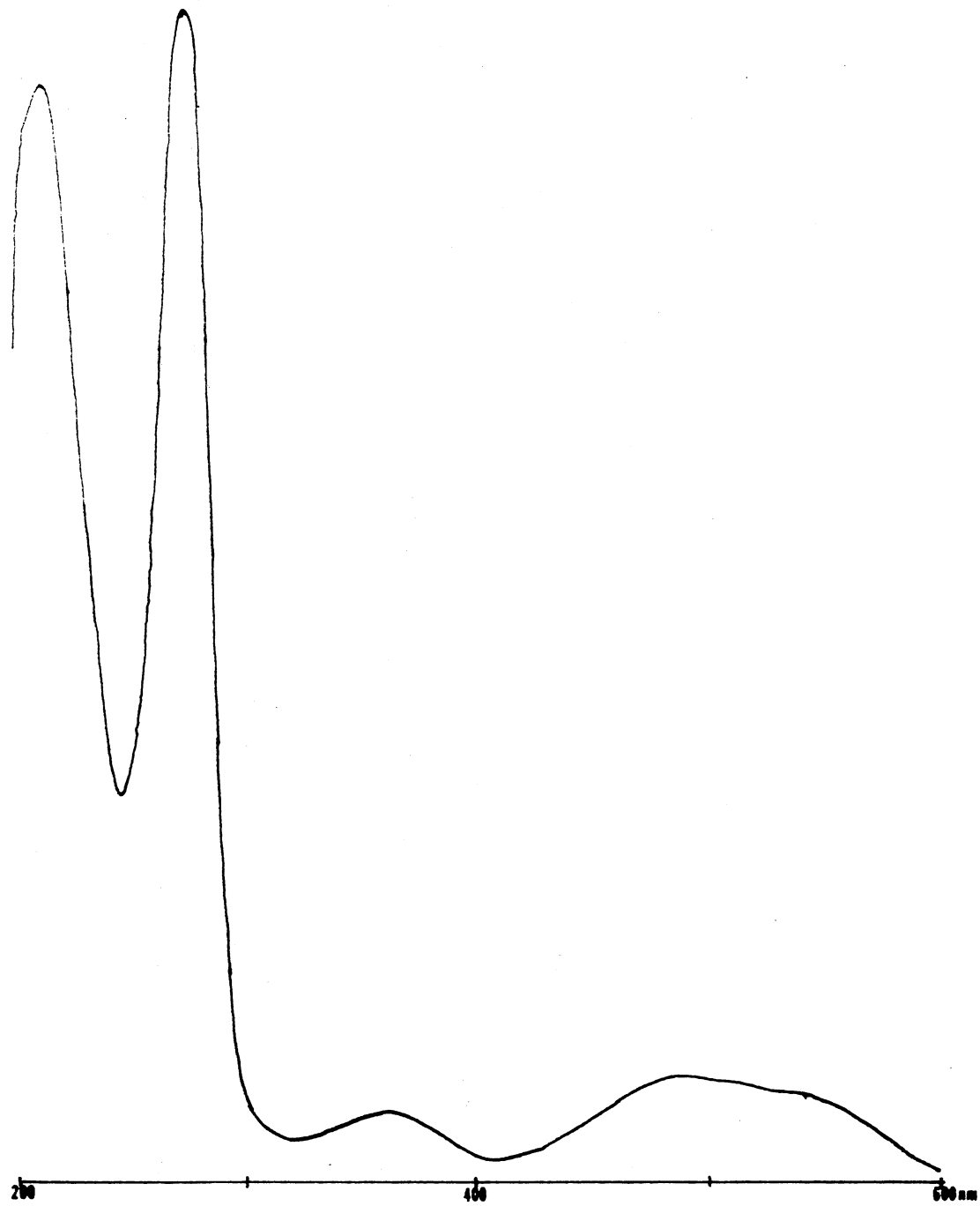


Fig. 25d

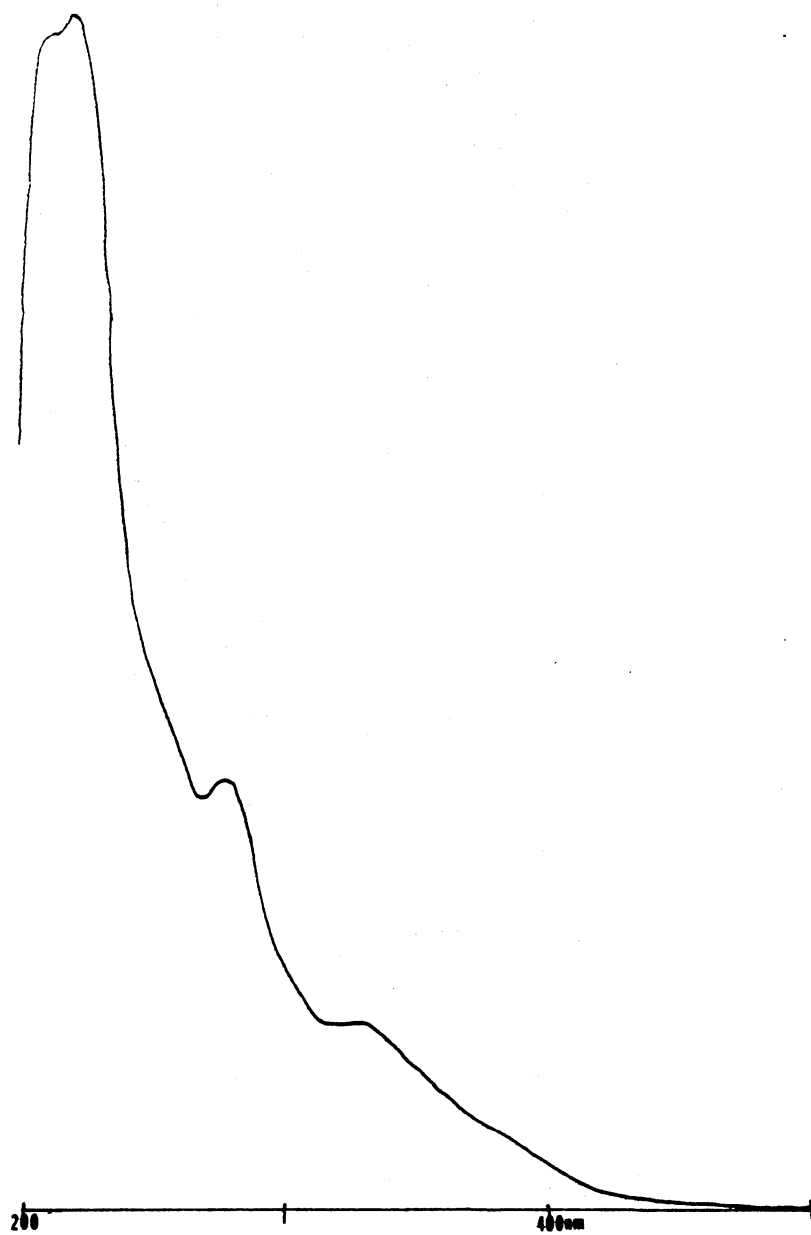


Fig. 25e

from each other. Both may have a role in the toxicity of DHC toward Xcm, in liquid culture assays and *in planta*, since DHC shows antibacterial activity in both light and dark conditions. Some property of the light reaction of DHC ensures that the concentration of DHC in liquid culture required to exert a toxic effect in the light is about one-half that needed for a bactericidal effect in the dark. (See Fig. 4, Chapter IV, this work).

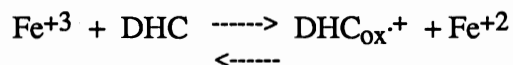
Fe-Dependent DHC Degradation in Dark Conditions

In the dark, DHC dissolved in MOPS medium (chosen as a reaction medium because it is the defined medium used for liquid culture bioassays) was degraded rapidly: the reaction was 76% complete in 1 hour. The reaction was slowed markedly by omitting Fe from the MOPS medium. Under these conditions, the degradation was only 59% complete after 4 hours. Addition of DTPA, an efficient Fe chelator, which prevents redox cycling of the bound Fe (10), almost completely blocked the dark degradation reaction. The two 'no-Fe' conditions (no added Fe, and with added DTPA) are compared in Fig. 7. DHC in both experiments was present at 0.374 mM. Fe in MOPS medium is $10\ \mu\text{M Fe}^{+3}$, and the concentration of Fe present in the MOPS prepared without Fe was unknown, but presumably well below $10\ \mu\text{M}$. Since Fe^{+3} , in a 1/37.4 ratio to DHC, was able to promote a rapid degradation, and Fe present in an even lower ratio still promoted the reaction, it is apparent that only catalytic amounts of Fe are needed. If Fe^{+3} acts as an oxidant, the resulting Fe^{+2} would rapidly and spontaneously autoxidize in this medium, permitting a catalytic recycling of Fe^{+3} . G. Cohen reported a complete autoxidation of ferrous ion in phosphate buffer (included in MOPS) in less than 30 seconds at neutral pH (4).

In Fig. 5b, the data from the DHC degradation shown in Fig. 5a are displayed in a semilog plot. The very low concentration Fe reaction ('no Fe, dk') shows a linear reaction progress, indicating first-order kinetics. The reaction was nearly completely blocked in the absence of redox-available Fe^{+3} . The apparent first-order (or pseudo-first-order)

kinetics of the dark degradation of DHC are probably due to a dependence on the DHC concentration, which declines throughout the reaction. The reaction is also clearly dependent on the presence and concentration of Fe^{+3} , as demonstrated by comparison of the 10 μM Fe^{+3} , trace Fe^{+3} , and DTPA treatments. However, it is probable that autoxidation of the Fe^{+2} generated is so rapid that the Fe^{+3} concentration remains essentially constant throughout. In this case, the Fe^{+3} effect on the rate would appear in the rate constant, leaving pseudo-first-order kinetics, in DHC concentration.

The effect of a large excess of Fe^{+2} (117X DHC) is shown in Fig. 9. Clean (glass-distilled) water was used in this experiment, at low pH, and without a chelator. The degradation of the DHC in the water controls in this experiment suggests that a catalytic amount of Fe^{+3} is present, even in the glass-distilled water. Ferrous ion in large excess almost completely blocked the degradation of DHC, probably by reducing the oxidized form of DHC to regenerate starting material:



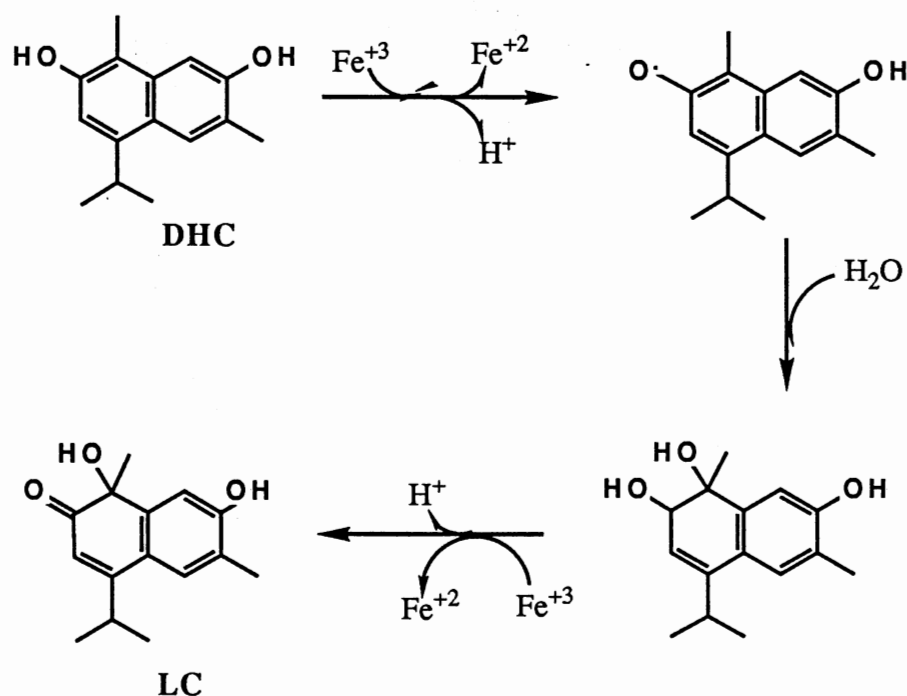
When Fe^{+2} was mixed with DHC in an 18.5/1 ratio (Fig. 10, "2 mM Fe^{+2} "), the degradation was initially prevented. Between 4 and 6 hours, however, the Fe^{+2} was apparently all oxidized, and the DHC was degraded at the same accelerated rate seen in the Fe^{+3} -treated samples. An approximately equimolar solution of DHC and Fe^{+2} showed a slight initial inhibition of the rate of DHC degradation. After 2 hours, the rate of degradation of the equimolar Fe^{+2} treatment was quite comparable to that of the corresponding Fe^{+3} treatment.

The same Fe concentrations were used in the experiments shown in Figs. 9 & 10. In Fig. 9, the Fe^{+2} treatment protected the DHC throughout the experiment (24 hours), and was assumed not to be autoxidized significantly during that time. Although the Fe^{+2} concentrations are the same, the DHC concentration in the experiment shown in Fig. 10 is 6.3-fold higher than that in Fig. 9. Therefore, it is more probable that the briefer

protection of DHC by Fe^{+2} in that experiment was due to oxidation of Fe^{+2} by an oxidized form of DHC, than to spontaneous autoxidation of the Fe^{+2} .

Fe^{+3} appears to function in this oxidative degradation as a one-electron carrier, helping to overcome the energy barrier to the two-electron oxidation of DHC to LC. A possible mechanism for such an oxidation is:

Fig. 26



However, it is not readily apparent how such a mechanism could account for the collapse of the initial observed protection by excess Fe^{+2} .

Free ionic iron is usually present only in extremely small amounts in living tissue and fluids. The demonstrated ability of a very low, but unknown concentration of Fe to catalyze the degradation of DHC may be adequate to account for the DHC dark degradation that occurs *in planta*. It is also possible that Fe, or other metallic ions, bound

to proteins may promote degradation, as demonstrated in the experiments shown in Figs. 14 and 16.

During the hypersensitive response of resistant cotton plants which generates the *de novo* synthesis of DHC, cotton cells at the site of infection are lysed, as shown by transmission electron microscopy (11). Some of the metallo-proteins liberated into the extracellular spaces following cell rupture could potentially contribute to the DHC 'dark' degradation.

Superoxide dismutase (SOD) catalyzed an extremely rapid (complete in 10 minutes) degradation of DHC (Fig. 14). The estimated SOD concentration in this reaction was 161 μM , a slight excess to DHC (99.8 μM). The reaction of DHC with SOD was more rapid than that observed with an equivalent amount of Fe^{+3} (Figs. 5 - 8). The SOD used was a Cu/Zn type, capable of being inhibited by KCN. The DHC degradation by SOD was slowed markedly by the addition of KCN, but was not prevented under these conditions. CN^- is believed to inhibit the dismutase activity of SOD by binding to the oxygen-binding site.

SOD may promote the oxidation of DHC by constraining the bound O_2 in such a way as to promote its ability to accept electrons from DHC. The interference of CN^- with oxygen-binding would account for the observed inhibition of the oxidative degradation. Alternatively, DHC may be able to interact directly with the metallic cofactors of SOD, which are believed to be slightly exposed at the binding site. Such a direct interaction seems improbable, given the disparity of size and shape between DHC and O_2 .

Three other metalloproteins were tested for effect on DHC, and catalase and cytochrome c (both heme proteins) were found to promote the dark degradation reaction. Peroxidase (also a heme protein) had very little effect on DHC.

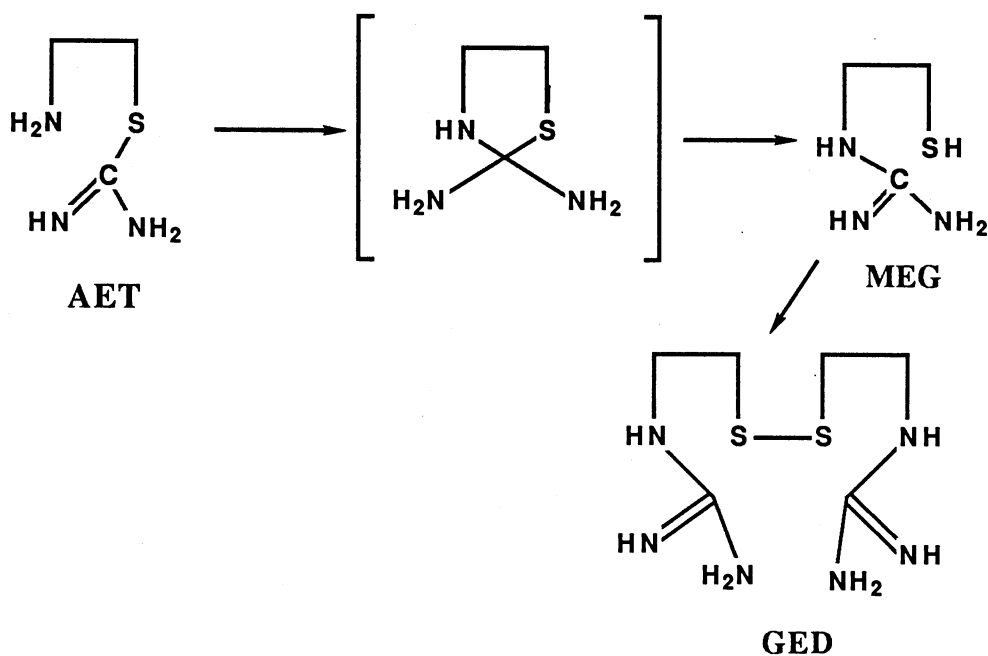
Protein-bound Fe or Cu and Zn, is, therefore, capable of promoting the dark degradation of DHC. The mechanism of this interaction is unknown, and may involve bound oxygen as a redox reactant.

When DHC was dissolved in rigorously anaerobic MOPS medium (prepared without added Fe), the oxidative degradation which produced LC was markedly inhibited, relative to a control sample in air (Fig. 18). The amount of Fe^{+3} present in this MOPS medium can be assumed to be very small. Presumably, only catalytic re-oxidation and recycling would permit this amount of Fe to stimulate the oxidative degradation of DHC to the degree observed in Figs. 5a, b & c, and in the control (O_2) sample in Fig. 19. When the re-oxidation of Fe^{+2} was blocked by the absence of O_2 , the ability of Fe^{+3} to catalyze the degradation of DHC was significantly inhibited.

Crocin, a water-soluble carotenoid capable of scavenging free radicals did not inhibit the dark degradation of DHC in MOPS medium. The 440 nm absorption of crocin, which is rapidly bleached by free radicals, was bleached no more by DHC in MOPS medium in the dark than by a MOPS medium control. This result may indicate that no free radical is involved in the dark oxidative degradation of DHC. Alternatively, a free radical intermediate may occur in the reaction, but may simply possess energetic or conformational properties unfavorable for an interaction with crocin.

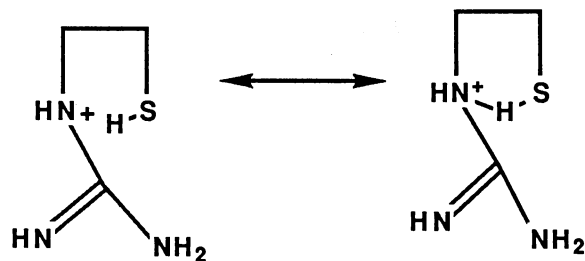
The degradation of DHC in the dark, like that in the light, was almost completely blocked by the presence of AET (structure below). AET is reported to undergo transguanylation at neutral or alkaline pH to form the aminothiols 2-mercaptoethyl guanidine-HBr (MEG), Fig. 27. MEG is reported to be the biologically active form of this radioprotectant (12).

Fig. 27 Transguanylation Rearrangement of AET



Aminothiols such as MEG are capable of scavenging free radicals and forming highly resonance stabilized free radical species with the unpaired electron shared between the N and S atoms (Fig. 28) (13).

Fig. 28



MEG is capable of acting as a reductant toward oxidized intermediates in the degradation of DHC, either as a single-electron interaction with a free radical, forming the free radical shown above, or as a two electron reduction, forming bis(2-guanidinoethyl)disulfide (GED).

The dark reaction of DHC is likely to occur *in planta*. It is not clear, however, whether it would function to detoxify the DHC (LC, the major product, requires much higher concentrations than DHC to inhibit Xcm) or as part of the toxic interaction with Xcm. The latter possibility would be strongly indicated if a free radical could be observed as an intermediate in the Fe-dependent oxidation.

Photo-Degradation of DHC

The photo-degradation of DHC, unlike the dark degradation, is not clearly dependent on Fe^{+3} . In the light treatments without Fe of Figs. 5a ("no Fe, It") and 6 ("no Fe, It"), the DHC samples were degraded very nearly as rapidly as the treatments with $10 \mu\text{M Fe}^{+3}$ present (Fig. 5a, "+ Fe, + It"; Fig. 6, "+ Fe, It"). The semilog plot in Fig. 5b, using data from the experiment shown in Fig. 5a, shows first-order decomposition of DHC for both the trace Fe^{+3} ("no Fe, It") and the $10 \mu\text{M Fe}^{+3}$ ("+ Fe, It") treatments. The slope of the $10 \mu\text{M Fe}^{+3}$ reaction data is steeper than that of the trace Fe^{+3} treatment. The very rapid autoxidation of Fe^{+2} under these conditions probably held the Fe^{+3} concentration constant throughout the reaction. Making this assumption, the effect of Fe^{+3} concentration would appear in the pseudo-first-order rate constant. Since even a large excess of the chelator DTPA did not markedly inhibit the photo-degradation of DHC relative to the trace Fe^{+3} treatment (Figs. 5a & 6), Fe^{+3} is unlikely to be directly involved in the rate-limiting step of the degradation. However, the photo-degradation of DHC probably involves several reactions, a supposition supported by the isolation of five major degradation products from a DHC photo-degradation mixture. One or more of the reactions leading to these products may be promoted by $10 \mu\text{M Fe}^{+3}$.

Somewhat surprisingly, the rate of photo-degradation of DHC appeared to be unaffected by anaerobic conditions (Fig. 17). This result suggests that either 1) the rate-limiting step of this series of reactions does not involve oxygen, and very small quantities of oxygen will suffice for degradation, or 2) oxygen is not involved in the photo-degradation of DHC. The result is surprising because most reported photo-activated toxic compounds (photosensitizers) exert their photo-toxicity by interacting with oxygen, generating singlet oxygen or superoxide anion. The fact that such an interaction does not appear to participate in the photo-degradation of DHC does not necessarily eliminate the possibility that it is part of the photo-activated bactericidal activity of DHC.

Catalase and SOD catalyze a net conversion of superoxide anion to water, but did not protect DHC from photo-degradation (Fig. 12). In fact, SOD, catalase, and lysozyme slightly accelerated this degradation, relative to a control without protein present. This result, and the result of the anaerobic light degradation, strongly suggest that photo-dynamic generation of superoxide anion is not involved in the photodegradation of DHC.

A fourth protein, BSA, was included in this experiment as a control protein without reactive oxygen catalytic capability. BSA quite markedly protected DHC from photodegradation. Human serum albumin interferes with resistant tobacco leaf blight hypersensitive response, probably by scavenging free radicals (14).

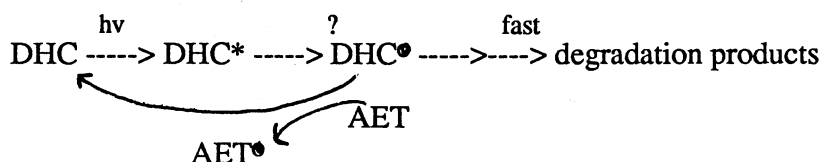
Further evidence for the involvement of a free radical in the photodegradation of DHC was provided by crocin. When crocin was mixed with DHC and exposed to light for 12 hours, the bleaching of its 440 nm absorption band specific to the DHC interaction (calculated by subtracting the amount of bleaching in a control in MOPS which was concurrently exposed to light) was 16% of the original (unbleached) 440 nm absorption. This corresponds to the absorption of 1.5 nmoles of crocin. The DHC mixed with crocin was partially protected from degradation (Fig. 19). The absorption at 237 nm remaining in a light-treated sample of DHC at 12 h was subtracted from that of the DHC/crocin sample, and the DHC protected from degradation by crocin was calculated to be 1.25

nmoles. The free-radical scavenging capability of crocin may act to regenerate DHC from a DHC-free radical species:



The nearly 1:1 correspondence between protected DHC and bleached crocin suggests that the collision between DHC^\bullet and crocin is sufficiently rare that few DHC molecules undergo more than one such collision in 12 hours. The slightly larger amount of bleached crocin indicates that some recycled DHC may go through this interaction more than once. The free radical species may be too reactive to have a high incidence of the protective crocin collisions. A larger excess of crocin might have increased the incidence of collisions and, therefore, provided more complete protection, but the intensity of the crocin absorbance would have interfered with spectral observation of the DHC.

AET provided nearly complete protection to DHC from photo-degradation, but only when present in large excess: 66.7-fold excess was effective in protecting DHC (Fig. 21, 10 mM AET), but 6.7-fold excess was only slightly protective (Fig. 12, 1 mM AET). The progress of DHC degradation in the AET treated samples was fairly linear with time, and did not display the delayed acceleration which would be observed if AET protected at high efficiency until it was consumed. The requirement for a large excess of AET, therefore, is probably due to the need for the collision of AET with the free radical to compete with a very rapid reaction of the DHC radical species:



The disappearance of DHC in the presence of mannitol, AET, or MOPS medium (experiment shown in Fig. 20) was plotted on a log scale (Fig. 20a) and shows linear

behavior, indicating first-order or pseudo first-order kinetics. The reaction is probably directly dependent on the concentration of DHC, with other factors (*e.g.*, presence of AET) influencing the rate constant.

The most direct evidence for involvement of a free radical in the photodegradation of DHC was obtained using a relatively light-stable spin trap (PBN). PBN developed the signal shown in the top spectrum, Fig 23, when it was mixed with DHC (PBN/DHC = 10/1) and exposed to light for two hours. The EPR spectrum of the free radical species trapped under these conditions had the hyperfine splitting constants $A_N = 15.24$ and $A_H = 3.53$ G. PBN has a β -H and produces hyperfine splitting due to both the β -H and to the nitroxide nitrogen. The magnitude of the hyperfine splitting by such a spin trap is useful in identification of the trapped species. In the particular case of the DHC/light generated free radical, the hyperfine constants suggest the presence of more than one free radical species: A_N is similar to that of a trapped $\text{OH}\cdot$, but the A_H splitting, much larger than that of a trapped $\text{OH}\cdot$, is similar to that reported for $\cdot\text{CH}_2\text{OH}$ or $\text{CH}_3\text{CH}\cdot\text{OH}$ (15). Other indications of trapping of mixed species seen in the spectrum are: the broadness of the peaks, and the jagged fine structure on the peaks. Since the photo-generation of free radicals from DHC is a rather low-yield reaction, it was necessary to expose the DHC-PBN solution to light for 2 hours in order to accumulate sufficient signal for observation. This prolonged incubation may permit secondary reactions of any of the initial free radical species which was not trapped, and some trapping of even a very low yield reaction product.

Some nitrones very readily undergo photochemical rearrangements which can generate nitroxide free radicals. DMPO rearranges to an oxazirane under UV-irradiation, which hydrolyzes to form the same nitroxide generated by trapping of $\text{OH}\cdot$. (16) PBN is considered to be relatively light-stable, but may undergo some photo-degradation during 2 hours of exposure, leading to the signal in the bottom spectrum shown in Fig. 23.

The spin trap also apparently partially protected the DHC sample from photodegradation. After approximately 4 hours of exposure to light, the DHC/PBN mixture (scanned against the PBN control to subtract the intense PBN absorption) still exhibited a marked DHC spectrum, corresponding to roughly 30% the original sample. Although no control DHC sample without PBN was included in the study, this time of exposure in similar treatments in MOPS produced complete degradation.

LC, like DHC, exhibits greatly stimulated antibacterial activity when exposed to light (see Fig. 5, Chapter IV). It was the major product of DHC degradation in the dark, but did not appear among the products isolated from DHC which was subjected to 24 hours of photodegradation. None of the time course samples of DHC photodegradation showed spectra with a peak or shoulder of absorption at 250 nm, the absorption maximum of LC.

The degradation of LC in light and dark conditions, with and without Fe, is shown in Fig. 11. LC was much more stable than DHC under all the conditions shown. The absorption spectra of all samples at 10.5 hours showed LC to be only about 50% degraded, or even less; whereas DHC in either light or dark conditions (except the dark/DTPA treatment) was completely degraded by 10.5 hours. Even after 24 hours, distinct LC spectra were apparent in the absorption spectra of all the samples, obscuring the spectra of the products, and indicating that the reactions had not gone to completion. The light degradation products appeared, nonetheless, to be spectrally distinct from those of the light reaction of DHC. The LC light degradation products showed an increasing absorption at 280 nm, unlike the DHC light product mixture. The dark treatments gave spectra with reduced concentrations of LC, but apparently no other strongly light-absorbing species. Also in contrast to DHC, LC was somewhat stabilized by the dark treatment with Fe^{+3} , relative to the other treatments.

These results suggest that LC is not an intermediate in the photo-degradation of DHC, since LC degrades much more slowly than DHC, and apparently forms different products. However, LC might be an intermediate if DHC or a reactive product of DHC interacts with

LC during DHC photodegradation to cause a rapid degradation to the previously described DHC light products.

HMC, a close structural analog of DHC, was degraded in methanol in the light at the same rate as DHC (Fig. 22). The light degradation products of HMC were spectrally indistinguishable from those of DHC, just as the absorption spectra of DHC and HMC are virtually identical. Apparently HMC undergoes a photo-degradation very similar to the reaction DHC undergoes in methanol, with the same or similar rate, mechanism, and products. Since the 7-methoxy group of HMC would be expected to be much less reactive than the 7-hydroxy of DHC, these results suggest that the light degradation reaction, at least in methanol, can proceed by reactions at the 2-hydroxy group alone. In bioassays (Fig. 6, Chapter IV), HMC showed no antibacterial activity, and was not apparently stimulated by light. Since HMC appears to undergo the same light reactions as DHC, its failure to display light-stimulated toxicity may be due solely to its severely limited water solubility.

Identification of the major products of DHC photo-degradation is a necessary part of characterizing this reaction. The mechanisms of oxidative coupling of many phenols are well studied, and if some of the products of DHC photo-degradation are dimers or multimers, a reaction can readily be proposed from this information. The identification will be pursued, using the separated products whose spectra are shown in Fig. 25.

It has been the goal of this study to understand the mechanism of toxicity of DHC toward Xcm, both in light and dark conditions. In the experiments described in Chapter IV, the problem was approached by attempting to interfere with the toxicity of DHC with reagents of reported capacity for scavenging or quenching various reactive oxygen species. Of the reagents tested, only DABCO gave a fairly significant protection from DHC toxicity in the light (Fig. 11a, Ch. IV). Bixin was itself photo-toxic, but showed a small protective effect in the dark, as did Na-benzoate (Figs. 13b & 14b, Ch. IV). The very limited success of this approach implied that either the toxic interaction occurs in a

compartment mostly inaccessible to the reagents tested or that multiple reactive species are present.

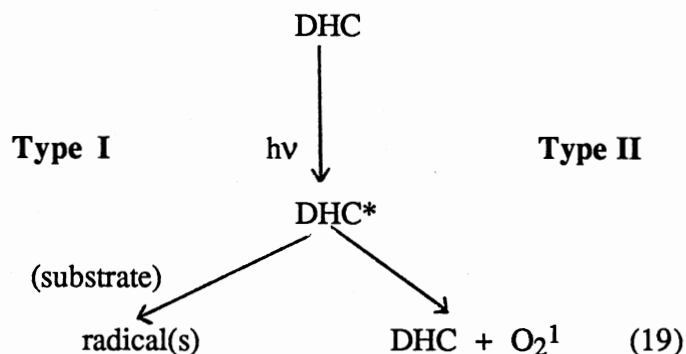
The experiments described in Chapter V were undertaken to investigate the reactions of DHC without the complicating effect of bacteria. Under these circumstances, the light reaction(s) of DHC was shown to involve a free radical species, as evidenced by interaction with crocin, AET, and PBN. The major free radical produced under these circumstances was probably a C-centered, rather than O-centered radical, as suggested by the epr spectrum and by the lack of effect of anaerobic conditions.

AET and crocin, which were effective reagents in interfering with the light reaction were shown to be toxic toward Xcm in concentrations even lower than those required to be effective in blocking DHC photo-degradation. (For toxicity tests of AET and crocin, see Appendix). BSA, which also inhibited the light reaction, was not bioassayed, due to the reported proteolytic capability of Xcm (17).

The dark reaction of DHC in the abiotic experiments was shown to be Fe^{+3} -dependent, and was blocked by DTPA, excess Fe^{+2} , and AET, and was inhibited by anaerobic conditions. Unfortunately, all of these conditions were shown to be toxic or inhibitory to Xcm, or, in the case of excess Fe^{+2} , incompatible with any growth medium.

The two approaches did not produce the desired independent confirmation of a clear-cut mechanism of toxicity. They suggest, instead, a highly reactive molecule, which can undergo a variety of reactions leading to degradation and/or toxic events.

DABCO, which partially inhibited the photo-stimulation of toxicity, did not inhibit the light degradation. Anaerobic conditions also did not inhibit the light degradation of DHC. Although these results do not support each other, they are not necessarily contradictory. In one of the reactions leading to photo-toxicity, DHC may act as a type-II photosensitizer. (See Fig. 29) In this case, ground-state DHC would be regenerated, along with the singlet oxygen. DABCO could quench this reaction, protecting Xcm, without interfering with a competing type-I reaction, leading to photo-degradation and free radicals.

Fig. 29 Proposed Toxic Reaction Pathways of Light-Activation

This apparent multiplicity of reactions available to the DHC molecule, while making characterization of the mechanism of toxicity difficult, probably contributes to its effectiveness as a phytoalexin.

EXPERIMENTAL

Preparation and Purification of Phytoalexins

DHC and HMC were prepared synthetically, as described in Chapter III (20). LC was prepared by oxidation of DHC in a solution of MOPS medium with additional Fe⁺³ (added as FeNH₄(SO₄)₂·12H₂O), as described in Ch. IV. DHC, HMC and LC were purified before use by reverse-phase HPLC on C-18 silica, in a methanol/water solvent system. DHC and LC were eluted with an isocratic methanol:water, 60:40, (v/v) solvent system, and HMC was eluted with methanol:water, 67:33, (v/v). All three compounds were kept under N₂ and handled under blue-deficient light from General Electric FO6T12/GO gold fluorescent lamps, except where specified.

Time-Course Degradations

The degradation reactions were carried out under conditions very similar to the DHC/Xcm bioassay conditions. The DHC, except where specifically noted, was diluted

in MOPS growth medium, which is based on the MOPS growth medium developed by Neidhardt *et al.* (20) and modified by McNally *et al.* (21). MOPS growth medium was prepared with 10 μM FeSO_4 . For several experiments, specifically noted, the FeSO_4 was omitted. The solution of DHC in MOPS medium, with other compounds where noted, was transferred to a 1.5 ml conical polypropylene centrifuge tube, and mounted 9 - 10 cm directly below a cool-white fluorescent lamp. The tubes were agitated on an orbital shaker at 30°C. Dark condition samples were double-wrapped with aluminum foil and otherwise treated as were the light samples. Aliquots were withdrawn at the stated times, diluted in MOPS medium, and scanned on a Hitachi 100-80A spectrophotometer.

Ferrous and Ferric Ion/ DHC Degradations

Fe^{+2} solutions were prepared freshly for each experiment, by dissolving $\text{FeSO}_4 \cdot 7\text{H}_2\text{O}$ in glass-distilled water, with a minimum volume of H_2SO_4 used to achieve solvation. Fe^{+3} solutions were prepared in the same way, from $\text{FeNH}_4(\text{SO}_4)_2 \cdot 12\text{H}_2\text{O}$, and were more stable than the Fe^{+2} solutions.

DHC was extracted away from the iron salts in these experiments for absorbance spectroscopy or HPLC. Aliquots were withdrawn from the reaction tube, diluted to 1 ml in water, and extracted three times with 0.4 ml CHCl_3 . The CHCl_3 was evaporated, and the extracted products redissolved in 60% methanol (v/v).

The eluting peaks in the experiment shown in Fig. 10 were cut out and weighed. Using a standard curve developed for these HPLC conditions, the peak weight was converted to nmoles of DHC or LC.

Protein/DHC Degradation Experiments

Horseradish SOD, bovine liver catalase, horseradish peroxidase and horse heart cytochrome c were obtained from Sigma. Buffered protein solutions were prepared in

either MOPS medium or 50 mM K_2HPO_4/KH_2PO_4 buffer, pH, 7.8. KCN solutions were prepared fresh and used promptly.

Crocin/DHC Experiments

Crocin was prepared by extraction from saffron, according to the published method (22). The crocin was stored in methanol at 0 °C until use, and protected from light.

Spin-Trapping of Free Radical

PBN was obtained from Aldrich, and a 2M stock solution in DMSO was prepared and stored at 0°C. DHC (0.1 mM) and PBN (0.1 M) were mixed in H₂O or MOPS medium without Fe. The spectra shown in Fig. 23 were taken in H₂O, but no significant differences were seen in spectra taken in MOPS medium without Fe. Instrument settings for the spectra in Fig. 23 were: modulation frequency, 100 kHz; modulation amplitude, 2.5 G; time constant, 0.1 s; microwave frequency, 9.76 GHz; microwave power, 10 mW; and scan rate, 100 s, on a Bruker ER 200D spectrometer.

REFERENCES

1. Essenberg, M., Doherty, M.d., Hamilton, B.K., Henning, V.T., Cover, E.C., McFaul, S.J., and Johnson, W.M. (1982) *Phytopathology*, **72**, 1349
2. Sun, T.J. (1987) Ph.D. Dissertation, Oklahoma State University
3. Stipanovic, R.D., Greenblatt, G.Z., Beier, R.C., and Bell, A.A. (1981) *Phytochemistry* **20**, 729
4. Cohen, G. (1985) *CRC Handbook of Methods for Oxygen Radical Research*, Ed. R. Greenwald, CRC Press, Boca Raton, FA, p. 55
5. Crapo, J.D., McCord, J.M., and Fridovich, I. (1978) *Methods in Enzymology, Biomembranes Part D*, Eds. S. Fleischer and L. Packer, Academic Press, New York, p. 382
6. Bors, W., Saran, M. and Michel, C. (1982) *Int. J. Radiat. Biol.* **41**, 493

7. Winston, G. W. and Cederbaum, A.I. (1985) CRC Handbook of Methods for Oxygen Radical Research, Ed. R. Greenwald, CRC Press, Boca Raton, FA, p. 169
8. Bors, W., Michel, C. and Saran, M. (1981) Oxygen and Oxy Radicals in Chemistry and Biology, Eds. M.A. Rogers and E.L. Powers, Academic Press, New York, p. 75
9. Casarett, A.P. (1968) Radiation Biology, Prentice-Hall, Englewood Cliffs, NJ, p. 257
10. Halliwell, B. (1978) FEBS Lett. **92**, 321
11. Al-Mousawi, A.H., Richardson, P.E., Essenberg, M. and Johnson, W.M. (1982) Phytopathology **72**, 1230
12. Shapira, F., Doherty, D.G. and Burnett, Jr., W.T. (1957) Radiation Research **7**, 22
13. Vijayan, K., Vedavathi, B.M., and Mani, A. (1983) Proc. Indian Acad. Sci. **92**, 457
14. Kiraly, Z., Hevesi, M. and Klement, Z. (1977) Acta Phyto. Acad. Scient. Hungaricae **12**, 247
15. Singh, A. (1982) Can. J. Physiol. Pharmacol. **60**, 1330
16. Finkelstein, E., Rosen, G.M. and Rauckman (1980) Arch. of Biochem. and Biophys. **200**, 17
17. Gholson, R.K., Rodgers, C. and Essenberg, M. (1987) Fed. Proc. **46**, 2212
18. Foote, C.S., Shook, F.C., and Abakerli, R.B. (1984) Methods in Enzymol., Oxygen Radicals in Biological Systems, Ed. L. Packer, Academic Press, New York, p.36
19. Stipanovic, R.D. and Steidl, J. (1986) Syn. Comm. **16**, 1809
20. Niedhardt, F., Bloch, P. and Smith, P. (1974) J. Bacter. **119**, 736
21. McNally, K., Gabriel, D. and Essenberg, M. (1984) Phytopathology **74**, abstract #A685, p. 875
22. Friend, J. and Mayer, M. (1960) Bioch, et Biophys. Acta **41**, 422

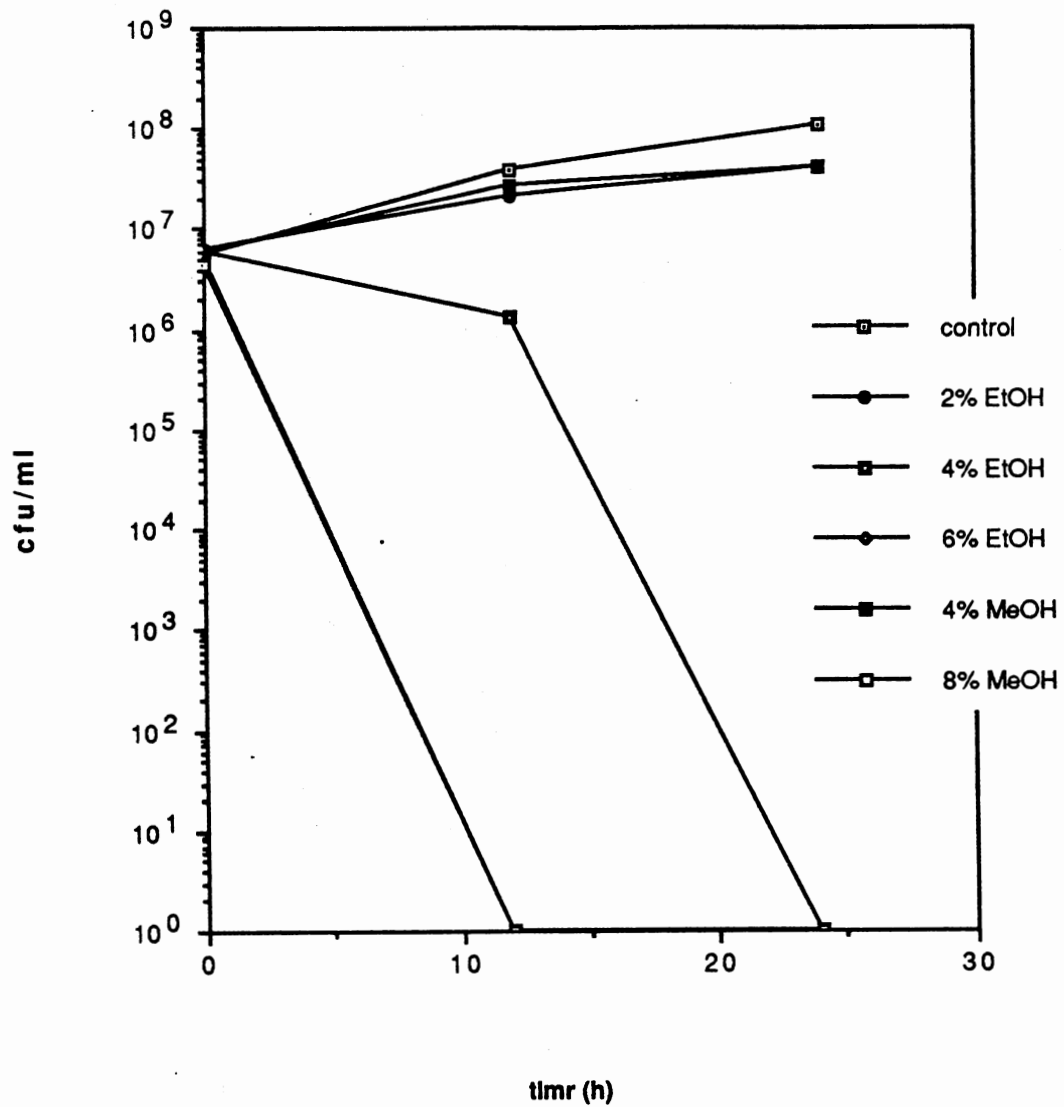
BIBLIOGRAPHY

- 1) Cho, V. S., Wilcoxon, R. D. and Froehner, F. I. (1973) *Phytopathology*, **63**, 760
- 2) Walker, J. C., and Shahmann, M. A. (1955) *Ann. Rev. Plant Physiol.* **6**, 351
- 3) Darvil, A. G. and Albersheim, P. (1984) *Ann. Rev. Plant Physiol.* **35**, 243
- 4) Klement, Z., Farkas, G. L. and Lovrekovic, L. (1964) *Phytopathology* **54**, 474
- 5) Turner, J. B. and Novacky, R. (1974) *Phytopathology* **61**, 862
- 6) Kunz, G. (1986) Ph. d. Dissertation, Technischen Hochschule Darmstadt, West Germany
- 7) *ibid*
- 8) Keppler, L.D., Atkinson, M. and Baker, J. (1988) 7th Ann. Plant Biochem. and Physiol. Symp., Univ. Missouri, Columbia, abstr # 16
- 9) Chai, H.B. and Doke, N. (1987) *Phytopathology* **77**, 645
- 10) Keppler, L.D. and Novacky, A. (1986) *Phytopathology*, **76**, 104,
- 11) Morgham, A.T., Richardson, P.E., Essenberg, M. and Cover, E. (1988) *Physiol. and Molec. Plant. Path.* **32**, 141
- 12) Sequeira, L., Gaard, G. and de Soeten, G. A. (1977) *Physiol. Plant Pathol.* **10**, 43
- 13) Al-Mousawi, A.H., Richardson, P. E., Essenberg, M. and Johnson, W. M. (1982) *Phytopathology* **72**, 1230
- 14) Al-Mousawi, A.H., Richardson, P.E., Essenberg, M. and Johnson, W.M. (1982) *Phytopathology* **72**, 1222
- 15) Essenberg, M., Doherty, M. d., Hamilton, B.K., Henning, V. , Cover, E., McFaul, S.J. and Johnson, W.M. (1982) *Phytopathology* **72**, 1349
- 16) Essenberg, M., Hamilton, B., Cason, Jr, E.T., Brinkerhoff, L. A., Gholson, R.K., and Richardson, P.E. (1979) *Physiol. Plant Pathol.* **15**, 69
- 17) Hamilton, B., Essenberg, M., Richardson, P.E. and Scholes, V.E. , unpublished
- 18) Essenberg, M., Cason, E.T., Jr, Hamilton, B., Brinkerhoff, L.A., Gholson, R.K., and Richardson, P.E. (1979) *Physiol. Plant Pathol.* **15**, 53
- 19) Pierce, M. and Essenberg, M. (1987) *Physiol. Molec. Plant Pathol.* **31**, 273

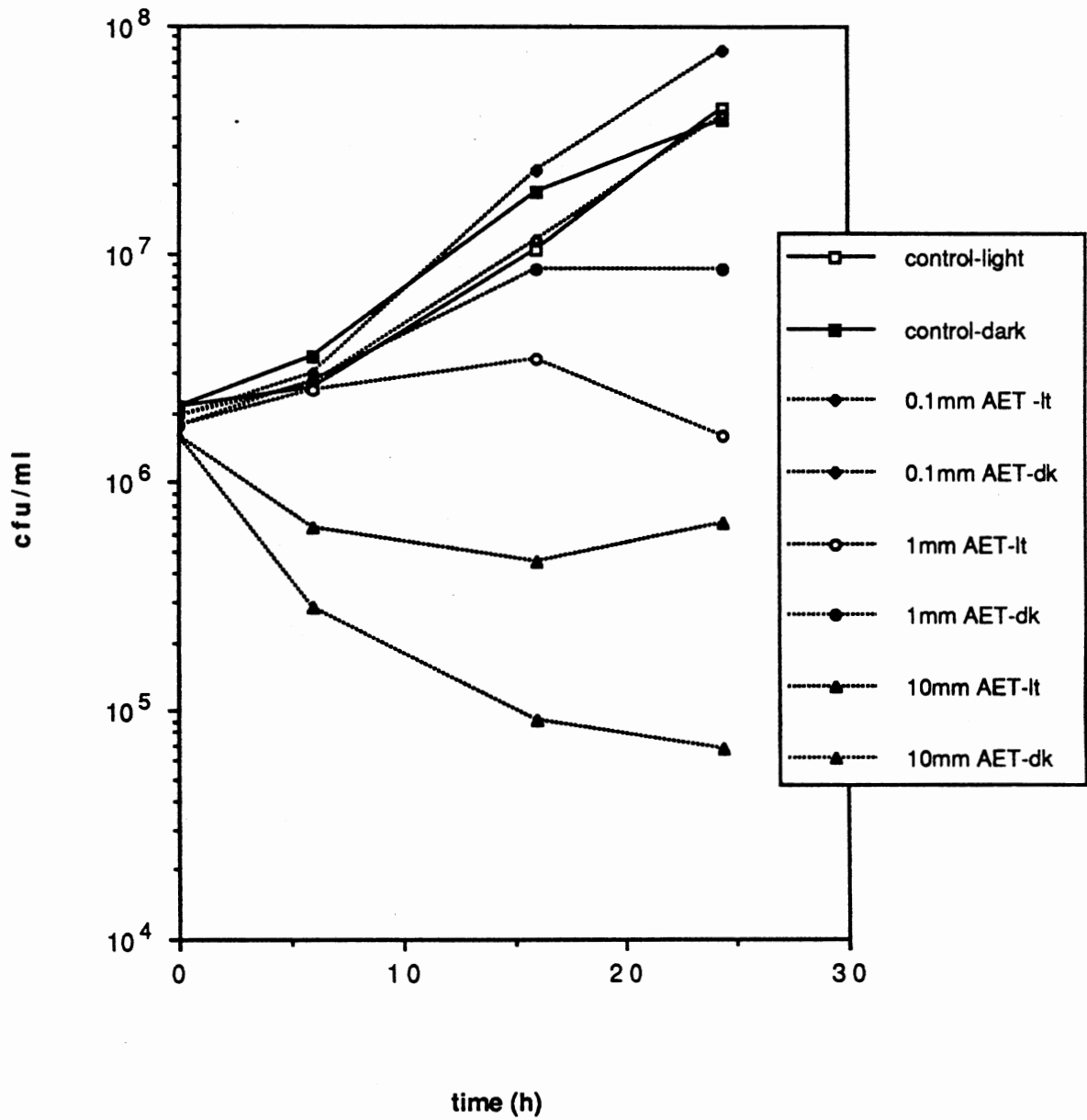
- 20) Essenberg, M., Pierce, M., Shevell, J.L., Sun, T.J. and Richardson, P.E. (1985) *Curr. Comm.*, 145
- 21) Weinstein, L. I. and Albersheim, P. (1983) *Plant Physiol.* **72**, 557
- 22) Boydston, J. R., Paxton, J.D. and Koeppe, D. (1983) *Plant Physiol* **72**, 151
- 23) Hargreaves, J. A. (1980) *Physiol. Plant Pathol.* **16**, 351
- 24) Skipp, R. A., Selby, C. and Bailey, J.A. (1977) *Physiol. Plant Pathol.* **10**, 221
- 25) Turrelli, M., Coulomb, C., Coulomb, Ph.J., Roggero, J.P., and Bounia, M. (1984) *Physiol. Plant Pathol.* **24**, 211
- 26) de Peyster, A., Hyslop, P.A., Kuhn, C.E, and Sauerheber, R.D. (1986) *Biochem. Pharm.* **35**, 3263
- 27) Frobisher, Hindsill, Crabtree, and Goodheart (1974) *Fundamentals of Microbiology*, W. B. Saunders Co., p. 309
- 28) Singer, M. and Wan, J. (1977) *Biochem. Pharm.* **26**, 2259
- 29) Davidson, P. M., and Branen, A.L. (1980) *J. of Food Science* **45**, 1607
- 30) Bakker, J., Gommers, F.J., Smits, L., Fuchs, A. and de Vries, F.W. (1983) *Photochem. and Photobiol.* **38**, 323
- 31) Sun, T.J. (1987) Ph.D. Dissertation, Oklahoma State University
- 32) Daub, J.E. and Hangarter, R.P. (1983) *Plant Physiol.* **73**, 855
- 33) Daub, M.E. (1982) *Phytopathology*, **72**, 370
- 34) Wilkinson, F. and Brummer, J.G. (1981) *J. Phys. Chem. Ref. Dat.* **10**, 809
- 35) Foote, C.S., Shook, F.C., and Abakerli, R.B. (1984) *Methods in Enzymology*, vol. 105 ed. L. Packer, Academic Press, Orlando, FA p. 36
- 36) Sawyer, D.T. and Gibian, M.T. (1979) *Tetrahedron* **35**, 1471
- 37) Singh, A. (1982) *Can. J. Physiol. Pharmacol.* **60**, 1330
- 38) von Sonntag, C. and Schutte, Frohlinde, D. *Effects of Ionizing Radiation on DNA. Physical, Chemical Biological Spect.* Eds. J. Hutterman, L. Kohn, R Teoule and A. J. Bertinchamps, Springer-Verlag, Berlin, p. 204(1978)
- 39) Bielski, B.H.J. and Shiue, B.B. (1979) *Oxygen Free Radicals and Tissue Damage*, CIBA Foundtion Series 65, Elsevier Press, Amsterdam, p. 43
- 40) Foote, C.S. and Denny, R.W. (1968) *J. Am. Chem. Soc.* **90**, 6233
- 41) Ouannes, C. and Wilson, T. (1968) *J. Am. Chem. Soc.* **90**, 6257

- 42) Foote, C.S., Denny, R.W., Weaver, L, Chang, Y. and Peters, J. (19?), Annals New York Acad. of Science. p.139
- 43) Winston, G.W. and Cederbaum, A.F. (1985) CRC Handbook of Methods for Oxygen Radical Research, R. Greenwald Ed., CRC Press, Boca Raton, FA, p.169
- 44) Halliwell, B. and Gutteridge, J.M. (1984) Methods in Enzymology, vol 105, Ed. L. Packer, Academic Press, Orlando FA p.47

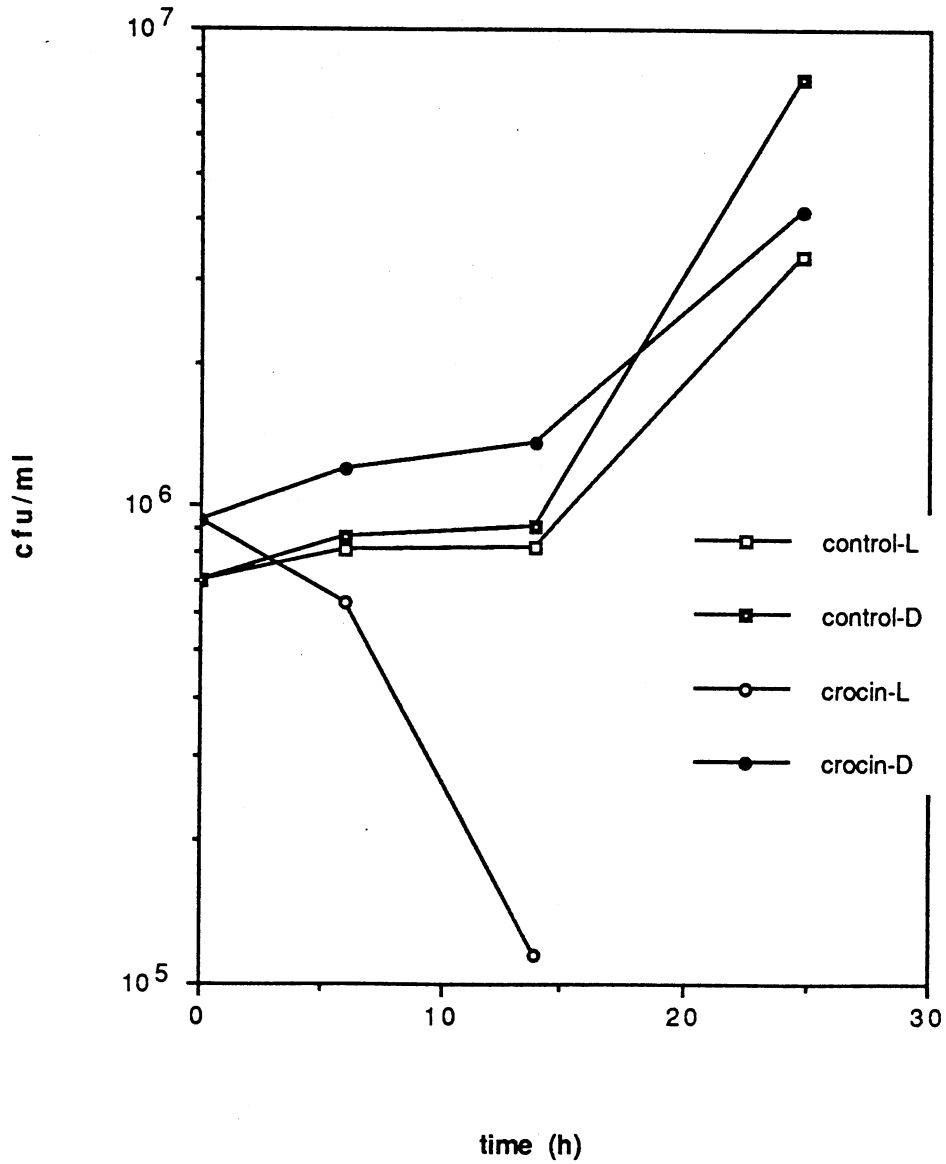
APPENDICES



APPENDIX A. The Effect of Two Alcohols on Growth of Xcm; Low Light Conditions. EtOH in final concentrations of 2, 4, and 6%, and MeOH in the final concentrations of 4 and 8%, were added to suspensions of Xcm in MOPS medium. Bioassay Method I.



APPENDIX B. Effect of AET on Growth of Xcm; Light and Dark Conditions. Suspensions of Xcm in MOPS medium were prepared containing AET in three concentrations: 0.1, 1.0, and 10.0 mM. Bioassay Method II.



APPENDIX C. Effect of Crocin on Growth of Xcm, Light and Dark Conditions. Crocin (0.3 mM) was added to suspensions of Xcm in MOPS medium. Bioassay Method II.

VITA

Joy Randall Steidl

Candidate for the Degree of

Doctor of Philosophy

Thesis: SYNTHESIS OF 2,7-DIHYDROXYCADALENE, A COTTON PHYTOALEXIN; PHOTO-ACTIVATED ANTIBACTERIAL ACTIVITY OF PHYTOALEXINS FROM COTTON; EFFECT OF REACTIVE OXYGEN SCAVENGERS AND QUENCHERS ON BIOLOGICAL ACTIVITY AND ON TWO DISTINCT DEGRADATION REACTIONS OF DHC

Major Field: Biochemistry

Biographical:

Personal Data: Born in Urbana, Illinois, June 2, 1955, seventh child of Raymond F. and Patsy Steidl.

Education: Bachelor of Science Degree in Biochemistry, University of Illinois, May, 1977; Master of Science in Chemistry, State University of New York at Albany, May 1981; completed requirements for Doctor of Philosophy degree at Oklahoma State University, December, 1988.

Professional Experience: Research Technician at State University of New York at Albany; Teaching Assistant, and Research Assistant, Department of Chemistry, State University of New York at Albany, and at Oklahoma State University; Visiting Assistant Professor, Oklahoma State University.